A HEURISTIC SLOW VOLTAGE CONTROL SCHEME

FOR

LARGE POWER SYSTEMS

By

JINGDONG SU

A dissertation submitted in partial fulfillment of
the requirements for the degree of

DOCTOR OF PHILOSOPHY

WASHINGTON STATE UNIVERSITY
School of Electrical Engineering and Computer Science

May 2006

To the Faculty of Washington State University:

The members of the Committee appointed to examine the dissertation of JINGDONG SU find it satisfactory and recommend that it be accepted.

Chair

ACKNOWLEDGEMENT

I would like to express my sincere appreciation to my advisor, Professor Vaithianathan Venkatasubramanian, for his valuable advice, skilled guidance and continuous support throughout my doctoral study. His profound knowledge and kindness will always be an inspiration to me. I am also grateful to Mr. Carson Taylor and Mr. Ramu Ramanathan for their counsel, insight and support. I have enjoyed the enlightening instruction and advisement of Professor Anjan Bose and Professor Kevin Tomsovic, and I am thankful for their participation in my advisory committee.

Funding in part from Bonneville Power Administration (BPA) is gratefully acknowledged. Funding in part from the Consortium for Electric Reliability Technology Solutions (CERTS) is gratefully appreciated. The valuable comments and feedback from BPA planning and operation engineers and National System Research (NSR) engineers are specially appreciated. The support of the Power System Engineering Research Center (PS_{ERC}) is gratefully acknowledged.

I am also deeply indebted to my friends and colleagues at Washington State University, for their friendship and their help, which made this long journey a joyful one. Finally I would like to thank my family for their encouragement, support and enduring love, without them I would never have been able to make it this far.

A HEURISTIC SLOW VOLTAGE CONTROL SCHEME

FOR

LARGE POWER SYSTEMS

Abstract

by Jingdong Su, Ph.D.
Washington State University
May 2006

Chair: Vaithianathan Venkatasubramanian

Automatic control of transmission network voltage provides significant improvements in security, quality and efficiency of power system operation. In Europe, voltage control is traditionally organized in a three levels hierarchical structure. At the second level, the so called “secondary voltage control” divides the network into multiple control regions based on the pilot node concept and all generators in a given region are operated in an “aligned” mode. In North America, transmission grid voltage control is mostly achieved through manual switching of capacitor/reactor banks and LTC transformers by operators. Recently, an automatic discrete slow voltage controller is proposed to regulate voltage of the western Oregon area in the Pacific Northwest. The controller acts upon SCADA measurements and relies on state estimator model to evaluate the incremental effects of control device switching by running localized power flow.

This dissertation first proposes an alternate heuristic slow voltage controller, which can be easily integrated with the above controller and implemented under a common framework. Then the controller scheme is extended so that it is applicable to any large

power systems. In view of a state estimator model maybe unavailable or unreliable because of topology errors under certain conditions, the proposed alternate controller operates independent of the state estimator model and can be either used as back-up controller under these conditions or used to reinforce the decision recommended by the model-based controller. A local voltage estimator is formulated based on linearized reactive power flow model to approximate switching effects by utilizing only the local SCADA measurements around the control devices.

For large power systems, several voltage problems may occur simultaneously in different areas, a multiple problematic area voltage control scheme is proposed to make simultaneous corrective control actions accordingly such that the system voltages are quickly brought back to normal range. This control scheme is quite open and can be easily extended to handle different objective functions. For many power systems, it is also necessary to consider generators as voltage control devices, which leads to the problem of coordinating generator controls and discrete device controls. A multi-phase hybrid voltage control scheme is proposed to deal with the problem by formulating generator and discrete device controls as continuous and discrete problems separately while taking reactive power security into consideration. The controller solves the problems in different operating phases using linear programming and integer programming algorithms respectively and sends alarms to operators if reactive power reserve limits are hit.

Contents

ACKNOWLEDGEMENT iii

ABSTRACT iv

LIST OF TABLES ix

LIST OF FIGURES xi

1. Introduction 1

1.1 Power System Voltage Control 1

1.2 Literature Review 8

1.3 Background and Motivation 16

1.4 Summary 18

2. Local Voltage Estimation 21

2.1 Formulation of the Local Voltage Estimator 21

2.1.1 Estimation of Capacitor/Reactor Switching Effects 23

2.1.2 Estimation of Transformer Tap Changing Effects 26

2.1.3 Estimation of Generator Voltage Adjusting Effects 28

2.2 Feasibility Studies of the Local Voltage Estimator 29

2.2.1 Tests on IEEE 30 Bus System 30

2.2.2 Tests on WECC System 33

2.3 Summary 40

3. Alternate Heuristic Voltage Control 42

3.1 On-line Slow Voltage Control Framework 42

3.2 Formulation of the Alternate Heuristic Control 47

3.3 Testing of the Alternate Voltage Controller 53

3.3.1 Tests on IEEE 30 Bus System 53

3.3.2 Tests on WECC System 56

3.4 Summary 68

4. Large Power System Considerations 70

4.1 Multiple Problematic Area Voltage Control 71

4.1.1 Multiple-area Voltage Control Scheme 71

4.1.2 Tests on WECC System 73

4.2 Multi-phase Hybrid Voltage Control 78

4.2.1 Multi-phase Hybrid Control Scheme 79

4.2.2 Formulation of the Optimization 81

4.2.3 Tests on IEEE 30 Bus System 87

4.2.4 Tests on WECC System 91

4.3 Summary 97

5. Conclusions and Future Works 99

5.1 Conclusions 99

5.2 Future Works 100

BIBLIOGRAPHY 102

APPENDIX 107

A. IEEE 30 Bus Test System 107

A.1 One-line Diagram of IEEE 30 Bus Test System 107

A.2 System Data of IEEE 30 Bus Test System 108

B. README of the Programs 110

B.1 Standard programs used and case studied 110

B.2 MATLAB files 111

B.3 C/C++ files 113

List of Tables

2.1 Selection of estimation parameters for IEEE 30 bus system 30

2.2 Estimation results for capacitor switching on IEEE 30 bus system 31

2.3 Estimation results for LTC tap changing on IEEE 30 bus system 31

2.4 Estimation results for generator voltage adjusting on IEEE 30 bus system 32

2.5 Estimation results for capacitor switching on WECC Base Case 34

2.6 Estimation results for capacitor switching on WECC Case #1. 35

2.7 Estimation results for capacitor switching on WECC Case #2. 35

2.8 Estimation results for transformer tap changing on WECC Base Case. 36

2.9 Estimation results for transformer tap changing on WECC Case #1 36

2.10 Estimation results for transformer tap changing on WECC Case #2 37

2.11 Estimation results for transformer tap changing on WECC Case #3 37

2.12 Estimation results for generator voltage adjusting on WECC Base Case. 38

2.13 Estimation results for generator voltage adjusting on WECC Case #1. 38

2.14 Estimation results for generator voltage adjusting on WECC Case #2. 38

2.15 Estimation results for generator voltage adjusting on WECC Case #3. 38

3.1 Rules to choose candidate device and its control action 48

3.2 Control devices available in IEEE 30 bus system 54

3.3 Results of voltage control on IEEE 30 bus system (A) 55

3.4 Results of voltage control on IEEE 30 bus system (B) 55

3.5 Control devices available in west Oregon area 57

3.6 Generator controlled buses 57

3.7 Voltage control results with capacitor/reactor only (LVE) 59

3.8 Voltage control results with capacitor/reactor only (PF) 60

3.9 Voltage control results with capacitor/reactor/LTC (LVE) 62

3.10 Voltage control results with capacitor/reactor/LTC (LPF) 63

3.11 System static limit increases with voltage controller 66

3.12 Capacitors available in the test case for generator control 67

3.13 Voltage control results with capacitor/reactor/LTC/generator (LVE) 68

4.1 Additional control devices available in Spokane area 73

4.2 Additional control devices available in Seattle/Tacoma area 74

4.3 Multiple area voltage control results [Oregon and Seattle areas] 75

4.4 Multiple area voltage control results [Oregon and Spokane areas] 77

4.5 Results of multi-phase hybrid voltage control (IEEE 30 – A) 89

4.6 Modified LTC tap range on IEEE 30 bus system 89

4.7 Results of multi-phase hybrid voltage control (IEEE 30 – B) 90

4.8 Control devices available in west Oregon area 92

4.9 Results of multi-phase hybrid voltage control (WECC - A) 94

4.10 Results of multi-phase hybrid voltage control (WECC - B) 96

List of Figures

1.1 Simple model of power transfer through transmission line 2

1.2 Load voltage versus active and reactive power 4

1.3 The normalized *P-V* curves 5

1.4 The hierarchical voltage control structure 14

2.1 Power transmission line π-equivalent model 22

2.2 Power transformer line π-equivalent model 26

2.3 Part of the one-line diagram for the west Oregon area of WECC 33

3.1 Common on-line slow voltage control framework 43

3.2 Alternate on-line slow voltage controller flowchart 46

3.3 Penalty function of voltage violation 51

4.1 Multiple problematic area voltage control diagram 72

4.2 Phase transition diagram of the multi-phase hybrid voltage control 80

A.1 One-line diagram of IEEE 30 bus test system. 95

To My Family

Chapter 1

Introduction

Power systems are sometimes referred to as the largest machines built by man. A modern power system is typically composed of a large number of equipments that perform generation, delivery and consumption of electricity. One of the main objectives in operating a power system is to maintain the system voltage properly to avoid equipment damage and transfer power efficiently. In recent years, voltage control has become more and more important for secure and economic operation of power systems because the grid is operated ever so nearer to its limits to meet continuously growing loads and more uncertainty in operating conditions is introduced by the electricity market. This dissertation is essentially concerned with the control of power system voltage with an emphasis on transmission network voltage control. In this chapter, a brief introduction to power system voltage control is presented in Section 1.1. Section 1.2 reviews the existing voltage control methods for transmission grid. Section 1.3 addresses the background and motivation of the research. The contributions and the structure of this dissertation are summarized in Section 1.4.

1.1 Power System Voltage Control

Active (real) and reactive power transfer depends on the voltage magnitudes and angles of transmission network, hence control of voltage is closely related to control of the real and reactive power. To facilitate understanding, let us first recall some fundamentals of the power transfer between a generator and a load, and use the simple model of Figure 1.1 to represents a constant voltage source with voltage *E* supplying a remote load through a transmission line modeled as a series reactance.

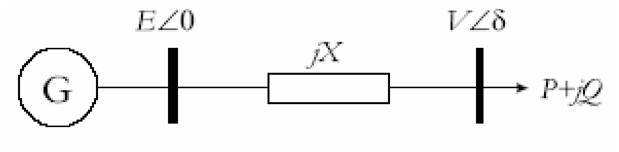

Figure 1.1 Simple model of power transfer through transmission line.

The receiving end voltage magnitude *V* and angle δ depend on the active power *P* and reactive power *Q* transmitted through the line. The active and reactive power received at the load end can be written as [1] - [3]

$$P = -\frac{EV}{X}\sin\delta = P_{\max}\sin\delta \tag{1.1}$$

$$Q = -\frac{V^2}{X} + \frac{EV}{X}\cos\delta \tag{1.2}$$

For practical power transfer and power angles, say less than 30°, the above equations can be approximated by using the relation $\sin\delta \cong \delta$ and $\cos\delta \cong 1$, then we have

$$P \cong P_{\max}\delta \tag{1.3}$$

$$Q = \frac{V(E-V)}{X} \tag{1.4}$$

Equations (1.3) and (1.4) imply that (a). Active (real) power transfer depends mainly on the power angles, i.e. *P* and δ are closely coupled. (b). Reactive power transmission depends mainly on voltage magnitudes and current from the high voltage to low voltage, i.e. Q and V are closely couples. These relationships are often taken advantage of in analysis of power systems, such as fast decoupled power flow algorithm.

Next, solving (1.1) and (1.2) with respect to V^2 yields

$$V^2 = \frac{E^2}{2} - QX \pm X\sqrt{\frac{E^4}{4X^2} - P^2 - Q\frac{E^2}{X}} \tag{1.5}$$

The problem has solution if the inner square root is large or equal to zero

$$P^2 + Q\frac{E^2}{X} \le \frac{E^4}{4X^2} \tag{1.6}$$

It can be observed from the inequality (1.6) that the active and reactive power transfer limits are proportional to the line admittance and to the square of the source voltage E. The reactive power transfer limit is $\frac{E^2}{4X}$ for all conditions. The active power transfer limit is $\frac{E^2}{2X}$ for $Q \ge 0$, but this limit can be exceeded by injection of reactive power at the load end, i.e. $Q < 0$. Thus, it appears more difficult to transfer reactive power than active power over the inductive line, and it seems that reactive power can influence the ability of the line to transfer active power.

Figure 1.2 shows the so-called "onion surface" given by equation (1.5) drawn in normalized variables (assuming power factor is $\tan\phi$). It illustrates how the receiving end voltage V changes with the transferred active power P and reactive power Q. Each point on the surface corresponds to a feasible operating point and in normal conditions the operating point lies on the upper part of the surface with load voltage V close to source voltage E. The solid lines drawn on the surface correspond to operating points with varying load and constant power factor. The figure also visualizes the set of maximum load power points located on the “equator” of the surface which corresponds to the transfer limit according to condition (1.6).

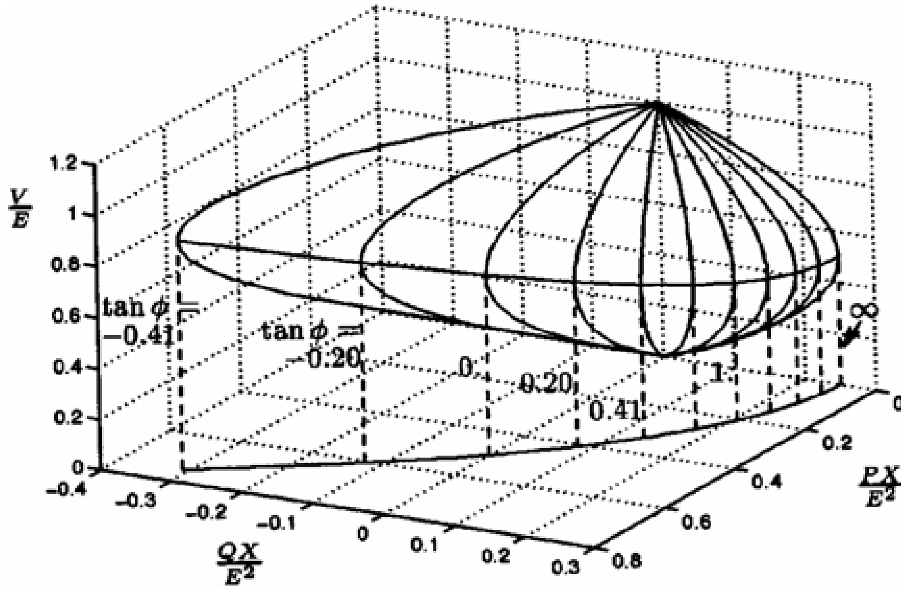

Figure 1.2 Load voltage versus active and reactive power (“onion surface”) [3].

A more traditional way (and common industry practice) of illustrating the phenomenon is to plot the curves that relate terminal voltage *V* to active power *P*. Figure 1.3 shows so-called *P-V* curves or “nose curves” which are projections of the solid lines drawn on the onion surface onto the *P-V* plane. The rightmost point of each *P-V* curve marks the maximum active power transfer (referred to as *theoretical transfer limit*) and the corresponding load end voltage (referred to as the *critical voltage*) for a particular load power factor. The critical voltage and theoretical transfer limit increase with decreasing power factor. In normal operation the voltages of both ends of the line are kept close (to the rated voltage, typical 5 % deviation from the nominal voltage. The *practical transfer limit* is therefore about $0.35\frac{E^2}{X}$ or even lower for the load with a lagging power factor. Reactive power injection at the load end, such as capacitor banks, decreases the apparent power factor of the load, thus the operating point shifts to another *P-V* curve for a lower value of $\tan\phi$ and the transfer limit increases correspondingly. However, the critical voltage is also brought closer to the nominal voltage, which makes the system more vulnerable to load variations and more prone to voltage collapse.

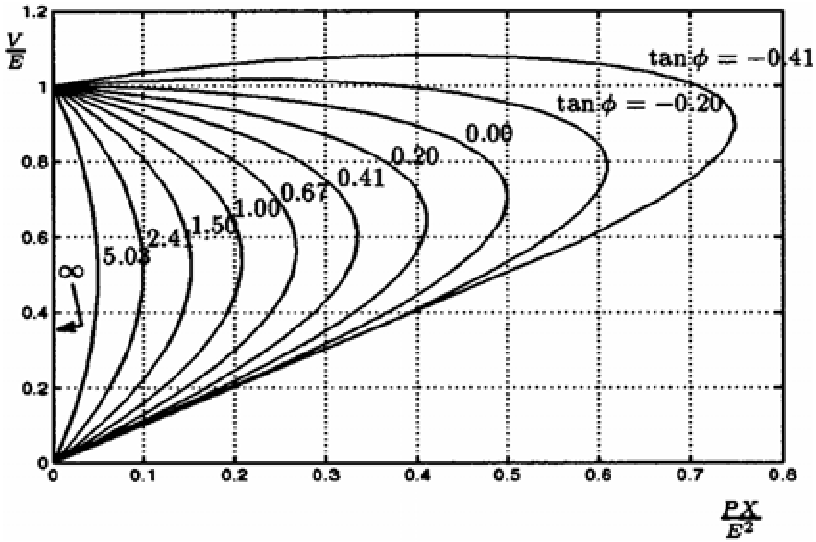

Figure 1.3 The normalized *P-V* curves ("nose curves") [3].

It is clear from the above analysis of the simple system that the real power transfer capability and load end voltage are highly dependent on the absorption or injection of reactive power; the control of voltage is in fact closely related to the control of reactive power. Since reactive power balance is a fundamental aspect of reactive power and voltage control, it is necessary to briefly review the power system components from the viewpoint of reactive power production and absorption [1] – [4].

Loads seen from the transmission system are usually inductive and therefore absorb reactive power. Typically, a transmission system load is composed of significant amount of induction motor loads, which exhibit potentially very complex voltage behavior. For small voltage excursions, say less than 5 %, the active power drawn by induction motors can be approximated as constant and the reactive power as proportional to an exponential of the voltage. Since the transmission loads are usually connected through tap changers that keep the load voltages close to their nominal values, they can normally be considered as constant power in the long term.

Transmission lines both produce and consume reactive power, which is one of the factors that make voltage control complicated. The reactive power production (V^2B) of transmission line due to the line shunt capacitance is relatively constant since voltage must be kept within about $\pm 5\%$ of nominal voltage, while the reactive power consumption (I^2X) of transmission line due to the line impedance varies because the current changes with the load level. Overhead lines thus generate reactive power under light load and absorb reactive power under heavy load. Underground cables always produce reactive power since the reactive losses never exceed the production because of their high shunt capacitance. However, because the production of reactive power by cables and overhead lines is quadratically dependent on the voltage, it provides less support at low voltages when reactive power is likely to be needed most.

Synchronous generators and synchronous condensers can be controlled to regulate bus voltage by continuously generating or absorbing reactive power according to the need of the surrounding network. Generators normally provide the most basic yet most effective means of system voltage control. The automatic voltage regulator (AVR) acts on the exciter of a synchronous machine to adjust field current within capability its limits, thus maintain a scheduled terminal voltage. The response time of the primary controllers is short, typically fractions of a second, for generators with modern excitation systems.

Synchronous condensers are nothing but synchronous machines designed to operate without mechanical power source. Because of their high initial and operating costs, they are not widely used nowadays.

Transformers always consume reactive power because of their reactive losses. In addition, transformers equipped with load tap changers (LTCs) can regulate network voltage by shifting reactive power between their primary and secondary sides. However, the regulation of the voltage of one side affects the voltage at the other side in the opposite direction. Thus it is necessary to carefully coordinate tap changing with other network voltage control methods such as switching capacitor/reactor banks.

Series capacitors are connected in series with the line conductors and can lower the inductive reactance of heavily loaded lines and thereby reduce their reactive losses. They have the effect of increasing the maximum transfer capability of the lines without increasing the critical voltage, thus appear to be the ideal compensation devices. However they could cause subsynchronous resonance and need complicated protection equipment to protect them from fault currents and therefore not in widespread use for the purpose of alleviating voltage problems.

Shunt capacitors and shunt reactors are passive devices that generate or absorb reactive power. Shunt capacitors act by adding capacitive admittance to improve the power factor of the load or compensate transmission system reactive power losses under heavy load conditions. The amount of reactive power generated by a capacitor is quadratically dependent on the voltage so it will provide less support at low voltages. Compensation by capacitor banks increases the practical transfer limit but also pushes the critical voltage closer to nominal voltage which makes the system more prone to voltage collapse. Shunt reactors have the opposite effect compared to capacitor banks and are sometimes used to absorb excess reactive power produced by lightly loaded lines and cables.

Static var compensators (SVCs) combine conventional capacitors and reactors with fast switching capability of modern power electronics. They provide rapid, direct and continuous regulation of voltage and are ideally suited for preventing transient voltage instability associated with motor loads. Because SVCs use capacitors, they suffer from the same degradation in reactive power capability as voltage drops and require harmonic filters to reduce the amount of harmonics injected into the power system.

In general, the reactive demand from loads close to generation areas is often supplied by the generators. Shunt capacitor/reactor banks are usually used to meet the reactive demand in load areas far from generators. In terms of time frames, power system voltage control can be classified as “fast” (transient, dynamic) control with a time frame less than 10 seconds, and “slow” (static, long-term) control with a time frame of tens of seconds or several minutes [1], [5], [6]. Another way to categorize voltage control is transmission system voltage control and distribution system voltage control because of the topological differences between them. Transmission grid voltage control is largely provided by generator AVRs, capacitor/reactor banks, LTC transformers and sometimes SVCs, while LTC transformers and capacitor/reactor banks are often coordinated to regulate distribution system voltage. This dissertation is mainly focused on “slow” control of transmission system steady state voltage. The following section contains review of different voltage control strategies for transmission network.

1.2 Literature Review

Voltage and reactive power control problems are not new in the operation of electric power systems but are receiving special attentions in recent years because the steadily growing loads (for instance, at 3% annually in the USA, [7]) force the grid to be operated much closer to its limits, but the transmission networks are hardly expanded due to social and economical reasons, and the operating uncertainty has greatly increased owing to the deregulation of electricity market. Under such circumstance, it is becoming more and more difficult for power system operators, based on their experience and offline studies, to determine proper control strategies that could ensure the quality of power supply and the power system security. For example, it is reported in [6] that incorrect switching action by operators has led to partial voltage collapse and loss of loads on the Olympic Peninsula in January 1995. Besides, with retirements of the experienced operators, this traditional man-in-loop way of voltage control will become more challenging. Automatic control of system voltages can improve voltage security greatly since the voltages of the transmission system will be quickly brought back to normal ranges following any contingency and reactive power resources are continuously managed to increase the operating margins for preventing potential collapse. Furthermore, transmission losses can be reduced by continuously keeping the system voltages near the optimal profile. However, the diversity of the control devices and the nonlinear interactions between them make the control problem particularly difficult. The literature of the past shows how different voltage control strategies have evolved over the years.

In the late seventies and early eighties, although the voltage magnitude changes were available through state estimator, these data were typically not used for any direct control of voltage. One reason is that it is much easier to monitor and understand smaller data sets, such as the system frequency and tie line flows, which clearly reflect the system-wide active power imbalances than the large amount of the voltage magnitudes associated with the load buses throughout the system. Another reason is that active power disturbances have stronger system-wide effect, whereas reactive power and voltage related problems tend to be more local in a geographical sense and relatively rare because transmission grid were seldom over-loaded at that time. Besides, there were not enough economic incentives for voltage and reactive power control, because the operation costs are mostly associated with real power generation and distribution.

After a number of severe voltage-related operational problems had been reported worldwide, the interest in voltage and reactive power control has increased dramatically [1], [2]. Considerable research efforts have been made to find effective ways of managing reactive power and maintaining desired system voltage profile. In the beginning, researchers were trying to adapt the well-developed planning tools such as optimal power flow (OPF) for this purpose [8] – [10]. The objective is generally modified to keep all bus voltages within acceptable bounds, while at the same time satisfying some optimality criteria (minimum losses, maximum reactive reserve, minimum shifts of controls, etc). However, the specific nature and some deficiencies of the OPF-related methods, such as hardness in defining a well-balanced objective, computational burden, infeasibility under certain conditions and complexity for human operators, have limited their scope of application, especially in real-time environment [11].

In the mid-eighties, improvements in the artificial intelligence (AI) technology, especially expert systems, had made it possible to develop some prototype rule-based tools to assist operators in reactive power/voltage control [12] – [15]. In [12] an expert system based on 28 rules is proposed to deal with voltage problems of low severity. Sensitivities of bus voltages to control variables are incorporated to enhance the capability of the expert system. Based on the ‘sparse” sensitivity matrix, a sensitivity tree is used in the expert system proposed in [13] to check if a control action will cause new voltage violations. The concept of “local network” (a set of load buses surrounded by some PV boundary buses) is adopted in [14] to simplify the task of computing, since effective control devices must lie on the boundary. Two rule-based techniques are presented in [15] based on the so-called “reactive path” concept. The first one allocates to each controller the load buses on which it has significant effects. Then two most efficient controllers are identified for a bus with voltage problems. Besides expert systems, other branches of AI technology, such as fuzzy logic and neural network, have also been explored to solve the reactive power /voltage control problem [16] - [18].

Strictly speaking, all of the above OPF-based methods and AI-based methods are not close-loop control because these methods are generally intended to be implemented as on-line decision-making tools that help system operators dispatching reactive resources to maintain desired voltage profile. Ideally, a system-wide voltage control should follow a philosophy similar to that of automatic generation control (AGC) which compares some feedback values with reference values and automatically establish appropriate control actions. However, the enormous amount of voltages makes this type of control impossible in real-time without reducing the amount of information. This is exactly the consideration that leads to another approach of voltage control - the so-called secondary voltage control originally proposed by EDF in late seventies and implemented in late eighties [19].

The French control concept is a pilot point based hierarchical information and control structure that works with fewer voltage data and therefore makes the real time monitoring and control more manageable. A pilot point is a carefully chosen load bus at which the voltage is to be measured in real-time and used as feedback value to controller for deriving control actions. At the primary control level of this structure, voltage-control devices, including automatic voltage regulator (AVR) of generators, load tap changing (LTC) transformers and capacitor banks, attempt to maintain local bus voltages within a threshold of the desired reference values. At the secondary control level, the network is divided in to several regions (or zones) by off-line studies using empirical methods or using the concept of *electrical distance* [21], an on-line control scheme using information from the pilot points in each region takes action to update the reference voltages of the primary control devices.

The pilot points are selected such that, although there are few of them, the information from them is sufficient to control the voltage profile of the region. At the beginning of the implementation in the French system, one pilot point is selected for each region that is simply the load bus with the largest short circuit current [21]. Once the pilot points are found, a control scheme is implemented such that all generators in a given region are operated at the same rate of relative reactive power ("aligned" operation). Thus control of the pilot point voltage in a given region involves only one measurement and one control decision. Since the pilot point selection is critical for the successful implementation of the reduced information control structure, several other algorithms for pilot point selection are explained in [20], [24], [26]. However, as modern power systems become more meshed and heavily loaded, it is quite difficult to divide a power system into separated control regions, and to determine a proper pilot node for a control region.

The secondary voltage control assumes negligible interaction with the neighboring region. As the power system has become increasingly meshed and is operated closer to its transmission limits, an improved control design at the secondary level was proposed, which uses additional measurements to cancel the effects of the neighboring regions on a regional performance criterion [23]. However, it is effective only when there are sufficient reactive power reserves. EDF and some other utilities also considered a coordinated secondary voltage control scheme to take into account operating constraints and to manage interaction between coupled area [22] [24] [25].

The tertiary voltage control operates at the highest hierarchical level to provide system-wide coordination of the reactive power flow between different regions. It coordinates in a centralized way the actions of the regional voltage control by defining and actuating in real-time the optimal voltage pattern of the pilot nodes [22][27]. In Italy ENEL, the tertiary voltage regulator has strong interaction with the reactive power scheduling functions [22]. In Belgium, coordinated voltage control has been in operation since 1998. Every 15 minutes or on request (e.g. following important disturbances) a tertiary voltage control scheme is computed using an optimal power flow (OPF) with dedicated objective function. It optimizes system-wide generator reactive reserves and shunt capacitor bank switching under constraints of voltage limits and reactive power area balance. The actual optimization is carried out by linear programming (LP), with the quadratic objective function linearized by segments and all control variables are basically treated as "continuous" [27].

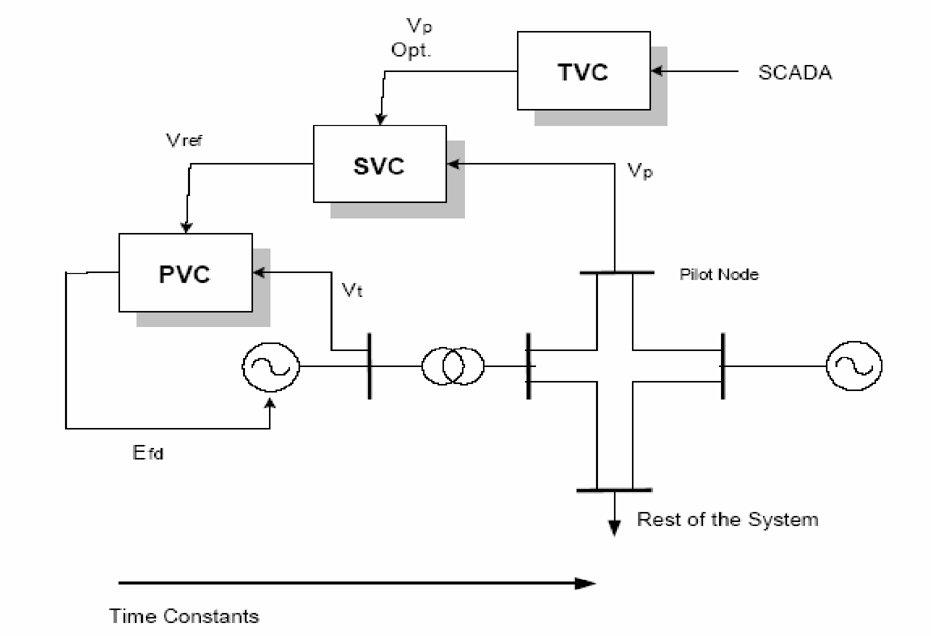

Figure 1.4 The hierarchical voltage control structure.

To ensure that different levels of control do not interact and thus reduce the risk of oscillation or instability, the hierarchical voltage control operates in a way such that the three levels of control are both spatially (or geographically) and temporally independent. At primary level, control devices such as generator AVRs act locally on fast and random voltage variations, attempt to maintain local voltage at its reference value. The time constant is generally in the range of hundreds of milliseconds to tens of seconds. At secondary level, slow and large regional voltage variations, such as those caused by hourly load changes, are fed back to the controller as the voltage deviations of several pilot bus voltages from their optimal values. The controllers act upon these deviations and update the reference values of the primary level controls within a time scale ranging from tens of seconds to a few minutes. Finally at tertiary level, system-wide information is used to compute optimal pilot bus voltages with the purpose of economy and security of power system operation. This is achieved by solving, either automatically or manually by operators, a large-scale optimization problem such as the optimal power flow with the objective of minimizing real power losses while taking security constraints into account. The time constant could range from about 15 minutes up to a few hours.

In the Unites State, an on-line voltage control using full SCADA (Supervisory Control and Data Acquisition) information was introduced in early nineties and implemented in the New England system in late nineties [28] – [30]. It is a generation-based scheme to maintain least square minimization of voltage deviations from their desired “optimal” voltage profile as system load level or topology changes. The localized echelon-based approach is proposed to reach the solution for a small portion of the system. In the above schemes, the formation is basically for a continuous control problem. In [30], it was indicated that the software developed based on [29] is not being used by the utility, partly because the operators hesitate to switch capacitors frequently.

In all of above schemes, the formulations are basically for continuous control problems, discrete controls are handled by solving a continuous problem first and later approximating the solution with nearest discrete values. These formulations have the potential deficiencies such as poor convergence and hunting for discrete problems. Recently, a discrete formulation of online voltage control scheme is proposed in [31]. This model-based controller targets primarily on the west Oregon area of WECC system, where there is little generation support but many discrete devices, such as capacitor/reactor banks and LTC transformers, available for voltage control purpose. The controller acts on SCADA measurements and utilizes localized power flow based on state estimator (SE) model to evaluate the incremental effects of control device switching. The control objective is to keep the voltages within constraints with minimum switching actions and minimum circular reactive flow. Bonneville Power Administration (BPA) and National System Research Inc. (NSR) have started to implement the controller prototype for evaluation on Pacific Northwest system since August 2001.

1.3 Background and Motivation

The Pacific Northwest power system is characterized by high spring and summer power transfer to California, and winter peaking of load. The major load centers are on the west side of the Cascade Mountains, including the Vancouver B.C., Seattle/Tacoma, Portland metropolitan areas, and the Willamette River Valley between Portland and Eugene, Oregon. Generation concentrations are along the Columbia River on the east side of the Cascade Mountains. Some power plants are far more distant in northern British Columbia, eastern Montana, and Wyoming.

During normal operation, reactive compensation switching is mainly done by SCADA operators. For voltage changes of several per cent or more, voltage relays with seconds of time delay will initiate compensation switching. With dozens of transmission-level shunt capacitor banks and shunt reactors, good coordination of control is challenging. BPA autotransformers (500/230-kV and 230/115-kV) have under-load tap changers, but are controlled by SCADA operators. Tap changing has lower priority than reactive power compensation switching. Switching frequency is restricted to several tap changes per day because tap changer failure results in transformer outage.

To improve wintertime voltage stability and provide spring/summer voltage support for high power transfer on the Pacific Intertie, Bonneville Power Administration (BPA) is developing a response-based wide-area stability and voltage control in close collaboration with Washington State University (WSU) [5], [6]. The wide-area control can be categorized as fast control to ensure transient stability following major disturbances, and slow control for wintertime voltage stability. Slow controls also provide reactive power “management” during normal operation. The fast controls are *corrective countermeasures* taken in less than one second following a disturbance. The slow controls are either corrective countermeasures taken in a time frame of tens of seconds following a disturbance, or *preventive countermeasures* ensuring security for potential disturbances.

Under BPA contract, Washington State University has been developing methods for automating the slow voltage control of the western Oregon region south of Portland. A model-based discrete slow voltage controller has been proposed for switching of the many capacitor/reactor banks and LTC autotransformers in western Oregon [31]. Owing to the close proximity of discrete devices in this area, the system is treated as one coupled system instead of several sub-control areas. The controller uses adaptive local computations based on state estimator models to evaluate the incremental effects of control switching. For each device, a small local area is constructed first by using the concept of electrical distance, and the power-flow computation is restricted to this small area. For switching decisions, the computed incremental values are added to the measured actual voltage values from SCADA. Based on the discrete nature of the problem, an integer-programming formulation is proposed with the objective of maintaining acceptable voltage profile while minimizing circulating VAR flows, minimizing number of control actions and respecting specified control preferences. A robust formulation is also proposed so that the controller decision is based upon a weighted average of current operating conditions together with the expected conditions from the short-term load forecast.

The advantage of the model based approach is that the effects of switching actions can be computed directly by power-flow calculations. However, state estimator model maybe unavailable or unreliable because of topology errors under certain conditions, thus an alternate formulation of heuristic voltage controller independent of the state estimator model is proposed in this dissertation. A multiple problematic area parallel control is also proposed to deal with voltage problems occurring simultaneously in different areas of large power system. For general large power systems with not only discrete devices but also many generators, a hybrid automatic voltage control scheme is proposed to coordinate continuous generator controls and discrete device controls while taking reactive power security into consideration.

1.4 Summary

Motivated by the BPA voltage control project, this dissertation first proposes an alternate heuristic slow voltage controller that can be easily integrated with the model-based controller and implemented under a common framework. Then the controller scheme is extended so that it is applicable to any large power systems. The time frame of the controller is similar to the secondary voltage control in Europe, namely about tens of seconds.

The major contributions of this dissertation include:

1) In view of a state estimator model maybe unavailable or unreliable because of topology errors under certain conditions, the proposed alternate voltage controller

operates independent of the state estimator model and can be either used as back-up controller under these conditions, or used to reinforce the decisions recommended by the model-based controller.

2) Based on the discrete nature of the problem, an integer programming formulation is used to find the optimal controls. The objective is to maintain an acceptable voltage profile with minimum number of switchings while respecting control preferences. Some heuristic rules are employed in search of optimal control actions.

3) A local voltage estimator is formulated based on linearized reactive power flow model to approximate switching effects by utilizing only the local SCADA measurements around the control devices. The control effects of capacitor/reactor switching, LTC tap changing, and generator voltage adjusting are evaluated in a unified way by treating them as some reactive power injection changes.

4) For large power systems covering vast geographical areas, several voltage problems may occur in different places at same time, a multiple problematic area parallel control scheme is proposed to make simultaneous corrective control actions accordingly to quickly bring the system voltages back to normal range.

5) To extend the control scheme to general power systems, a hybrid automatic voltage control scheme is proposed to deal with the problem of coordinating continuous generator controls and discrete device controls while taking reactive power security into consideration. The controller operates in three phase with the generators and discrete devices control formulated as continuous and discrete problems and solved using linear programming and integer programming respectively.

6) The prototypes of the above control schemes are implemented with MATLAB and C/C++ languages. Feasibility tests of the controls are performed on both standard IEEE 30 bus system and a few actual WECC planning test cases. Simulation results show that the proposed controllers are very effective for solving the coordinated voltage control problem in large power systems.

The rest of this dissertation is organized as follows. Chapter 2 describes the formulation of the local voltage estimator. The feasibility studies of the local voltage estimator are also presented at the end of the chapter. In chapter 3, an on-line control framework integrated both model-based controller and heuristic controller is presented. The formulation of the heuristic controller and some heuristic rules are addressed and the test results are shown in the same chapter. Chapter 4 extends the voltage control to general large power systems. A multiple problematic area parallel control scheme and a multi-phase hybrid automatic voltage control scheme are proposed and formulated with their feasibility demonstrated by simulation results on IEEE 30 bus system and WECC planning cases. In Chapter 5, the conclusions of this dissertation are made and possible future research directions are pointed out.

Chapter 2

Local Voltage Estimation

The alternate heuristic voltage control differs from the model-based voltage control in that the state estimator model is assumed to be unavailable; hence the switching effects can not be evaluated by power flow computation. For the heuristic approach of voltage control, the challenge is how to "predict" or "estimate" the load bus voltage changes after a switching action under different topology/load conditions. In this chapter, a local voltage estimator (LVE) is formulated to approximate the bus voltage changes after a switching action by using only the local measurements from SCADA before switching. Section 2.1 presents the formulation of the local voltage estimator in details. The feasibility studies of the proposed local voltage estimation method are presented in Section 2.2. The conclusions are made in Section 2.3.

2.1 Formulation of the Local Voltage Estimator

The formulation of the local voltage estimator is based on the fact that reactive power flow and voltage magnitude are closely coupled, and their relationship is considered as linear for small changes under normal operating conditions. For the voltage control problem, it is also a valid assumption that a reactive power control device only has a limited geographic effect. The local control area can be formed using the concept of *electrical distance* as in [21], [31] or the localized echelon-based approach in [29]. In this dissertation, a tier-based method similar to localized echelon-based approach is employed to make the local area formation process simple and fast, without the hassle of inverting system susceptance matrix.

If the parameters of transmission lines are known and measurements of bus voltage magnitudes and reactive line flows are available from SCADA near the buses with candidate control devices, here our goal is to find an alternate method to approximate the effects of candidate device switching actions by using these available measurements and known parameters only without running state estimator model-based power flow.

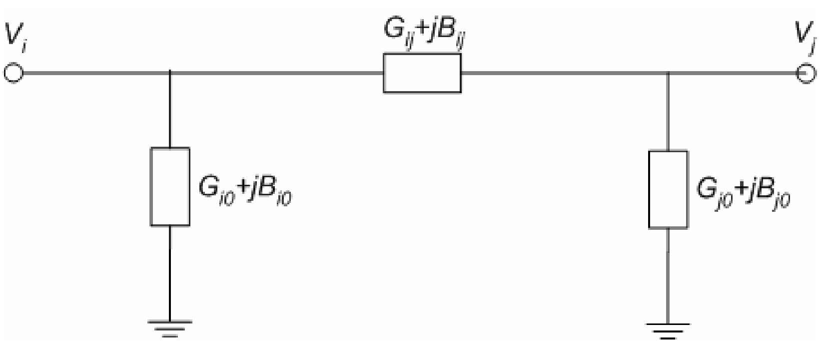

Figure 2.1 Power transmission line π-equivalent model.

As a starting point, the detailed reactive power line flow model needs to be developed and investigated. Let the transmission line between bus i and bus j be represented by π-equivalent model with known line admittance $Y_{ij} = G_{ij} + jB_{ij}$ and shunt admittances $Y_{i0} = G_{i0} + jB_{i0}$ and $Y_{j0} = G_{j0} + jB_{j0}$ as shown in Figure 2.1. If the two complex terminal voltages are represented by $\vec{V}_i = V_i \angle \delta_i$ and $\vec{V}_j = V_j \angle \delta_j$, the complex power line flow equation is [2], [32], [33]

$$\vec{S}_{ij} = \vec{V}_i \left[(\vec{V}_i - \vec{V}_j) Y_{ij} \right]^* + \vec{V}_i \left[(\vec{V}_i - 0) Y_{i0} \right]^* \quad (2.1)$$

Substitute line/shunt admittances and bus voltages/angles into (2.1), the active and reactive power line flow equations are

$$P_{ij} = V_i^2 (G_{ij} + G_{i0}) - V_i V_j (G_{ij} \cos\delta_{ij} + B_{ij} \sin\delta_{ij}) \tag{2.2}$$

$$Q_{ij} = -V_i^2 (B_{ij} + B_{i0}) - V_i V_j (G_{ij} \sin\delta_{ij} - B_{ij} \cos\delta_{ij}) \tag{2.3}$$

where $\delta_{ij} = \delta_i - \delta_j$ is the difference between two bus voltage angles.

2.1.1 Estimation of Capacitor/Reactor Switching Effects

Under normal operating conditions, capacitor/reactor switching could be treated as nearly constant reactive power injection change which will be distributed along the transmission lines connected to the shunt switching bus and cause the voltage changes on the buses in surrounding area. Assume that the changes of reactive flow of transmission lines are related only to terminal voltage magnitude changes under normal conditions, the following linearized reactive power line flow equation can be derived from (2.3)

$$\Delta Q_{ij} = \Delta Q_{ij}(\Delta V_i, \Delta V_j) = \frac{\partial Q_{ij}}{\partial V_i}\Delta V_i + \frac{\partial Q_{ij}}{\partial V_j}\Delta V_j \tag{2.4}$$

where

$$\frac{\partial Q_{ij}}{\partial V_i} = -2V_i (B_{ij} + B_{i0}) - V_j (G_{ij} \sin\delta_{ij} - B_{ij} \cos\delta_{ij}) \tag{2.5}$$

$$\frac{\partial Q_{ij}}{\partial V_j} = -V_i (G_{ij} \sin\delta_{ij} - B_{ij} \cos\delta_{ij}) \tag{2.6}$$

From equation (2.3), the following equation holds

$$(G_{ij} \sin\delta_{ij} - B_{ij} \cos\delta_{ij}) = \frac{-V_i^2 (B_{ij} + B_{i0}) - Q_{ij}}{V_i V_j} \tag{2.7}$$

Substitute (2.7) into (2.5) and (2.6), the two partial derivatives now become

$$\frac{\partial Q_{ij}}{\partial V_i} = -V_i(B_{ij} + B_{i0}) + \frac{Q_{ij}}{V_j} \tag{2.8}$$

$$\frac{\partial Q_{ij}}{\partial V_j} = \frac{V_i^2}{V_j}(B_{ij} + B_{i0}) + \frac{Q_{ij}}{V_j} \tag{2.9}$$

Note that in (2.8) and (2.9) only transmission line parameters, measurements of reactive power line flow and measurements of bus voltage magnitudes are needed to calculate those derivatives, thus given the voltage changes at two terminal buses, the change of reactive power line flow could be estimated by (2.4) without running power flow.

Now assume that a small local control area has been formed around the switching capacitor/reactor, let us investigate how reactive power injection change at certain bus is distributed along all the lines connected to the bus. Such reactive power injection change could be the change caused by shunt device switching or the propagated change on a bus within the small local area around the switching bus. Let the bus with reactive power injection change be bus *i*, and denote the set of buses connected directly to bus *i* as J_i, then the following reactive power injection change equation can be obtained from (2.4)

$$\Delta Q_i = \sum_{j \in J_i} \Delta Q_{ij} = \sum_{j \in J_i} \left(\frac{\partial Q_{ij}}{\partial V_i} \Delta V_i + \frac{\partial Q_{ij}}{\partial V_j} \Delta V_j \right) \tag{2.10}$$

Since the voltage changes of the voltage-controlled buses are zero, they can be excluded from the above equation by setting $\frac{\partial Q_{ij}}{\partial V_j} = 0$, denote the set of voltage-controlled buses connected directly to bus *i* as $J_c \in J_i$, then equation (2.10) becomes

$$\Delta Q_i = \sum_{j \in J_i} \Delta Q_{ij} = \sum_{j \in J_i} \left(\frac{\partial Q_{ij}}{\partial V_i} \right) \Delta V_i + \sum_{\substack{j \in J_i \\ j \notin J_c}} \left(\frac{\partial Q_{ij}}{\partial V_j} \Delta V_j \right) \tag{2.11}$$

If bus i is a boundary bus of the local control area, because of the local nature of the reactive power change, we could assume that the voltage change of an outside bus j connected to the boundary bus can be approximated by $\Delta V_j = \alpha_j \Delta V_i$ with a constant α between 0 and 1. Denote the set of outside buses connected directly to bus i as $J_o \in J_i$, then equation (2.11) can be written as

$$\Delta Q_i = \sum_{j \in J_i} \Delta Q_{ij} = \left[\sum_{j \in J_i} \left(\frac{\partial Q_{ij}}{\partial V_i} \right) + \sum_{\substack{j \in J_o \\ j \notin J_c}} \left(\frac{\partial Q_{ij}}{\partial V_j} \alpha_j \right) \right] \Delta V_i + \sum_{\substack{j \in J_i \\ j \notin J_c}} \left(\frac{\partial Q_{ij}}{\partial V_j} \Delta V_j \right) \tag{2.12}$$

Finally assume that the small local control area around the switching capacitor/reactor has N buses inside, the following vector-form equation can be derived from (2.12)

$$\begin{bmatrix} \Delta Q_1 \\ \Delta Q_2 \\ \vdots \\ \Delta Q_N \end{bmatrix} = \begin{bmatrix} B_{11} & B_{12} & \cdots & B_{1N} \\ B_{21} & B_{22} & \cdots & B_{2N} \\ \vdots & \vdots & \ddots & \vdots \\ B_{N1} & B_{N2} & \cdots & B_{NN} \end{bmatrix} \begin{bmatrix} \Delta V_1 \\ \Delta V_2 \\ \vdots \\ \Delta V_N \end{bmatrix} \tag{2.13}$$

where

$$B_{ii} = \left[\sum_{j \in J_i} \left(\frac{\partial Q_{ij}}{\partial V_i} \right) + \sum_{\substack{j \in J_o \\ j \notin J_c}} \left(\frac{\partial Q_{ij}}{\partial V_j} \alpha_j \right) \right]; \quad i = 1,2,\ldots,N \tag{2.14}$$

$$B_{ij} = \begin{cases} \dfrac{\partial Q_{ij}}{\partial V_j}; & j \notin \bigcup J_c \\ 0; & j \in \bigcup J_c \end{cases}; \quad i = 1,2,\ldots,N \tag{2.15}$$

Since the local area constructed is quite small, so is the number of buses inside N, thus the following equation can be used to estimate the voltage changes on the buses inside the control area very quickly

$$\Delta V = [B]^{-1} \Delta Q = [S] \Delta Q \tag{2.16}$$

where $\Delta Q = [0,...,0, Q_{sh}, 0,...,0]$ is the vector of reactive power injection changes with switching device's capacity denoted as Q_{sh}.

2.1.2 Estimation of Transformer Tap Changing Effects

For transformer, reactive power line flow equation (2.3) needs some modification to include transformer ratio or tap position such that they can be used to estimate the effects of transformer tap changing. Let the transformer between bus *i* and bus *j* be represented by *π*-equivalent model with the transformer ratio t, the original transformer admittance $Y_T = G_T + jB_T$, the equivalent line admittance $Y_{ij} = G_{ij} + jB_{ij}$, and shunt admittances $Y_{i0} = G_{i0} + jB_{i0}$ and $Y_{j0} = G_{j0} + jB_{j0}$ as shown in Figure 2.2.

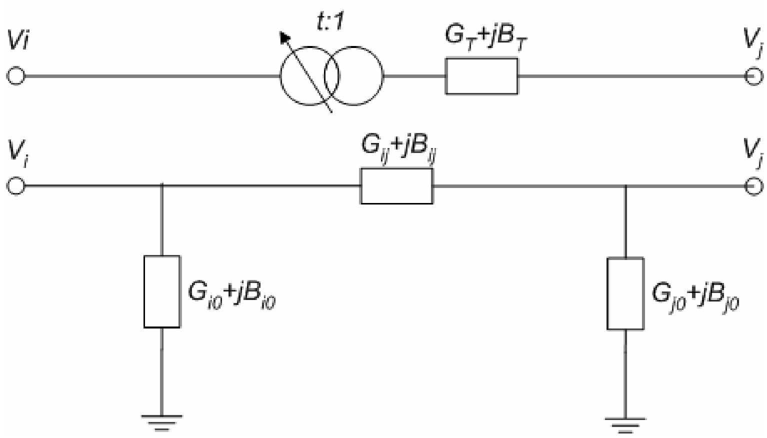

Figure 2.2 Power transformer line *π*-equivalent model.

The relationship between the original transformer's parameters and the equivalent line model's parameters can be written as

$$G_{ij} = G_{ji} = \frac{G_T}{t}; \quad B_{ij} = B_{ji} = \frac{B_T}{t} \tag{2.17}$$

$$G_{i0} = G_T \frac{1-t}{t^2}; \quad B_{i0} = B_T \frac{1-t}{t^2} \tag{2.18}$$

$$G_{j0} = G_T \frac{t-1}{t}; \quad B_{j0} = B_T \frac{t-1}{t} \tag{2.19}$$

Substitute (2.17), (2.18) and (2.19) to (2.3), the equations for reactive power line flows of both directions are

$$Q_{ij} = -V_i^2 \frac{B_T}{t^2} - V_i V_j (\frac{G_T}{t} \sin \delta_{ij} - \frac{B_T}{t} \cos \delta_{ij}) \tag{2.20}$$

$$Q_{ji} = -V_j^2 B_T - V_j V_i (\frac{G_T}{t} \sin \delta_{ji} - \frac{B_T}{t} \cos \delta_{ji}) \tag{2.21}$$

Assume that reactive line flow changes of transformer line are related only to terminal voltage changes and transformer ratio change (or equivalently the reactive line flow changes caused by factors other than voltage and ratio changes are close to zero), then the linearized reactive power line flow equations for transformer can be derived from (2.20) and (2.21) and written as

$$\Delta Q_{ij} = \Delta Q_{ij}(\Delta V_i, \Delta V_j, \Delta t) = \frac{\partial Q_{ij}}{\partial t} \Delta t + \frac{\partial Q_{ij}}{\partial V_i} \Delta V_i + \frac{\partial Q_{ij}}{\partial V_j} \Delta V_j = 0 \tag{2.22}$$

$$\Delta Q_{ji} = \Delta Q_{ji}(\Delta V_j, \Delta V_i, \Delta t) = \frac{\partial Q_{ji}}{\partial t} \Delta t + \frac{\partial Q_{ji}}{\partial V_j} \Delta V_j + \frac{\partial Q_{ji}}{\partial V_i} \Delta V_i = 0 \tag{2.23}$$

where

$$\frac{\partial Q_{ij}}{\partial V_i} = -V_i (B_{ij} + B_{i0}) + \frac{Q_{ij}}{V_j}; \quad \frac{\partial Q_{ji}}{\partial V_j} = -V_j (B_{ji} + B_{j0}) + \frac{Q_{ji}}{V_i} \tag{2.24}$$

$$\frac{\partial Q_{ij}}{\partial V_j} = \frac{V_i^2}{V_j} (B_{ij} + B_{i0}) + \frac{Q_{ij}}{V_j}; \quad \frac{\partial Q_{ji}}{\partial V_i} = \frac{V_j^2}{V_i} (B_{ji} + B_{j0}) + \frac{Q_{ji}}{V_i} \tag{2.25}$$

$$\frac{\partial Q_{ij}}{\partial t} = \frac{V_i^2}{t^3} B_T - \frac{Q_{ij}}{t} = \frac{V_i^2}{t} (B_{ij} + B_{i0}) - \frac{Q_{ij}}{t} \tag{2.26}$$

$$\frac{\partial Q_{ji}}{\partial t} = -\frac{V_j^2}{t} B_T - \frac{Q_{ji}}{t} = -\frac{V_j^2}{t} (B_{ji} + B_{j0}) - \frac{Q_{ji}}{t} \tag{2.27}$$

Note that in (2.24) – (2.27) only transformer line parameters, transformer ratio, and measurements of reactive power line flows and bus voltage magnitudes are needed to calculate these derivatives. In fact, (2.24) and (2.25) are exactly same as the equations (2.8) and (2.9) in transmission line reactive power flow model. If we define virtual reactive power injection changes caused by transformer ratio change at two terminal buses of the transformer line as $\Delta Q_{Ti} = -\frac{\partial Q_{ij}}{\partial t}\Delta t$ and $\Delta Q_{Tj} = -\frac{\partial Q_{ji}}{\partial t}\Delta t$, then equations (2.22) and (2.23) become

$$\Delta Q_{Ti} = -\frac{\partial Q_{ij}}{\partial t}\Delta t = \frac{\partial Q_{ij}}{\partial V_i}\Delta V_i + \frac{\partial Q_{ij}}{\partial V_j}\Delta V_j \tag{2.28}$$

$$\Delta Q_{Tj} = -\frac{\partial Q_{ji}}{\partial t}\Delta t = \frac{\partial Q_{ji}}{\partial V_j}\Delta V_j + \frac{\partial Q_{ji}}{\partial V_i}\Delta V_i \tag{2.29}$$

Comparing equations (2.28) and (2.29) with equation (2.4), it is obvious that they are almost same, thus the effects of transformer tap changing can be approximated in a way similar to the one used for capacitor/reactor switching. For a transformer tap change, the corresponding transformer ratio change is a fixed value, thus transformer tap changing action is in effect equivalent to two constant reactive power injection changes at both ends of the transformer line. With this consideration, the voltage changes on the buses inside the local control area around the LTC transformer can be estimated using equations (2.13) – (2.16) with the only difference in vector of injection changes

$$\Delta Q = \left[0,\ldots,\Delta Q_{Ti},\ldots,\Delta Q_{Tj},\ldots,0\right] = \left[0,\ldots,-\frac{\partial Q_{ij}}{\partial t}\Delta t,\ldots,-\frac{\partial Q_{ji}}{\partial t}\Delta t,\ldots,0\right] \tag{2.30}$$

2.1.3 Estimation of Generator Voltage Adjusting Effects

For generators, the terminal voltage setpoint adjusting values ΔQ_{Gi}, instead of reactive power injection changes ΔV_{Gi}, on the control generator buses are known. To estimate the effects of generator voltage setpoint adjusting in a way similar to that of capacitor/reactor switching, the generator bus is temporarily treated as PQ bus with variable shunt capacity. With an initial guess of reactive power injection change $\Delta V_{Gi}{}^{0}$, the voltage changes on the buses within local area (including control generator bus i) can be estimated by (2.13) – (2.16), and the generator reactor power output change can be updated with following equation until the difference becomes less than certain tolerance.

$$\Delta Q_{Gi}^{m+1} = \frac{2\Delta V_{Gi}}{\Delta V_{Gi}^{m} + \Delta V_{Gi}} \Delta Q_{Gi}^{m} \tag{2.30}$$

In summary, a local voltage estimator (LVE) has been formulated to approximate the effects of the shunt switching, LTC transformer tap changing and generator voltage setpoint adjusting in a unified way. By treating these control actions as some reactive power injection changes inside their local control areas, the local voltage estimator is able to predict the bus voltage changes using linearized computations based only on the local measurements from SCADA before control actions.

2.2 Feasibility Studies of the Local Voltage Estimator

In this section, the local voltage estimator formulated in the last section will be evaluated with numerical examples. The standard IEEE 30-bus system and an actual WECC 2001-2003 Winter (case ID 213SNK) planning case will be used to test the accuracy and feasibility of the local voltage estimator formulation. The simulations of local voltage estimator and power flow on IEEE 30 bus system are all done with

MATLAB programs, while the simulations of local voltage estimator and power flow on WECC system are done with C/C++ program and BPA Power Flow package [39].

2.2.1 Tests on IEEE 30 Bus System

The standard IEEE 30-bus system is a widely used test case for power system researchers. The system data is available at the website of power research group of University of Washington [34], the system one-line diagram is shown in Figure A.1 of Appendix A. The local control areas are chosen such that the buses within 3 tiers of the control bus are included. Before the tests on the local voltage estimator, let us choose a proper parameter α for this system to approximate the voltage changes on outside buses. The results are shown as in the following table

α	Bus 10 (19 Mvar)			Bus 24 (4.3 Mvar)		
	Max error		Total error	Max error		Total error
0.75	25	0.0039	0.0244	20	-0.0018	0.0044
0.85	12	0.0031	0.0167	24	-0.0015	0.0028
0.95	19	-0.0053	0.0270	24	-0.0019	0.0032

Table 2.1 Selection of estimation parameters for IEEE 30 bus system.

It is obvious from the above table that $\alpha = 0.85$ is the best for this system in terms of both maximum error and total error and will be applied in the following tests. The IEEE 30 bus test case is slightly modified to facilitate the test. All capacitors are switched out and all voltage setpoints of generators are set to 0.01 lower than their original values. The tests include switching in each of the shunt capacitors, changing ratios of each transformer, and adjusting voltage setpoints of all generators. Table 2.2, Table 2.3 and Table 2.4 show the simulation results.

Control Cap.	Action	First tier buses and Max error bus						Total err
		Tier	Bus	V_0	V_{PF}	V_{LVE}	V_{ERR}	
10	19 Mvar In	1	6	1.0080	1.0102	1.0103	-0.0001	0.0152
		1	9	1.0397	1.0509	1.0513	-0.0004	
		1	10	1.0233	1.0451	1.0460	-0.0009	
		1	17	1.0206	1.0399	1.0400	-0.0002	
		1	20	1.0116	1.0297	1.0319	-0.0021	
		1	21	1.0118	1.0327	1.0334	-0.0007	
		1	22	1.0127	1.0332	1.0339	-0.0006	
		3	18	1.0138	1.0281	1.0317	-0.0035	
24	3.4 Mvar In	1	22	1.0283	1.0332	1.0329	0.0003	0.0037
		1	23	1.0214	1.0272	1.0275	-0.0003	
		1	24	1.0124	1.0216	1.0227	-0.0012	
		1	25	1.0110	1.0173	1.0176	-0.0003	
		3	20	1.0263	1.0297	1.0283	0.0014	

Table 2.2 Estimation results for capacitor switching on IEEE 30 bus system.

Control LTC	Action	First tier buses and Max error bus						Total err
		Tier	Bus	V_0	V_{PF}	V_{LVE}	V_{ERR}	
6-9	0.978 to 0.988	1	4	1.0119	1.0117	1.0116	0.0001	0.0025
		1	6	1.0107	1.0102	1.0102	0.0000	
		1	7	1.0026	1.0024	1.0023	0.0000	
		1	9	1.0472	1.0509	1.0506	0.0003	
		1	10	1.0428	1.0451	1.0449	0.0002	
		1	28	1.0071	1.0068	1.0067	0.0001	
		3	15	1.0367	1.0377	1.0369	0.0008	
4-12	0.932 to 0.942	1	3	1.0217	1.0207	1.0208	-0.0001	0.0034
		1	4	1.0129	1.0117	1.0118	-0.0001	
		1	6	1.0106	1.0102	1.0102	0.0000	
		1	12	1.0541	1.0571	1.0565	0.0006	
		3	20	1.0283	1.0297	1.0285	0.0012	

Table 2.3 Estimation results for LTC tap changing on IEEE 30 bus system.

Control Gen.	Action	First tier buses and Max error bus						Total err
		Tier	Bus	V_0	V_{PF}	V_{LVE}	V_{ERR}	
2	1.0330 To 1.0430	1	2	1.0330	1.0430	1. 0430	0.0000	0.0025
		1	4	1.0089	1.0117	1.0114	0.0003	
		1	6	1.0083	1.0102	1.0100	0.0003	
		3	20	1.0284	1.0297	1.0290	0.0007	
5	1.0000 to 1.0100	1	5	1. 0000	1. 0100	1. 0100	0.0000	0.0003
		1	7	0.9976	1.0024	1.0023	0.0001	
		3	12	1.0567	1.0571	1.0569	0.0002	
8	1.0000 to 1.0100	1	6	1.0047	1.0102	1.0101	0.0001	0.0023
		1	8	1. 0000	1. 0100	1. 0100	0.0000	
		1	28	1.0003	1.0068	1.0066	0.0002	
		3	20	1.0266	1.0297	1.0283	0.0014	
11	1.0720 to 1.0820	1	9	1.0468	1.0509	1.0509	0.0000	0.0000
		1	11	1. 072	1. 0820	1. 0820	0.0000	
		3	20	1.0274	1.0297	1.0294	0.0003	
13	1.0610 to 1.0710	1	12	1.0515	1.0571	1.0572	-0.0001	0.0006
		1	13	1. 061	1. 0710	1. 0710	-0.0000	
		3	17	1.0369	1.0399	1.0403	-0.0004	

Table 2.4 Estimation results for generator voltage adjusting on IEEE 30 bus system.

In above tables, V_0 are the voltages before any control actions, V_{PF} are the voltages after control actions obtained from power flow, V_{LVE} are the estimated voltages after control actions given by local voltage estimator, and V_{ERR} are normalized estimation errors. The total error shown is the summation of the absolute estimation errors on the local buses excluding the boundary buses (tier 3 buses).

From above tables, it can be seen that the estimation errors for most local buses are quite small, especially for those buses in the first tier. The maximum errors usually occur on the boundary buses (tier 3 buses), which may caused by our approximation using a constant α for all boundary buses. The errors could be further reduced by using different parameters for each boundary buses. Also it is observed that the total error increases as the switching capacity increases in table 2.2, which is reasonable due to the linearization model. The results could be improved by extending the computations to say four or five tier local subsystems instead of the three tier networks used in the study above.

2.2.2 Tests on WECC System

The simulations are based on WECC 2001-2003 Winter (case ID 213SNK) planning case which has more than 6000 buses in the system. For the part of the system of our interest, west Oregon area of WECC northwest system has dozens of 230KV, 115 KV and 69 KV capacitor banks, a couple of 500 KV reactor banks, a few 500/230-kV and 230/115-kV LTC autotransformers. Part of the one-line diagram for the west Oregon area of WECC northwest system is shown in Figure 2.3. For test purpose, the local control areas are constructed such that the buses within 6 tiers of the control bus are included. To facilitate the test, a base case is setup by modifying the original planning case slightly. All capacitors are switched out and reactors are switched in, the voltage setpoints of generators are also adjusted a little bit different from their original values.

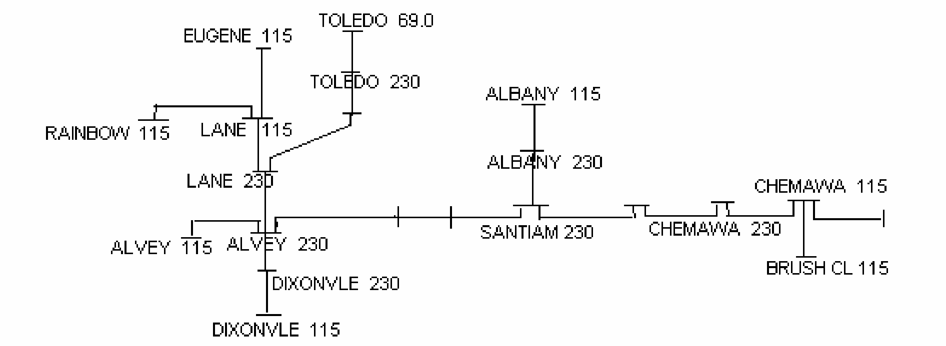

Figure 2.3 Part of the one-line diagram for the west Oregon area of WECC.

First the local voltage estimator is applied to capacitor/reactor switching and part of the tests results on the base case and several modified cases under different topology and loading conditions are shown in Table 2.5, Table 2.6 and Table 2.7.

Base Case [213snk0b]: All capacitors are OFF, all reactors are ON.							
Tier	Bus Name	V_0	V_{PF}	$\alpha = 0.85$		$\alpha = 0.98$	
				V_{LVE}	*Err%*	V_{LVE}	*Err%*
ALVEY 230 capacitor [58.9 Mvar] switching IN.							
1	ALVEY 230	1.0200	1.0250	1.0245	0.0452	1.0251	-0.0125
2	ALVEY 115	1.0250	1.0290	1.0283	0.0715	1.0289	0.0139
2	ALVEY 500	1.0750	1.0780	1.0773	0.0666	1.0779	0.0079
2	E SPRING 230	1.0210	1.0260	1.0251	0.0895	1.0257	0.0337
2	LANE 230	1.0220	1.0260	1.0249	0.1102	1.0254	0.0564
2	MARTINTP 230	1.0200	1.0250	1.0236	0.1364	1.0242	0.0811
2	MCKEN TP 230	1.0130	1.0170	1.0166	0.0403	1.0172	-0.0224
2	SPENCER 230	1.0200	1.0250	1.0245	0.0536	1.0250	-0.0045
MARION 500 reactor [-149.0 Mvar] switching OUT.							
1	MARION 500	1.0750	1.0820	1.0805	0.1397	1.0810	0.0907
2	ALVEY 500	1.0750	1.0800	1.0788	0.1145	1.0796	0.0416
2	ASHE 500	1.0860	1.0870	1.0860	0.0000	1.0860	0.0000
2	BUCKLEY 500	1.0910	1.0930	1.0924	0.0525	1.0927	0.0273
2	JOHNDAY 500	1.0900	1.0900	1.0900	0.0000	1.0900	0.0000
2	LANE 500	1.0730	1.0790	1.0770	0.1894	1.0778	0.1117
2	PEARL 500	1.0770	1.0800	1.0787	0.1171	1.0790	0.0914
2	SANTIAM 500	1.0740	1.0810	1.0794	0.1505	1.0799	0.1008

Table 2.5 Estimation results for capacitor switching on WECC Base Case.

Case #1 [213snk0b1]: Line JOHN DAY 500 – MARION 500 out of service, Load change on ALVEY 115 [P_L = 300 MW, Q_L = 100 MW], DIXONVLE 115 [P_L = 259 MW, Q_L = 107 MW].							
Tier	Bus Name	V_0	V_{PF}	$\alpha = 0.85$		$\alpha = 0.98$	
				V_{LVE}	*Err%*	V_{LVE}	*Err%*
ALBANY 115 capacitor [50.0 Mvar] switching IN.							
1	ALBANY 115	0.9920	1.0080	1.0028	0.4914	1.0042	0.3790
2	ADAIR 115	0.9910	1.0060	0.9995	0.6237	1.0010	0.5036

2	ALBANY 230	0.9780	0.9890	0.9854	0.3375	0.9867	0.2306
2	BURNTWD 115	0.9910	1.0070	1.0018	0.4909	1.0033	0.3783
2	CONSER 115	0.9940	1.0080	1.0026	0.5128	1.0041	0.3933
2	HARRISBG 115	0.9840	0.9940	0.9893	0.3076	0.9925	0.1551
2	HAZELWOD 115	0.9910	1.0080	1.0017	0.6017	1.0032	0.4891
2	LOCKNER 115	0.9940	1.0100	1.0039	0.5821	1.0052	0.4792
MARION 500 reactor [-248.0 Mvar] switching OUT.							
1	MARION 500	1.0600	1.0740	1.0706	0.3207	1.0718	0.2114
2	ALVEY 500	1.0600	1.0710	1.0672	0.3547	1.0688	0.2039
2	ASHE 500	1.0830	1.0840	1.0830	0.0000	1.0830	0.0000
2	BUCKLEY 500	1.0840	1.0870	1.0867	0.0250	1.0873	-0.0266
2	LANE 500	1.0540	1.0670	1.0616	0.5086	1.0634	0.3457
2	PEARL 500	1.0710	1.0770	1.0744	0.2460	1.0749	0.1915
2	SANTIAM 500	1.0590	1.0730	1.0694	0.3417	1.0705	0.2315

Table 2.6 Estimation results for capacitor switching on WECC Case #1.

Case #2 [213snk0b2]: Base on Case #1, Load change on ALVEY 115 [P_L = 600 MW, Q_L = 200 MW].							
Tier	Bus Name	V_0	V_{PF}	$\alpha = 0.85$		$\alpha = 0.98$	
				V_{LVE}	*Err%*	V_{LVE}	*Err%*
TOLEDO 69.0 capacitor [15.4 Mvar] switching IN.							
1	TOLEDO 69.0	0.9430	0.9560	0.9563	-0.0359	0.9566	-0.0644
2	TOLEDO 230	0.9550	0.9660	0.9645	0.1568	0.9648	0.1289
3	WENDSON 230	0.9860	0.9900	0.9887	0.1338	0.9889	0.1106
3	WREN 230	0.9700	0.9770	0.9762	0.0823	0.9765	0.0532
4	LANE 230	0.9800	0.9820	0.9805	0.1507	0.9809	0.1112
4	TAHKNICH 230	0.9990	1.0040	1.0005	0.3509	1.0006	0.3381
4	WENDSON 115	0.9900	0.9940	0.9919	0.2087	0.9922	0.1839
4	SANTIAM 230	0.9980	0.9990	0.9987	0.0282	0.9990	-0.0027
DIXONVLE 500 reactor [-149.0 Mvar] switching OUT.							
1	DIXONVLE 500	1.0520	1.0690	1.0642	0.4578	1.0653	0.3481
2	ALVEY 500	1.0450	1.0570	1.0524	0.4354	1.0536	0.3225
2	DIXONVLE 230	0.9910	1.0030	0.9986	0.4478	0.9997	0.3296
2	MERIDINP 500	1.0730	1.0850	1.0814	0.3392	1.0824	0.2398

Table 2.7 Estimation results for capacitor switching on WECC Case #2.

Next, we apply the local voltage estimator with modification for LTC transformer to west Oregon area of WECC northwest system. The simulations are done on base case and several modified cases, part of the results are given below in Table 2.8, Table 2.9, Table 2.10 and Table 2.11.

Base Case [213snk0b]: All capacitors are OFF, all reactors are ON.							
Tier	Bus Name	V_0	V_{PF}	$\alpha = 0.85$		$\alpha = 0.98$	
				V_{LVE}	$Err\%$	V_{LVE}	$Err\%$
ALVEY 230 →|− ALVEY 115 (3) LTC tap DOWN from 4/9 to 3/9.							
1	ALVEY 230	1.0200	1.0190	1.0189	0.0098	1.0189	0.0107
2	ALVEY 115	1.0250	1.0280	1.0278	0.0157	1.0279	0.0110
2	ALVEY 500	1.0750	1.0750	1.0745	0.0477	1.0744	0.0536
2	E SPRING 230	1.0210	1.0210	1.0200	0.0961	1.0200	0.0975
2	LANE 230	1.0220	1.0230	1.0219	0.1076	1.0219	0.1056
2	MARTINTP 230	1.0200	1.0200	1.0191	0.0856	1.0191	0.0883
2	MCKEN TP 230	1.0130	1.0130	1.0126	0.0350	1.0126	0.0346
2	SPENCER 230	1.0200	1.0190	1.0189	0.0077	1.0189	0.0089

Table 2.8 Estimation results for transformer tap changing on WECC Base Case.

Case #1 [213snk0b1]: Line JOHN DAY 500 – MARION 500 out of service, Load change on ALVEY 115 [P_L = 300 MW, Q_L = 100 MW], DIXONVLE 115 [P_L = 259 MW, Q_L = 107 MW].							
Tier	Bus Name	V_0	V_{PF}	$\alpha = 0.85$		$\alpha = 0.98$	
				V_{LVE}	$Err\%$	V_{LVE}	$Err\%$
DIXONVLE 230 →|− DIXONVLE 115 (1) LTC tap DOWN from 11/17 to 10/17.							
1	DIXONVLE 230	1.0010	1.0000	1.0003	-0.0319	1.0003	-0.0270
2	DIXONVLE 115	1.0100	1.0150	1.0145	0.0525	1.0144	0.0565
2	DIXONVLE 500	1.0640	1.0640	1.0637	0.0237	1.0637	0.0284
2	HANNA 230	1.0130	1.0130	1.0125	0.0499	1.0124	0.0559
2	RESTON 230	1.0030	1.0020	1.0025	-0.0501	1.0025	-0.0452
2	SPENCER 230	0.9990	0.9990	0.9989	0.0135	0.9988	0.0192

Table 2.9 Estimation results for transformer tap changing on WECC Case #1.

Case #2 [213snk0b2]: Base on Case #1, Load change on ALVEY 115 [P_L = 600 MW, Q_L = 200 MW].							
Tier	Bus Name	V_0	V_{PF}	$\alpha = 0.85$		$\alpha = 0.98$	
				V_{LVE}	*Err%*	V_{LVE}	*Err%*
ALVEY 230 →|− ALVEY 115 (4) LTC tap DOWN from 4/9 to 3/9.							
1	ALVEY 230	0.9760	0.9750	0.9749	0.0098	0.9749	0.0117
2	ALVEY 115	0.9580	0.9620	0.9606	0.1432	0.9607	0.1394
2	ALVEY 500	1.0450	1.0450	1.0445	0.0503	1.0444	0.0570
2	E SPRING 230	0.9790	0.9790	0.9780	0.1002	0.9780	0.1026
2	LANE 230	0.9800	0.9810	0.9799	0.1160	0.9799	0.1149
2	MARTINTP 230	0.9820	0.9810	0.9811	0.0132	0.9811	-0.0097
2	MCKEN TP 230	0.9670	0.9680	0.9666	0.1427	0.9666	0.1434
2	SPENCER 230	0.9760	0.9760	0.9749	0.1102	0.9749	0.1123
ALVEY 500 →|− ALVEY 230 (5) LTC tap DOWN from 9/9 to 8/9.							
1	ALVEY 500	1.0450	1.0430	1.0415	0.1441	1.0417	0.1196
2	ALVEY 230	0.9760	0.9810	0.9793	0.1709	0.9799	0.1144
2	DIXONVLE 500	1.0520	1.0500	1.0494	0.0539	1.0496	0.0388
2	MARION 500	1.0480	1.0480	1.0469	0.1088	1.0470	0.0912

Table 2.10 Estimation results for transformer tap changing on WECC Case #2.

Case #3 [213snk0b3]: Base on Case #1, Load change on ALVEY 115 [P_L = 900 MW, Q_L = 300 MW].							
Tier	Bus Name	V_0	V_{PF}	$\alpha = 0.85$		$\alpha = 0.98$	
				V_{LVE}	*Err%*	V_{LVE}	*Err%*
DIXONVLE 230 →|− DIXONVLE 115 (2) LTC tap DOWN from 11/17 to 10/17.							
1	DIXONVLE 230	0.9760	0.9760	0.9753	0.0722	0.9752	0.0774
2	DIXONVLE 115	0.9900	0.9940	0.9947	-0.0745	0.9947	-0.0702
2	DIXONVLE 500	1.0360	1.0350	1.0357	-0.0714	1.0357	-0.0665
2	HANNA 230	0.9970	0.9970	0.9965	0.0524	0.9964	0.0586
2	RESTON 230	0.9810	0.9800	0.9805	-0.0496	0.9804	-0.0445
2	SPENCER 230	0.9470	0.9470	0.9469	0.0147	0.9468	0.0209
ALVEY 500 →|− ALVEY 230 (5) LTC tap DOWN from 9/9 to 8/9.							
1	ALVEY 500	1.0260	1.0250	1.0224	0.2539	1.0226	0.2303
2	ALVEY 230	0.9460	0.9520	0.9493	0.2875	0.9498	0.2311
2	DIXONVLE 500	1.0360	1.0350	1.0334	0.1586	1.0335	0.1446
2	MARION 500	1.0360	1.0360	1.0348	0.1144	1.0350	0.0975

Table 2.11 Estimation results for transformer tap changing on WECC Case #3.

Finally the modified local estimator for generators is applied to west Oregon area of WECC northwest system and part of the tests results on the base case and several modified cases are shown in Table 2.12, Table 2.13, Table 2.14 and Table 2.15.

Base Case [213snk0c]: All capacitors are OFF, all reactors are ON.							
Tier	Bus Name	V_0	V_{PF}	$\alpha = 0.85$		$\alpha = 0.98$	
				V_{LVE}	*Err%*	V_{LVE}	*Err%*
BIG EDDY 230 generator voltage setpoint UP from 1.050 to 1.060.							
1	BIG EDDY 230	1.0500	1.0600	1.0600	0.0000	1.0600	0.0000
2	BIG EDDY 500	1.0720	1.0770	1.0775	-0.0473	1.0775	-0.0475
2	CELILO 230	1.0510	1.0610	1.0594	0.1549	1.0594	0.1548
2	CHEMAWA 230	0.9920	0.9950	0.9929	0.2118	0.9931	0.1910
2	CHENOWTH 230	1.0420	1.0510	1.0505	0.0439	1.0506	0.0381
2	MABTON 230	1.0450	1.0480	1.0482	-0.0166	1.0482	-0.0173
2	MAUPIN 230	1.0490	1.0570	1.0563	0.0631	1.0564	0.0542
2	MCLOUGLN 230	1.0380	1.0380	1.0389	-0.0861	1.0390	-0.0952
2	PARKDALE 230	1.0410	1.0480	1.0479	0.0128	1.0479	0.0128

Table 2.12 Estimation results for generator voltage adjusting on WECC Base Case.

Case #1 [213snk0c1]: Line JOHN DAY 500 – MARION 500 out of service.							
Tier	Bus Name	V_0	V_{PF}	$\alpha = 0.85$		$\alpha = 0.98$	
				V_{LVE}	*Err%*	V_{LVE}	*Err%*
JOHN DAY 500 generator voltage setpoint UP from 1.050 to 1.060.							
1	JOHN DAY 500	1.0500	1.0600	1.0600	0.0000	1.0600	0.0000
2	BIG EDDY 500	1.0720	1.0760	1.0720	0.3720	1.0720	0.3718
2	GRIZZLY 500	1.0770	1.0800	1.0776	0.2183	1.0778	0.2087
2	HANFORD 500	1.0810	1.0830	1.0810	0.1840	1.0810	0.1838
2	MARION 500	1.0620	1.0660	1.0637	0.2144	1.0638	0.2060
2	SLATT 500	1.0740	1.0790	1.0765	0.2298	1.0765	0.2287

Table 2.13 Estimation results for generator voltage adjusting on WECC Case #1.

Case #2 [213snk0c2]: Base on Case #1, Load change on ALVEY 115 [P_L = 300 MW, Q_L = 100 MW], DIXONVLE 115 [P_L = 259 MW, Q_L = 107 MW].							
Tier	Bus Name	V_0	V_{PF}	α = 0.85		α = 0.98	
				V_{LVE}	*Err%*	V_{LVE}	*Err%*
BIG EDDY 230 generator voltage setpoint UP from 1.050 to 1.060.							
1	BIG EDDY 230	1.0500	1.0600	1.0600	0.0000	1.0600	0.0000
2	BIG EDDY 500	1.0720	1.0780	1.0775	0.0461	1.0775	0.0459
2	CELILO 230	1.0510	1.0610	1.0594	0.1549	1.0594	0.1549
2	CHEMAWA 230	0.9830	0.9850	0.9839	0.1117	0.9841	0.0917
2	CHENOWTH 230	1.0420	1.0510	1.0505	0.0439	1.0506	0.0381
2	MABTON 230	1.0440	1.0470	1.0472	-0.0168	1.0472	-0.0175
2	MAUPIN 230	1.0490	1.0560	1.0563	-0.0313	1.0564	-0.0405
2	MCLOUGLN 230	1.0360	1.0370	1.0369	0.0098	1.0370	0.0012
2	PARKDALE 230	1.0410	1.0480	1.0479	0.0127	1.0479	0.0127

Table 2.14 Estimation results for generator voltage adjusting on WECC Case #2.

Case #3 [213snk0c3]: Base on Case #2, Load change on ALVEY 115 [P_L = 600 MW, Q_L = 200 MW].							
Tier	Bus Name	V_0	V_{PF}	α = 0.85		α = 0.98	
				V_{LVE}	*Err%*	V_{LVE}	*Err%*
JOHN DAY 500 generator voltage setpoint UP from 1.050 to 1.060.							
1	JOHN DAY 500	1.0500	1.0600	1.0600	0.0000	1.0600	0.0000
2	BIG EDDY 500	1.0720	1.0760	1.0720	0.3720	1.0720	0.3718
2	GRIZZLY 500	1.0800	1.0870	1.0806	0.5891	1.0807	0.5797
2	HANFORD 500	1.0790	1.0810	1.0790	0.1843	1.0790	0.1842
2	MARION 500	1.0470	1.0510	1.0487	0.2185	1.0488	0.2102
2	SLATT 500	1.0720	1.0780	1.0745	0.3237	1.0745	0.3226

Table 2.15 Estimation results for generator voltage adjusting on WECC Case #3.

In above tables, V_0 are the voltages before any control actions, V_{PF} are the voltages after each control actions obtained by running BPA power flow on the whole WECC system. The estimated voltages V_{LVE} after control actions given by local voltage estimator and normalized estimation errors $Err\% = \frac{|V_{LVE} - V_{PF}|}{V_{PF}} 100\%$ under $\alpha = 0.85$ and $\alpha = 0.98$ are also shown in the table.

From above tables, it can be seen that the estimated voltages in most buses of the system under different conditions are quite close to the voltages obtained by running power flow, and the results are better with $\alpha = 0.98$ than those with $\alpha = 0.85$. The estimation results for capacitor/reactor and generator voltage adjusting are generally better than those for transformer tap changing. Actually, because the voltage changes caused by the tap change are much smaller that those cause by switching capacitor/reactor banks, the absolute voltage changes on some buses with very small changes are different in direction from those obtained from running power flow. For the buses with large enough voltage changes, the estimation results are still quite close to power flow results.

It is also observed that in some cases, the estimated results are not very good. The reason seems to be that in the formulation of the B matrix used in estimation algorithm, the 'BX', 'BQ' and 'BC' type of buses are assumed to be PV buses, but this assumption does not always hold in BPA power flow program [39]. The 'BX' type bus voltages are controlled by switched capacitor/reactor banks and the voltages may not be constant because the devices are discrete. The 'BC' and 'BQ' type voltages are controlled by "BG' generators or other reactive resources such as static var compensators (SVC), if the reactive powers or generator voltages hit the limits, the 'BC' and 'BQ' type bus voltages may be far from their setpoint values. Also the 'BG' type buses change their voltage setpoint values automatically, which cause voltages of the surrounding buses change accordingly. Besides, there are some buses with regulating transformers (e.g. LANE 230, MCKEN TP 230, etc) change their voltage automatically in BPA power flow, although the solution option of the program is set to turning on DC line terminal transformer automatic control only.

2.3 Summary

A local voltage estimator has been formulated based on linearized reactive power flow model. For each device, a small local area is constructed and local voltage estimator is used to evaluate the switching effects. The local estimator treats switching of capacitor/reactor, adjusting LTC tap and generator voltage setting in a unified way, and is able to approximate voltage changes after a switching action based only on the local measurements from SCADA before switching. The accuracy and feasibility of the local voltage estimator formulation are proven by the simulation results on the standard IEEE 30-bus system and the actual WECC planning case.

Chapter 3

Alternate Heuristic Voltage Control

The discrete slow voltage controller proposed in [31] relies on the availability of state estimator model to make correct control decisions. In practice, state estimator model maybe unavailable or unreliable because of topology errors under certain conditions. With the local voltage estimator (LVE) formulated in last chapter, the effects of any control actions can be evaluated without state estimator model, thus make a model-free voltage control scheme possible under such conditions. In this chapter, an alternate on-line heuristic slow voltage controller is formulated to make control decisions based on SCADA measurements only. In section 3.1, a common slow voltage control framework integrated the model-based controller and the alternate controller is presented. The optimization problem of the alternate voltage control is formulated in Section 3.2. The feasibility tests results on small and large power systems are given in Section 3.3. Finally, Section 3.4 summarizes the conclusions of this chapter.

3.1 On-line Slow Voltage Control Framework

Since the goal of on-line slow voltage control is to automate actions of an alert and experienced operator, it is necessary to briefly review the current operation practice on western Oregon subsystem in Pacific Northwest before introducing the slow voltage controller framework. This part of system is a large load area without significant local generation. Power is imported from other parts of Pacific Northwest and western Canada. There are tens of small capacitor/reactor banks and LTC transformers available for voltage control purpose in this area. During normal operation, voltage problems are alleviated by reactive compensation performed by system operators based on their experience, current and predicted network conditions. Switching out in-service devices is preferable than switching in alternate devices such that the maximum number of devices are available for future exercises. Tap changing has lower priority than reactive power compensation switching and tap changing frequency is restricted to several tap changes per day because tap changer failure results in transformer outage. Circular VAR flows are monitored by routinely checking the VAR flows on specific transformer banks and transmission paths and are mitigated by switching of capacitor banks or transformer tap changer settings.

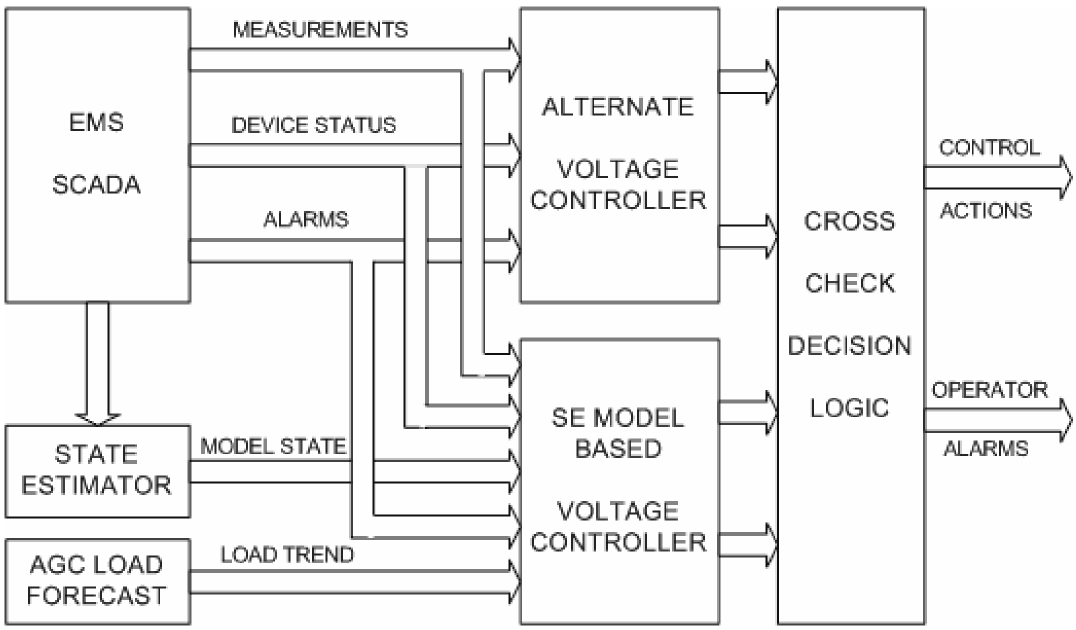

Figure 3.1 Common on-line slow voltage control framework.

The common slow voltage control framework integrated the state estimator model-based controller and the alternate heuristic controller is shown in Figure 3.1. The controller is intended to be used for “slow” control and has a time frame of tens of seconds or a few minutes. Similar to a system operator, the automatic controller primarily acts upon voltage alarms and checks SCADA measurements for the acceptability of the system voltage profile. As a first step, the controllers can be required to process only the voltage alarms. Other types of alarms relating to outages and contingencies can be handled directly by the system operators.

The common slow voltage controller consists of two sub-controllers that operate independently. Under normal conditions when state estimator program has valid results, the model-based controller will act as main controller and its control decisions will be cross-checked against the outputs of the alternate controller. If the control decisions made by the two controllers are different but similar, the decisions made by model-based controller will be adopted. If there are significant differences between the actions recommended by the two controllers, the system operator will be notified and responsible for making the final control decisions. When the state estimator model is unavailable or unreliable because of topology errors under certain conditions, the model-based controller will go into standby state, and the backup alternate controller will take over to make control decisions based on SCADA measurements only.

The model-based controller proposed in [31] calculates the incremental changes in bus voltages after switching control devices by carrying out an adaptive local power-flow starting from the system model output of the state estimation program. Then these incremental changes are assessed with respect to actual SCADA measurements to compute the expected voltage profile after the switching actions. In order to reduce the number of switchings during periods of rapid load growths and declines (for instance, during morning and evening pick-ups), load forecasting estimates for individual loads in the area are computed using existing distribution factor formulas and the system total load forecast available from the EPRI AGC load forecasting program. These forecasted loads are then used to form a set of possible future power flow cases in the robust formulation of the controller and each future power-flow case is associated with a confidence level that gradually increases after verifying its reliability during operation.

The model-based controller decides whether any control action is necessary by analyzing the SCADA measurement data and the expected voltage levels from future power-flow runs. If an action is required, a subset of candidate control devices which will have an impact on the problem is selected by using the concept of *electrical distance*. The controller as formulated minimizes the switching cost associated with these devices while keeping the voltage feasible in a robust sense by incorporating load forecast models, and while minimizing circular reactive flow through transformers. Specifically, the penalty for switching each device is a weighted average of the following terms: 1) switching penalty based on the switching history and the type of the device, 2) voltage violation penalty based on expected voltages after switching from state estimation power-flow model and future power-flow models, and 3) circular VAR flow penalty computed from the state estimation power-flow model and future power-flow models. Switching action on the device with the minimum penalty will be recommended by the controller.

The alternate controller, in contrast, calculates the incremental changes in bus voltages after switching control devices using local voltage estimator proposed in last chapter based purely on the available local measurements from SCADA. The expected voltages after the switching actions also can be computed directly by adding the incremental changes to the actual SCADA voltage measurements. The following flowchart shows the computation procedure of the alternate voltage controller.

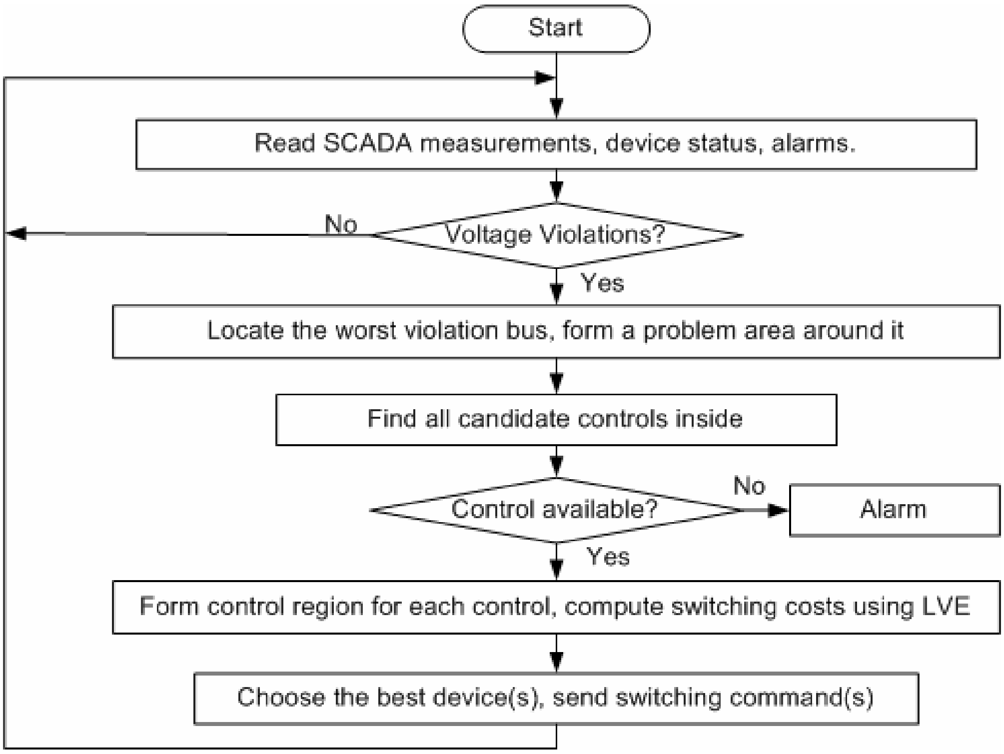

Figure 3.2 Alternate on-line slow voltage controller flowchart.

By checking the SCADA voltage measurements, the alternate controller first decides whether there is any voltage outside a specified band around some "optimal" voltage profile. If any voltage violation exists, the controller locates the bus with the worst violation, forms a problem area within several tiers of the bus, and tries to find a subset of candidate control devices that will have an impact on the problem inside the area. If there is no control device available, an alarm will be sent to the operator. Otherwise, a small local control area will be formed for each control device, and the switching costs will be calculated using the local voltage estimator (LVE) formulated in last chapter. The controller as formulated minimizes the switching cost associated with these devices while keeping the voltage as close as possible to the "optimal" profile. Specifically, the penalty for any control device is a weighted average of the switching penalty calculated based on the type and switching history of the device and the voltage violation penalty based on expected voltages after switching obtained from local voltage estimator. Switching action on the device with the minimum penalty is then recommended by the controller.

After issuing switching commands, the two sub-controllers will compare the voltages after the switching with their expected voltages from the state estimation based computations or local voltage estimator computations. Significant mismatches between expected and actual voltage levels will be reported to the operator via alarms.

The main features of the common voltage controller are

1) Efficient automation of switching slow voltage control devices no matter state estimator model is available or not.
2) Cross checking of the decisions made by two controllers to ensure correct control device switching.
3) Loss minimization in the sense that voltage profile is maintained as close as possible to the "optimal" profile.
4) Reactive reserve maximization in the sense that fewer reactive compensation devices are switched in.
5) Operating cost minimization in a deregulated market.

3.2 Formulation of the Alternate Heuristic Control

Assuming that the desired "optimal" voltage profile V_{dsr}, maximum voltage $V_{\max}$, and minimum voltage $V_{\min}$ at each bus for different time periods of the day are pre-determined through off-line studies, the proposed alternate heuristic control scheme is designed to find the "best" control actions to keep all bus voltage within the pre-specified limits while respecting some practical rules. This actually involves finding the available candidate control devices inside the problem area and choosing effective control devices by solving optimization problem.

Problem Type	LTC Transformer			Shunt		Generator
	$V_{Tap} > V_{load}$	$V_{Tap} < V_{load}$	$V_{Tap} = V_{load}$	Capacitor	Reactor	
V_{load} High	Tap Up	Tap Down	None	Out	In	V_{gen} Down
V_{load} Low	Tap Down	Tap Up	None	In	Out	V_{gen} Up

Table 3.1 Rules to choose candidate device and its control action.

Some heuristic rules are used in searching for the candidate control devices. First, a breadth-first search (BFS) algorithm [40] is employed to find all control devices within several tiers around the problem center bus (i.e. the bus with worst violation), then some rules are applied to determine the availability of a control device. For low-limit violating voltage problem, only the in-service reactor banks and out-of-service capacitor banks are chosen as shunt type candidate control devices, generators that do not reach their high reactive power or voltage limits are chosen as generation type control devices. For a transformer, if the tap-side nominal voltage is higher than the worst-violating bus nominal voltage, then the transformer is selected only if its tap position does not reach its low limits. If the tap-side nominal voltage is lower than the worst-violating bus nominal voltage, then the transformer is selected only if its tap position does not reach its high limit. Similar rules are also applied to low-limit violating voltage problem. By using these selection rules, the number of available candidate control devices can be reduced so as to speed up the computation. These rules are also used to determine proper direction of a control action as shown in Table 3.1.

To choose "best" or most effective control actions by optimization, a cost needs to be set for each control action, including capacitor/reactor bank switching, LTC transformer tap changing and generator-controlled bus reference voltage adjusting, such that it reflects the practical rules and preference used by system operators. In general, it is preferable to switching out a device in service than switching in another so that maximum numbers of control devices are available for control purposes at any time. Accordingly, a higher cost is set for switching in a device as compared to switching out the same device. Tap change should be avoided whenever the voltages can be maintained by switching of capacitor/reactor banks alone, because the maintenance costs for transformer banks are higher than those for capacitor banks and tap changer failure results in transformer outage. If in some case tap changes have to be implemented, only one tap change is allowed each time, which is consistent with the BPA operating policy. The switching costs for transformer banks are thus set significantly higher than those for capacitor/reactor banks in the formulation. The generator-controlled bus reference voltage adjusting also has lower priority than capacitor/reactor bank switching. However, depending on being within or outside the system, it may have higher or lower priority than LTC tap changing. For all devices, switching cost increases substantially after one switching and the cost then decreases slowly. This is used to prevent repeated switching in and out of the same shunt device or adjusting tap of the same LTC transformer.

With the cost well defined above, now the problem of choosing “best” control actions can be formulated as an integer programming optimization problem as follows

$$
\begin{aligned}
&\min : \sum_{i=1}^{N_D} |k_i| C_i(k_i) \\
&s.t.: V_{j\min} < V_j^0 + \sum_{i=1}^{N_D} \Delta V_{i,j} < V_{j\max}\ ; \quad j = 1,\ldots, N \\
&\quad \sum_{i=1}^{N_D} |k_i| \le N_{sw}\ ; \qquad k_i \in \{-1,0,1\}
\end{aligned}
\tag{3.1}
$$

In the above formulation, k_i represents the switching type: -1 for switching out capacitor/reactor, one tap decrease of LTC or one step decrease of generator voltage setting, 0 for no control action and +1 for switching in capacitor/reactor, one tap increase of LTC or one step increase of generator voltage setting. $C_i(k_i)$ denotes the cost of the *ith* control device under control action type k_i. V_j^0 is the bus voltage before control actions, $\Delta V_{i,j}$ is the voltage change on j_{th} bus caused control action of *ith* device, which can be calculated using the local voltage estimator equation (2.16). N, N_D and N_{sw} are the number of buses inside the local area, the number of feasible control devices, and the maximum number of control actions, respectively.

The objective of optimization as formulated is to find the minimum control cost while keeping all the voltages within limits. However, it may turn out that for some power flow scenario, no feasible solution exists. In this case, a penalty function can be defined to indicate how far the solution is away from the feasibility region, as shown in Figure 3.3. If the voltage at a bus is within limits, the penalty is zero. If it is too high or too low (higher than $V_{\max}$ or lower than $V_{\min}$) then a very large value P_0 is set to the penalty term. Between $(V_{high}, V_{\max})$ or $(V_{\min}, V_{low})$, the penalty function is linear. For any control actions, the estimated bus voltages are checked against their limits. If any violation exists, penalty functions are calculated for all the voltage violating buses. The penalty cost is defined as the norm of the voltage-violating vector. Either the summation of all the absolute value of the voltage violation (i.e. $F_1 \; |\cdot|_1 \; norm$) or the maximum absolute voltage violation (i.e. $F_\infty (|\cdot|_\infty) \; norm$) can be used for this purpose. Here $F_1 \; |\cdot|_1 \; norm$ is used to define the penalty cost.

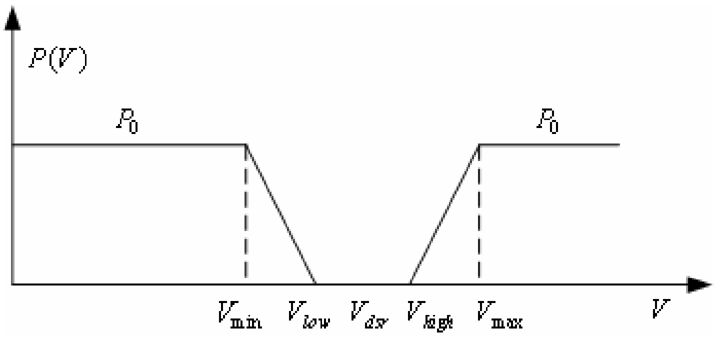

Figure 3.3 Penalty function of voltage violation

Now the optimization problem (3.1) can be transformed as follows

$$\begin{aligned} &\min : \sum_{i=1}^{N_D} |k_i| \left[C_i(k_i) + \lambda \sum_{j=1}^{N} P_i(\Delta V_{i,j}) \right] \\ &s.t.: \sum_{i=1}^{N_D} |k_i| \le N_{sw}; \qquad k_i \in \{-1,0,1\} \end{aligned} \tag{3.2}$$

Here $P_i(\Delta V_{i,j})$ denotes the voltage penalty value of *jth* bus under *ith* control action. λ represents the weighting factor of voltage violation penalty cost. As noted earlier, the cost $C_i(k_i)$ for tap changing action is significantly higher than that for capacitor or reactor bank switching action. Moreover, the cost associated with switching in a device (with $k_i = 1$) is set higher than the cost for switching out a device (with $k_i = -1$).

The optimization problem can also be formulated as minimizing active power loss or maximizing reactive reserves. The formulation in (3.2) is equivalent to minimizing the number of switching actions. In some sense, the formulation also maximizes the reactive resource reserves in the subsystem, since (3.2) keeps the minimum number of control devices in service, and therefore keeps the maximum number of control devices available for future control exercises.

Algorithms for integer programming problems typically go through a sequence of steps, with a set of choices at each step. However, using dynamic programming to determine the best choices is overkill for many optimization problems; simple, more efficient algorithms will do. A greedy algorithm always makes the choice that looks best at the moment. That is, it makes a locally optimal choice in the hope that this choice will lead to a globally optimal solution, but the greedy algorithm does not guarantee to yield globally optimal solutions.

In (3.2), N_{sw} defines the maximum number of control actions, which are permitted in any one of the iteration of the controller. For the formulation with $N_{sw} > 1$, the optimization problem needs to be solved using dynamic programming algorithm. However, N_{sw} is set to be 1 at present, since the operators usually hesitate to switch a large number of devices at one time, and $N_{sw} = 1$ is consistent with a conservative policy for an automatic controller. With the maximum number of switching $N_{sw} = 1$, the solution of optimization (3.2) becomes easy to handle. Basically, we evaluate voltage change after the control action of each candidate control device by a local voltage estimator described in Chapter 2 and select the one with minimum cost. This is equivalent to choose the locally optimal control action at each step, so it is a greedy algorithm. Although the final result is not necessarily the global optimum for this integer problem, it is good enough for the backup controller. More importantly, this one device at a time conservative control action make it easy for the operators to understand and to keep track of the decision taken by the automatic controller.

3.3 Testing of the Alternate Voltage Controller

In this section, feasibility tests of the alternate voltage controller formulated in section 3.2 will be performed on the standard IEEE 30-bus system and an actual WECC 2001-2003 Winter planning case (case ID 213SNK) with more than 6000 buses. The simulations of alternate controller and power flow on IEEE 30 bus system are done with MATLAB programs, while the simulations of alternate controller and power flow on WECC system are conducted with C/C++ program and BPA Power Flow package [39].

3.3.1 Tests on IEEE 30 Bus System

The system data for the standard IEEE 30-bus system is available at the website of power research group of University of Washington [34], and the system one-line diagram is shown in Figure A.1 of Appendix A. Table 3.2 lists all control devices in IEEE 30 bus system available for voltage control purpose and their initial settings.

Device Type	Bus / Transformer	Capacity / Range	Setting / Status
Capacitor	Bus 10	19.0	OFF
	Bus 24	4.3	OFF

LTC Transformer	Bus 6 →|– Bus 9	0.938 ~ 1.018	0.988
	Bus 6 →|– Bus 10	0.929 ~ 1.009	0.979
	Bus4 →|– Bus 12	0.892 ~ 0.972	0.942
	Bus 28 →|– Bus 27	0.928 ~ 1.008	0.978
Generator	Bus 1	-80.0 ~ 100.0 Mvar	1.050
	Bus 2	-40.0 ~ 50.0 Mvar	1.033
	Bus 5	-40.0 ~ 40.0 Mvar	1.000
	Bus 8	-100.0 ~ 40.0 Mvar	1.000
	Bus 11	-6.0 ~ 24.0 Mvar	1.072
	Bus 13	-6.0 ~ 24.0 Mvar	1.061

Table 3.2 Control devices available in IEEE 30 bus system.

In the following tests, the local control areas are chosen such that the buses within 3 tiers of the control bus are included. The step-sizes for LTC tap changing and generator voltage adjusting are set to be 0.01 p.u. The costs of different control device's actions are calculated according the following rules: the cost for switching out a capacitor or reactor bank is set to zero, the cost for switching in a capacitor or reactor bank is set to 10.0, the cost for LTC tap changing is set to 20.0, and cost for generator voltage adjusting is set to larger than 10.0, but may or may not larger than 20.0, depending the priority of the LTC and generator. For any type of device, the cost of next action will increase by 5.0, and decrease by 1.0 at each time step. The control objective is to maintain all bus voltages within 2% band around the normal voltage profile, and the maximum allowed voltage deviation is 5% away from the normal value. The voltage penalty coefficient λ is set to 1.0 and the maximum voltage penalty P_0 is set to 1.0 for test purpose.

Many scenarios with different load levels, load distributions and topology have been tested on the system. The results on one of the scenarios are shown in Table 3.3 and 3.4.

Tim Step	ΔV_{max} (Before Control)	Control Device (Bus)	Control Action	ΔV_{max} (After Control)
Stage 1: Line 16 – 17 out of service				
1	-0.0492 Bus 17	Bus 10 19 Mvar	In	-0.0279 Bus 24
2	-0.0279 Bus 24	Bus 24 4.3 Mvar	In	-0.0216 Bus 17
3	-0.0216 Bus 17	LTC Bus 28 →|– Bus 27	0.978→ 0.968	-0.0208 Bus 17
4	-0.0208 Bus 17	LTC Bus 6 →|– Bus 9	0.988→ 0.978	No Violation
Stage 2: Loads on Bus 16 and 17 increases by 50%.				
5	- 0.0271 Bus 17	LTC Bus 6 →|– Bus 10	0.979→ 0.969	- 0.0249 Bus 17
6	- 0.0249 Bus 17	LTC Bus 4 →|– Bus 12	0.942→ 0.932	- 0.0245 Bus 17
7	- 0.0245 Bus 17	LTC Bus 6 →|– Bus 9	0.978→ 0.968	- 0.0217 Bus 17
8	- 0.0217 Bus 17	LTC Bus 28 →|– Bus 27	0.968→ 0.958	- 0.0209 Bus 17
9	- 0.0209 Bus 17	LTC Bus 6 →|– Bus 10	0.969→ 0.959	No Violation
Stage 3: Line 16 – 17 in service, loads on Bus 16 and 17 back to normal.				
10	No Violation			

Table 3.3 Results of voltage control on IEEE 30 bus system (A).

Tim Step	ΔV_{max} (Before Control)	Control Device (Bus)	Control Action	ΔV_{max} (After Control)
Stage 1: Line 16 – 17 out of service				
1	-0.0492 Bus 17	Bus 10 19 Mvar	In	-0.0279 Bus 24
2	-0.0279 Bus 24	Bus 24 4.3 Mvar	In	-0.0216 Bus 17
3	-0.0216 Bus 17	Gen. Bus 11	1.072 →1.082	No Violation
Stage 2: Loads on Bus 16 and 17 increases by 50%.				
4	- 0.0274 Bus 17	Gen. Bus 13	1.061 →1.071	- 0.0258 Bus 17
5	- 0.0258 Bus 17	Gen. Bus 8	1.000 →1.010	- 0.0222 Bus 17
6	- 0.0222 Bus 17	LTC Bus 6 →|– Bus 9	0.988→ 0.978	No Violation
Stage 3: Line 16 – 17 in service, loads on Bus 16 and 17 back to normal.				
7	No Violation			

Table 3.4 Results of voltage control on IEEE 30 bus system (B).

From above tables, it can be seen that the alternate controller correctly locates the worst violation buses, identifies the most effective control devices with the lowest costs at each step, and finally brings voltage back to normal range. For this system, capacitors are switched in first; then LTC taps are changed or generator voltage setpoint are adjusted depending on their relative priority. The effects of the relative priority are shown clearly by the different control actions between Table 3.3 and Table 3.4 after step 3. In Table 3.4, the switching costs of LTC tap changing and generator voltage adjusting are set equal, thus the generators are chosen before LTCs as controls because the voltage penalties of generator actions are smaller than that of LTC. In contrast, the switching costs of generator voltage adjusting are set significantly higher than that of LTC tap changing in Table 3.3, thus the LTCs are chosen to act before generators at each step. It is also noted that the control steps taken in Table 3.4 are less than that in Table 3.3, since the adjusting generator voltage setpoints is more effective than changing transformer taps in terms of the bus voltage magnitude increments.

3.3.2 Tests on WECC System

The WECC 2001-2003 Winter (case ID 213SNK) planning case has more than 6000 buses in the system, specifically west Oregon area of WECC northwest system has dozens of 230KV, 115 KV and 69 KV capacitor banks, a couple of 500 KV reactor banks, a few 500/230-kV and 230/115-kV LTC autotransformers. For test purpose, only parts of these devices are selected as candidate devices for voltage control and a modified base case is setup to facilitate the tests. Table 3.5 lists these control devices and their initial settings. Note that the bus names listed as generator type controls are actually generator-controlled high-side voltage buses, the control generators are shown in table 3.6.

<table>
<tr><th>Device Type</th><th>Bus / Transformer</th><th>Capacity / Range</th><th>Setting / Status</th></tr>
<tr><td rowspan="11">Capacitor</td><td>ALBANY 115</td><td>50.0</td><td>OFF</td></tr>
<tr><td>ALVEY 115</td><td>19.5, 19.5, 25.6</td><td>OFF</td></tr>
<tr><td>ALVEY 230</td><td>58.9, 58.9, 58.9, 117.8</td><td>OFF</td></tr>
<tr><td>CHEMAWA 115</td><td>23.7</td><td>OFF</td></tr>
<tr><td>CHEMAWA 230</td><td>54.0</td><td>OFF</td></tr>
<tr><td>LANE 115</td><td>30.4</td><td>OFF</td></tr>
<tr><td>LANE 230</td><td>108.2</td><td>OFF</td></tr>
<tr><td>SANTIAM 230</td><td>147.0, 58.9</td><td>OFF</td></tr>
<tr><td>TILLAMOK 115</td><td>30.4, 22.8</td><td>OFF</td></tr>
<tr><td>TOLEDO 69.0</td><td>27.1, 15.4, 15.4</td><td>OFF</td></tr>
<tr><td>TOLEDO 230</td><td>30.0</td><td>OFF</td></tr>
<tr><td rowspan="2">Reactor</td><td>DIXONVLE 500</td><td>-149.0</td><td>ON</td></tr>
<tr><td>MARION 500</td><td>-248.0, -149.0</td><td>ON</td></tr>
<tr><td rowspan="5">LTC Transformer</td><td>ALVEY 230 →|– ALVEY 115 3</td><td>1/9 ~ 9/9</td><td>4/9</td></tr>
<tr><td>ALVEY 230 →|– ALVEY 115 4</td><td>1/9 ~ 9/9</td><td>4/9</td></tr>
<tr><td>ALVEY 500 →|– ALVEY 230 5</td><td>1/9 ~ 9/9</td><td>9/9</td></tr>
<tr><td>DIXONVLE 230 →|– DIXONVLE 115 1</td><td>1/17 ~ 17/17</td><td>11/17</td></tr>
<tr><td>DIXONVLE 230 →|– DIXONVLE 115 2</td><td>1/17 ~ 17/17</td><td>11/17</td></tr>
<tr><td rowspan="2">Generator</td><td>JOHN DAY 500</td><td>1.03 ~ 1.10</td><td>1.05</td></tr>
<tr><td>BIG EDDY 230</td><td>1.03 ~ 1.10</td><td>1.05</td></tr>
</table>

Table 3.5 Control devices available in west Oregon area.

<table>
<tr><th>Controlled Bus</th><th>Control Generator</th><th>V_{ref} range</th></tr>
<tr><td>JOHN DAY 500</td><td>JOHN DAY 13.8</td><td>1.03 ~ 1.10</td></tr>
<tr><td rowspan="3">BIG EDDY 230</td><td>DALLES 3 13.8</td><td rowspan="3">1.03 ~ 1.10</td></tr>
<tr><td>DALLES 21 13.8</td></tr>
<tr><td>DALLES 22 13.8</td></tr>
</table>

Table 3.6 Generator controlled buses.

In the following simulations, the local control areas are constructed such that the buses within 6 or 7 tiers of the control bus are included. The step-size for LTC tap changing is set to one tap at a time and the step-size for generator voltage adjusting is set to 0.02 p.u. The following rules are used to calculate the costs of different control actions: the cost for switching out a capacitor or reactor bank is zero, the cost for switching in a capacitor or reactor bank is 100.0, the cost for LTC tap changing is 200.0, and cost for generator voltage adjusting is set to 300.0, since it is assumed to be have lower priority than the other two types of actions. For any type of device, the cost of next action will increase by 10.0, and decrease by 1.0 at each time step. The control objective is to maintain all bus voltages within 2% band around the pre-defined voltage profile, and the maximum allowed voltage deviation is 5% away from the optimal value. The voltage penalty coefficient λ is set to 1.0 and the maximum voltage penalty P_0 is set to 7.5 for test purpose. Numerous tests have been conducted on the WECC planning cases under different topology and loading conditions, only parts of the results are shown here.

First the results of alternate voltage control with only capacitor/reactor banks available are shown in Table 3.7. The simulation scenario is that a line is out of service along with load increase, and then the line goes back to service with load back to normal. To investigate the feasibility of the local voltage estimator applied to voltage control, the control results using voltage sensitivities obtained from running power flow (PF) under current condition are also presented in Table 3.8.

Tim Step	ΔV_{max} (Before Control)	Control Device (Bus)	Control Action	ΔV_{max} (After Control)
Stage 1: Line Outage: JOHN DAY 500 – MARION 500 Load Increase: ALVEY 115 → [P_L = 300 MW, Q_L = 100 Mvar] DIXONVLE 115 → [PL = 259 MW, QL = 107 Mvar]				

1	-0.053 TOLEDO 69.0	MARION 500 -248 Mvar	OFF	-0.042 TOLEDO 69.0
2	-0.042 TOLEDO 69.0	MARION 500 -149 Mvar	OFF	-0.039 TOLEDO 69.0
3	-0.039 TOLEDO 69.0	ALVEY 230 118 Mvar	ON	-0.034 TOLEDO 69.0
4	-0.034 TOLEDO 69.0	LANE 230 108 Mvar	ON	-0.028 TOLEDO 69.0
5	-0.028 TOLEDO 69.0	TOLEDO 230 30 Mvar	ON	-0.026 DIXONVLE 115
6	-0.026 DIXONVLE 115	DIXONVLE 115 -149 Mvar	OFF	No Violation
Stage 2: Load Increase: ALVEY 115 → [P_L = 600 MW, Q_L = 200 Mvar]				
7	-0.040 GOSHN 115	ALVEY 230 58.9 Mvar	ON	-0.034 GOSHN 115
8	-0.034 GOSHN 115	ALVEY 230 58.9 Mvar	ON	-0.028 GOSHN 115
9	-0.028 GOSHN 115	ALVEY 230 58.9 Mvar	ON	-0.021 ALVEY 115
10	-0.021 ALVEY 115	ALVEY 115 25.6 Mvar	ON	No Violation
Stage 3: Line In-service: JOHN DAY 500 – MARION 500 Load Decrease: ALVEY 115 → [P_L = 4.4 MW, Q_L = 1.4 Mvar] DIXONVLE 115 → [PL = 130 MW, QL = 57.7 Mvar]				
11	+0.039 LANE 500	ALVEY 230 118 Mvar	OFF	+0.031 LANE 500
12	+0.031 LANE 500	LANE 230 108 Mvar	OFF	+0.023 DIXONVLE 500
13	+0.023 DIXONVLE 500	ALVEY 230 58.9 Mvar	OFF	No Violation

Table 3.7 Voltage control results with capacitor/reactor only (LVE).

Tim Step	ΔV_{max} (Before Control)	Control Device (Bus)	Control Action	ΔV_{max} (After Control)
Stage 1: Line Outage: JOHN DAY 500 – MARION 500 Load Increase: ALVEY 115 → [P_L = 300 MW, Q_L = 100 Mvar] DIXONVLE 115 → [PL = 259 MW, QL = 107 Mvar]				
1	-0.053 TOLEDO 69.0	MARION 500 -248 Mvar	OFF	-0.042 TOLEDO 69.0
2	-0.042 TOLEDO 69.0	MARION 500 -149 Mvar	OFF	-0.039 TOLEDO 69.0
3	-0.039 TOLEDO 69.0	ALVEY 230 118 Mvar	ON	-0.034 TOLEDO 69.0
4	-0.034 TOLEDO 69.0	DIXONVLE 115 -149 Mvar	OFF	-0.030 TOLEDO 69.0
5	-0.030 TOLEDO 69.0	SANTIAM 230 147 Mvar	ON	-0.022 TOLEDO 69.0
6	-0.022 TOLEDO 69.0	CHEMAWA 230 54 Mvar	ON	-0.021 TOLEDO 69.0
7	-0.021 TOLEDO 69.0	TOLEDO 230 30 Mvar	ON	No Violation
Stage 2: Load Increase: ALVEY 115 → [P_L = 600 MW, Q_L = 200 Mvar]				
8	-0.042 ALVEY 115	LANE 230 108 Mvar	ON	-0.032 LANE 500
9	-0.032 ALVEY 115	ALVEY 230 58.9 Mvar	ON	-0.027 VILLAGEG 115
10	-0.027 VILLAGEG 115	ALVEY 230 58.9 Mvar	ON	-0.021 GOSHN 115

11	-0.021 GOSHN 115	SANTIAM 230 58.9 Mvar	ON	-0.021 GOSHN 115
12	-0.021 GOSHN 115	ALVEY 230 58.9 Mvar	ON	No Violation
Stage 3: Line In-service: JOHN DAY 500 – MARION 500 Load Decrease: ALVEY 115 → [P_L = 4.4 MW, Q_L = 1.4 Mvar] DIXONVLE 115 → [PL = 130 MW, QL = 57.7 Mvar]				
13	+0.049 LANE 500	LANE 230 108 Mvar	OFF	+0.035 LANE 500
14	+0.035 LANE 500	ALVEY 230 118 Mvar	OFF	+0.028 LANE 500
15	+0.028 LANE 500	SANTIAM 230 147 Mvar	OFF	+0.025 DIXONVLE 500
16	+0.025 DIXONVLE 500	ALVEY 230 58.9 Mvar	OFF	+0.022 DIXONVLE 500
17	+0.022 DIXONVLE 500	SANTIAM 230 58.9 Mvar	OFF	No Violation

Table 3.8 Voltage control results with capacitor/reactor only (PF).

It can be seen from above tables that the alternate controller locates the worst violation buses, identifies the most effective control devices at each step, and brings bus voltages back to normal range. Since the switching out action has higher priority (or lower cost) than switching in action, the reactors are normally switched out before capacitors are switched in, such as in the first two step. However, if the voltage penalty cost for switching out reactor is larger than the difference between costs of switching-out and switching-in actions, capacitor may be switched out even a reactor is available. For example in step 3, capacitor at ALVEY 230 is switched in although reactor at DIXONVLE 115 is still in-service.

Note that in above two tables, the control actions taken are quite similar for same problematic bus. The different order of the control actions is due to the fact that the local control area constructed in Table 3.8 has one more tier than that of Table 3.7. This difference along with the coefficient of the voltage penalty may affect the control action orders made by the voltage control algorithm. For example, TOLEDO 69.0 is in the 7th tier of DIXONVLE 115, thus in Table 3.8 the reactor on DIXONVLE 115 is switched out at step 4 before capacitors on other control buses are switched in. However in Table 3.7, since TOLEDO 69.0 is not inside the 6-tier local area of DIXONVLE 115, the reactor on this bus is switched out later in step 6 when the worst bus has been changed to DIXONVLE 115. The total control steps made in Table 3.7 (using local voltage estimator) are actually less than that in Table 3.8 (using “real” voltage sensitivities), thus the local voltage estimator could be successfully used in alternate voltage control scheme.

Next, the LTC transformers will be included along with capacitor/reactor banks as available control devices, the results are shown in Table 3.9. The simulation scenario is same as before. For comparison of the model-based controller and the alternate controller, the control results from model-based control running localized power flow (LPF) are taken from Table 2.12 of [31] and listed in Table 3.10.

Tim Step	ΔV_{max} (Before Control)	Control Device (Bus)	Control Action	ΔV_{max} (After Control)
Stage 1: Line Outage: JOHN DAY 500 – MARION 500 Load Increase: ALVEY 115 → [P_L = 300 MW, Q_L = 100 Mvar] DIXONVLE 115 → [PL = 259 MW, QL = 107 Mvar]				
1	-0.053 TOLEDO 69.0	MARION 500 -248 Mvar	OFF	-0.042 TOLEDO 69.0
2	-0.042 TOLEDO 69.0	MARION 500 -149 Mvar	OFF	-0.039 TOLEDO 69.0
3	-0.039 TOLEDO 69.0	ALVEY 230 118 Mvar	ON	-0.034 TOLEDO 69.0
4	-0.034 TOLEDO 69.0	LANE 230 108 Mvar	ON	-0.028 TOLEDO 69.0
5	-0.028 TOLEDO 69.0	TOLEDO 230 30 Mvar	ON	-0.026 DIXONVLE 115
6	-0.026 DIXONVLE 115	DIXONVLE 115 -149 Mvar	OFF	No Violation
Stage 2: Load Increase: ALVEY 115 → [P_L = 600 MW, Q_L = 200 Mvar]				
7	-0.040 GOSHN 115	ALVEY 230 58.9 Mvar	ON	-0.034 GOSHN 115
8	-0.034 GOSHN 115	ALVEY 230 58.9 Mvar	ON	-0.028 GOSHN 115
9	-0.028 GOSHN 115	ALVEY 230 58.9 Mvar	ON	-0.021 ALVEY 115
10	-0.021 ALVEY 115	ALVEY 115 25.6 Mvar	ON	No Violation
Stage 3: Load Increase: ALVEY 115 → [P_L = 900 MW, Q_L = 300 Mvar]				
11	-0.054 GOSHN 115	LANE 115 30.4 Mvar	ON	-0.050 GOSHN 115

12	-0.050 GOSHN 115	ALVEY 115 25.6 Mvar	ON	-0.045 GOSHN 115
13	-0.045 GOSHN 115	ALVEY 115 19.5 Mvar	ON	-0.041 GOSHN 115
14	-0.041 GOSHN 115	ALVEY 230 →|– ALVEY 115 (3)	4/9→3/9	-0.037 VILLAGEG 115
15	-0.037 VILLAGEG 115	ALVEY 230 →|– ALVEY 115 (4)	4/9→3/9	-0.033 VILLAGEG 115
16	-0.033 VILLAGEG 115	ALVEY 500 →|– ALVEY 230 (5)	9/9→8/9	-0.028 VILLAGEG 115
17	-0.028 VILLAGEG 115	ALVEY 230 →|– ALVEY 115 (3)	3/9→2/9	-0.025 DIXONVLE 115
18	-0.025 DIXONVLE 115	DIXONLE 230→|– DIXONLE 115 (1)	11/17→ 10/17	-0.024 VILLAGEG 115
19	-0.024 VILLAGEG 115	ALVEY 230 →|– ALVEY 115 (4)	3/9→2/9	-0.023 BURNT WD 115
20	-0.023 BURNT WD 115	CHEMAWA 230 54 Mvar	ON	No Violation
Stage 4: Line In-service: JOHN DAY 500 – MARION 500 Load Decrease: ALVEY 115 → [P_L = 4.4 MW, Q_L = 1.4 Mvar] DIXONVLE 115 → [PL = 130 MW, QL = 57.7 Mvar]				
21	+0.069 CRESWELL 115	ALVEY 230 118 Mvar	OFF	+0.054 ALVEY 115
22	+0.054 ALVEY 115	LANE 230 108 Mvar	OFF	+0.044 ALVEY 115
23	+0.044 ALVEY 115	ALVEY 230 58.9 Mvar	OFF	+0.037 ALVEY 115
24	+0.037 ALVEY 115	ALVEY 230 58.9 Mvar	OFF	+0.030 ALVEY 115
25	+0.030 ALVEY 115	ALVEY 230 58.9 Mvar	OFF	+0.024 CRESWELL 115
26	+0.024 CRESWELL 115	ALVEY 115 25.6 Mvar	OFF	No Violation

Table 3.9 Voltage control results with capacitor/reactor/LTC (LVE).

Tim Step	ΔV_{max} (Before Control)	Control Device (Bus)	Control Action	ΔV_{max} (After Control)
Stage 1: Line Outage: JOHN DAY 500 – MARION 500 Load Increase: ALVEY 115 → [P_L = 300 MW, Q_L = 100 Mvar] DIXONVLE 115 → [PL = 259 MW, QL = 107 Mvar]				
1	-0.052 TOLEDO 69.0	MARION 500 -248 Mvar	OFF	-0.041 TOLEDO 69.0
2	-0.041 TOLEDO 69.0	MARION 500 -149 Mvar	OFF	-0.037 TOLEDO 69.0
3	-0.037 TOLEDO 69.0	LANE 230 108 Mvar	ON	-0.031 TOLEDO 69.0
4	-0.031 TOLEDO 69.0	SANTIAM 230 147 Mvar	ON	-0.027 DIXONVLE 115
5	-0.027 DIXONVLE 115	DIXONVLE 115 -149 Mvar	OFF	-0.022 TOLEDO 69.0
6	-0.022 TOLEDO 69.0	ALVEY 230 118 Mvar	ON	No Violation
Stage 2: Load Increase: ALVEY 115 → [P_L = 600 MW, Q_L = 200 Mvar]				
7	-0.034 VILLAGEG 115	ALVEY 230 58.9 Mvar	ON	-0.029 VILLAGEG 115
8	-0.029 VILLAGEG 115	ALVEY 230 58.9 Mvar	ON	-0.023 VILLAGEG 115
9	-0.023 VILLAGEG 115	ALVEY 230 58.9 Mvar	ON	No Violation

Stage 3: Load Increase: ALVEY 115 → [P_L = 900 MW, Q_L = 300 Mvar]				
10	-0.052 VILLAGEG 115	ALVEY 115 25.6 Mvar	ON	-0.046 VILLAGEG 115
11	-0.046 VILLAGEG 115	ALVEY 115 19.9 Mvar	ON	-0.042 GOSHN 115
12	-0.042 GOSHN 115	ALVEY 115 19.5 Mvar	ON	-0.039 GOSHN 115
13	-0.039 GOSHN 115	LANE 115 30.4 Mvar	ON	-0.035 VILLAGEG 115
14	-0.035 VILLAGEG 115	ALVEY 500 →|– ALVEY 230 (5)	9/9→8/9	-0.030 VILLAGEG 115
15	-0.030 VILLAGEG 115	ALVEY 500 →|– ALVEY 230 (5)	8/9→7/9	-0.025 GOSHN 115
16	-0.025 GOSHN 115	SANTIAM 230 58.9 Mvar	ON	-0.023 GOSHN 115
17	-0.023 GOSHN 115	ALVEY 230 →|– ALVEY 115 (1)	4/9→3/9	-0.021 DIXONVLE 115
18	-0.021 DIXONVLE 115	DIXONVLE230→|–DIXONVLE11 (5)	11/17→ 10/17	-0.020 VILLAGEG 115
19	-0.020 VILLAGEG 115	ALVEY 230 →|– ALVEY 115 (2)	4/9→3/9	No Violation
Stage 4: Line In-service: JOHN DAY 500 – MARION 500 Load Decrease: ALVEY 115 → [P_L = 4.4 MW, Q_L = 1.4 Mvar] DIXONVLE 115 → [PL = 130 MW, QL = 57.7 Mvar]				
20	+0.071 VILLAGEG 115	ALVEY 115 25.6 Mvar	OFF	+0.071 VILLAGEG 115
21	+0.065 VILLAGEG 115	ALVEY 230 118 Mvar	OFF	+0.065 VILLAGEG 115
22	+0.051 CRESWELL 115	LANE 230 108 Mvar	OFF	+0.051 CRESWELL 115
23	+0.040 VILLAGEG 115	ALVEY 230 58.9 Mvar	OFF	+0.040 VILLAGEG 115
24	+0.033 CRESWELL 115	ALVEY 230 58.9 Mvar	OFF	+0.033 CRESWELL 115
25	+0.025 VILLAGEG 115	ALVEY 230 58.9 Mvar	OFF	+0.025 VILLAGEG 115
26	+0.020 LANE 500	LANE 115 30.4 Mvar	OFF	No Violation

Table 3.10 Voltage control results with capacitor/reactor/LTC (LPF) [31].

It can be observed from above tables that when loads increase, the reactors are first switched out, and then the capacitors are switched in. The LTC taps are changed only if there is no suitable capacitor/reactor bank available. When loads are restored to the original values, capacitor banks are switched out to make the voltage within limits. The results show that the preferences of the operators are properly implemented into the algorithm. It is also noted that the order of control actions made by two controllers are almost same, especially in stage1 and state 4. The major difference in control decisions is in stage 3, more LTC tap changing are made by the alternate controller than that of the model-based controller, because the alternate controller does not include circular VAR flow penalty into objective function while the model-based controller does. Overall the tests show that the alternate controller can be used to reinforce the decisions made by model-based controller and act as backup controller effectively.

In above tests, we have shown that the alternate slow voltage controller successfully recover the violating voltages back to their normal ranges. We will now go further to investigate how the controller defers system collapse, or equivalently increases the system static limit, in extreme cases. Ten load buses in western Oregon area are chosen for the test: ALBANY 115, ALVEY 115, DIXONVLE 115, RAINBOW 115, EUGENE 115, LANE 115, CURRIN 115, WILLOW C 115, KEELER 115, and CHEMAWA 115. The simulation scenario is that the total active load keeps increasing while one line is out of service. The increased load is allocated to each of the above load bus in such a way that the power factors on those buses remain unchanged. Table 3.11 shows the total load increase when the system collapse with or without the control actions.

Tim Step	ΔV_{max} (Before Control)	Control Device (Bus)	Control Action	ΔV_{max} (After Control)
Stage 1: Line Outage: JOHN DAY 500 – MARION 500 Load Increase: P_L + 200 MW on 10 buses, Q_L keep power factor			Without Control -0.044 TOLEDO 69.0	
1	-0.044 TOLEDO 69.0	MARION 500 -248 Mvar	OFF	-0.038 TOLEDO 69.0
2	-0.038 TOLEDO 69.0	MARION 500 -149 Mvar	OFF	-0.033 TOLEDO 69.0
3	-0.033 TOLEDO 69.0	ALVEY 230 118 Mvar	ON	-0.032 TOLEDO 69.0
4	-0.032 TOLEDO 69.0	ALBANY 115 50 Mvar	ON	-0.030 TOLEDO 69.0
5	-0.030 TOLEDO 69.0	TOLEDO 69.0 27 Mvar	ON	No Violation
Stage 2: Load Increase: P_L + 400 MW on 10 buses, Q_L keep power factor			Without Control -0.051 TOLEDO 69.0	
6	-0.025 EUGENE 115	DIXONVLE 115 -149 Mvar	OFF	-0.021 ALDRWD T 115
7	-0.021 ALDRWD T 115	ALVEY 115 19.59 Mvar	ON	No Violation

Stage 3: Load Increase: P_L + 600 MW on 10 buses, Q_L keep power factor			Without Control -0.064 PARKER 12.5	
8	-0.029 PARKER 12.5	LANE 230 108 Mvar	ON	No Violation
Stage 4: Load Increase: P_L + 800 MW on 10 buses, Q_L keep power factor			Without Control -0.083 PARKER 12.5	
9	-0.031 PARKER 12.5	LANE 115 30.4 Mvar	ON	-0.027 ALDRWD T 115
10	-0.027 ALDRWD T 115	SANTIAM 230 147 Mvar	ON	-0.024 ALDERWOD 115
11	-0.024 ALDERWOD 115	Out of range		
Stage 5: Load Increase: P_L + 1000 MW on 10 buses, Q_L keep power factor			Without Control -0.103 PARKER 12.5	
12	-0.039 PARKER 12.5	ALVEY 230 58.9 Mvar	ON	-0.033 PARKER 12.5
13	-0.033 PARKER 12.5	ALVEY 230 58.9 Mvar	ON	-0.028 PARKER 12.5
14	-0.028 PARKER 12.5	ALVEY 230 58.9 Mvar	ON	-0.025 BURNT WD 115
15	-0.025 BURNT WD 115	SANTIAM 230 58.9 Mvar	ON	-0.022 BURNT WD 115
16	-0.022 BURNT WD 115	TOLEDO 230 30 Mvar	ON	-0.021 BURNT WD 115
17	-0.021 BURNT WD 115	CHEMAWA 115 23.7 Mvar	ON	0.021 TOLEDO 69.0
18	0.021 TOLEDO 69.0	SANTIAM 230 58.9 Mvar	OFF	-0.022 BURNT WD 115
19	-0.022 BURNT WD 115	CHEMAWA 230 54 Mvar	ON	No Violation
Stage 6: Load Increase: P_L + 1200 MW on 10 buses, Q_L keep power factor			Without Control -0.125 PARKER 12.5	
20	-0.031 PARKER 12.5	ALVEY 115 25.6 Mvar	ON	-0.027 ALDRWD T 115
21	-0.027 ALDRWD T 115	ALVEY 115 19.5 Mvar	ON	-0.026 DIXONVLE 115
22	-0.026 DIXONVLE 115	ALVEY 230 →|– ALVEY 115 (3)	4/9→3/9	-0.026 DIXONVLE 115
23	-0.026 DIXONVLE 115	DIXONLE 230→|– DIXONLE 115 (1)	11/17→ 10/17	-0.025 PARKER 12.5
24	-0.025 PARKER 12.5	ALVEY 230 →|– ALVEY 115 (4)	4/9→3/9	-0.023 ALDERWOD 115
25	-0.023 ALDERWOD 115	Out of range		
Stage 7: Load Increase: P_L + 1400 MW on 10 buses, Q_L keep power factor			Without Control -0.151 PARKER 12.5	
26	-0.036 PARKER 12.5	ALVEY 230 →|– ALVEY 115 (3)	3/9→2/9	-0.035 PARKER 12.5
27	-0.035 PARKER 12.5	ALVEY 230 →|– ALVEY 115 (4)	3/9→2/9	-0.034 ALDRWD T 115
28	-0.034 ALDRWD T 115	SANTIAM 230 58.9 Mvar	ON	-0.031 ALDERWOD 115
29	-0.031 ALDERWOD 115	Out of range		
Stage 8: Load Increase: P_L + 1600 MW on 10 buses, Q_L keep power factor			Without Control -0.211 PARKER 12.5	
30	-0.049 PARKER 12.5	ALVEY 230 →|– ALVEY 115 (3)	2/9→1/9	-0.047 PARKER 12.5
31	-0.047 PARKER 12.5	ALVEY 230 →|– ALVEY 115 (4)	2/9→1/9	-0.045 ALDRWD T 115
32	-0.045 ALDRWD T 115	Out of range		

Stage 9: Load Increase: P_L + 1800 MW on 10 buses, Q_L keep power factor			Without Control -0.242 PARKER 12.5	
33	-0.056 PARKER 12.5	Out of range		
Stage 10: Load Increase: P_L + 2000 MW on 10 buses, Q_L keep power factor			Without Control -0.406 PARKER 12.5	
34	-0.079 PARKER 12.5	Out of range		
Stage 11: Load Increase: P_L + 2200 MW on 10 buses, Q_L keep power factor			Without Control Diverge	
35	-0.107 PARKER 12.5	Out of range		
Stage 12: Load Increase: P_L + 2400 MW on 10 buses, Q_L keep power factor			Without Control Diverge	
36	-0.107 PARKER 12.5	Out of range		
Stage 13: Load Increase: P_L + 2600 MW on 10 buses, Q_L keep power factor			Without Control Diverge	
37	Diverge			

Table 3.11 System static limit increases with voltage controller.

From table above, it is obvious that the system static limit increases about 400 MW with the voltage controller switching available control devices in. The system without control collapses as the active load increases about 2200 MW, while the collapse is deferred to load increase of 2600 MW when the controller is used. The total capacity of capacitors that are switched in is about 880 MW. At some intermediate stages, when the worst violating bus is out of control region of any available control devices, the controller just stop making control decision. But as the scenario evolves, the worst violating bus may move to another bus and thus controller can act again as shown in the table.

Finally the alternate controller will be tested with generators available as control devices. Two generator-controlled buses in west Oregon area are included as shown in Table 3.5. To facilitate studying the generator control effects, lesser capacitors are chosen as control devices in Table 3.12, as compared to the capacitors considered in the previous cases (Table 3.5). The available reactors and LTC transformers are remained the same. The voltage control results are shown in Table 3.13.

Device Type	Bus / Transformer	Capacity / Range	Setting / Status
Capacitor	ALBANY 115	50.0	OFF
	ALVEY 115	19.5	OFF
	CHEMAWA 230	54.0	OFF
	LANE 115	30.4	OFF
	TILLAMOK 115	30.4, 22.8	OFF
	TOLEDO 69.0	27.1	OFF
	TOLEDO 230	30.0	OFF

Table 3.12 Capacitors available in the test case for generator control.

Tim Step	ΔV_{max} (Before Control)	Control Device (Bus)	Control Action	ΔV_{max} (After Control)
Stage 1: Line Outage: ALVEY 500 – MARION 500				
1	-0.045 TOLEDO 69.0	MARION 500 -248 Mvar	OFF	-0.038 TOLEDO 69.0
2	-0.038 TOLEDO 69.0	MARION 500 -149 Mvar	OFF	-0.034 TOLEDO 69.0
3	-0.034 TOLEDO 69.0	TOLEDO 230 30 Mvar	ON	-0.025 BURNT WD 115
4	-0.025 BURNT WD 115	ALBANY 115 50 Mvar	ON	-0.024 COYO D1 250
5	-0.024 COYO D1 250	JOHN DAY 500	1.050 →1.060	-0.021 ALVEY 230
6	-0.021 ALVEY 230	DIXONVLE 115 -149 Mvar	OFF	No Violation
Stage 2: Load Increase: ALVEY 115 → [P_L = 300 MW, Q_L = 200 Mvar] DIXONVLE 115 → [P_L = 259 MW, Q_L = 107 Mvar]				
7	-0.039 GOSHN 115	LANE 115 30.4 Mvar	ON	-0.036 VILLAGEG 115
8	-0.036 VILLAGEG 115	ALVEY 115 19.5 Mvar	ON	-0.034 GOSHN 115
9	-0.034 GOSHN 115	ALVEY 500 →|– ALVEY 230 (5)	9/9→8/9	-0.031 DIXONVLE 115
10	-0.031 DIXONVLE 115	ALVEY 230 →|– ALVEY 115 (3)	4/9→3/9	-0.031 DIXONVLE 115
11	-0.031 DIXONVLE 115	ALVEY 230 →|– ALVEY 115 (4)	4/9→3/9	-0.032 DIXONVLE 115
12	-0.032 DIXONVLE 115	DIXONLE 230 →|– DIXONLE 115 (2)	11/17→ 10/17	-0.027 DIXONVLE 115
13	-0.027 DIXONVLE 115	DIXONLE 230 →|– DIXONLE 115 (1)	11/17→ 10/17	-0.026 ALVEY 500
14	-0.026 ALVEY 500	TOLEDO 69.0 27.1 Mvar	ON	-0.025 ALVEY 500

15	-0.025 ALVEY 500	JOHN DAY 500	1.060 →1.080	-0.024 ALVEY 500
16	-0.024 ALVEY 500	JOHN DAY 500	1.080 →1.100	No Violation
Stage 3: Line In-service: ALVEY 500 – MARION 500 Load Decrease: ALVEY 115 → [P_L = 4.4 MW, Q_L = 1.4 Mvar] DIXONVLE 115 → [PL = 130 MW, QL = 57.7 Mvar]				
17	+0.023 TOLEDO 69.0	TOLEDO 69.0 27.1 Mvar	OFF	No Violation

Table 3.13 Voltage control results with capacitor/reactor/LTC/generator (LVE).

The control sequences in Table 3.13 clearly show the preference of capacitor and LTC actions to generator-controlled bus voltage adjusting. Also it can be seen that the generator-controlled bus voltage settings are continuously adjusted twice at stage 2, because the voltage settings are treated as discrete "tap" as LTC taps in this formulation. The multiple adjustments could be removed either by using linear approximation to evaluate the voltage changes for multiple voltage tap adjustment or formulating generator voltage adjusting as a continuous problem as shown in next chapter.

3.4 Summary

A common slow voltage control framework is proposed to integrate the model-based controller and a backup heuristic controller. The common controller acts upon voltage alarms and SCADA measurements to make control decisions. Under normal conditions when state estimator program has valid results, two sub-controller make their own control decisions and cross-checked against each other to make the final decisions. When the state estimator model is unavailable, the backup alternate controller will take over to make control decisions based on SCADA measurements only.

An integer programming formulation of the heuristic alternate voltage controller is also presented, which is based on the local voltage estimator proposed in chapter 2. The alternate controller is essentially formulated to simulate how the operators would act when the voltage problems happen. The one switching at a time formulation is essentially straightforward and the solving process is exhaustive. The decision is based on the local voltage estimation results from current measurements instead of operator's experience and off-line studies. Therefore the one switching decision by the controller would be more efficient than that of the operators. The simulation results on the standard IEEE 30-bus system and the actual WECC planning case clearly show that the controller is feasible, scalable to large-scale power system and suitable for on-line implementation.

Chapter 4

Large Power System Considerations

The discrete slow voltage controller presented in last chapter mainly targets on controlling voltages of the west Oregon area of Pacific Northwest. Since this area is relatively small, the controller assumes that all voltage problems will be within several tiers around the control devices, and form a single problematic area. Besides, because of the discrete nature of the available control devices in this area, the integer programming formulation is adopted and the generator's voltage settings are treated as discrete values. However, for general large power systems that expand large geographic areas, voltage problems may happen simultaneously in several places that are far away from each others. Moreover, for power systems with a large amount of generators close to load centers, it is more natural to consider generator's voltage settings as continuous control devices and coordinate their actions with discrete devices. In this chapter, the on-line slow voltage control scheme is extended to be applicable to general large power systems. In section 4.1, a multiple problematic area voltage control scheme is presented and tested on a large power system. In section 4.2, a multi-phase hybrid voltage control scheme is proposed to coordinate continuous and discrete controls. The tests results on small and large power systems are also given in this section. Finally, the conclusions of this chapter are summarized in Section 4.3.

4.1 Multiple Problematic Area Voltage Control

For a large power system such as Pacific Northwest, it is highly possible that several voltage problems occur simultaneously in different places that are too far to be considered as one control area. It is desirable to make simultaneous corrective control actions accordingly such that the system voltages could be quickly brought back to normal range. The secondary voltage control scheme introduced by EDF handles this situation by dividing the network into separate “control regions” through offline studies. Any voltage problems inside a given region are assumed to be reflected by the feedback voltages from some pilot point of that region, and will be mitigated by corresponding control actions inside the region. However, for a heavily-meshed system such as Pacific Northwest, it is not easy to divide into separate control regions. Thus, a multiple problematic area voltage control scheme is proposed under such considerations.

4.1.1 Multiple-area Voltage Control Scheme

The proposed multi-area voltage control scheme is essentially “problem-oriented”, which closely follows system operator’s philosophy. It divides the network into separate control areas dynamically according to current system conditions. The basic control framework is same as the one presented in Section 3.1. The computation procedure of the control scheme is shown in Figure 4.1. First, the SCADA voltage measurements are checked to decide whether there is any voltage outside a specified band around some “optimal” voltage profile. If any voltage violation exists, the violating buses are located and grouped into separate problematic control areas. The grouping is actually achieved by finding the worst violation bus and forming a problematic area that includes several tiers of buses around the bus, then expanding the area diameter 3 times to preventing control interference of neighboring areas. After excluding all busses inside the expanded area, the voltages on remaining buses are checked. If any violation buses exist, a new problematic area is formed around the worst violation bus, and the process is repeated until there is no violation bus. For each problematic area, the best control actions are found by using some optimization algorithms. If there is no control device available, an alarm will be sent to the operator. After issuing switching commands, the voltages after the switching will be compared with their expected voltages. Significant mismatches between expected and actual voltage levels will be reported to the operator via alarms.

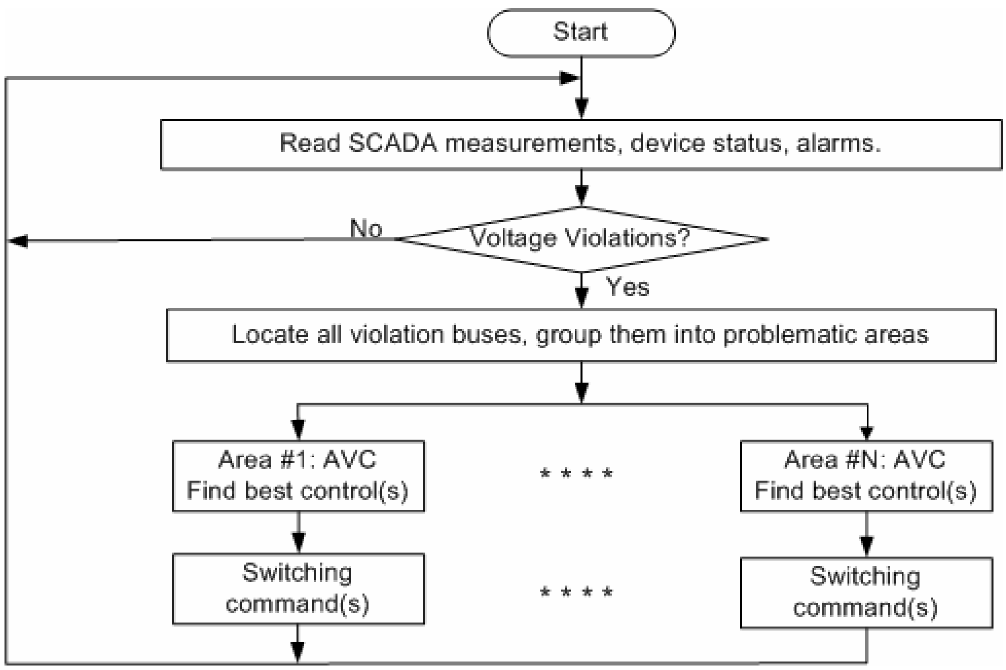

Figure 4.1 Multiple problematic area voltage control diagram.

Note that this control scheme is in general an expansion of the voltage control presented in chapter 3 to handle multiple voltage problems simultaneously. The scheme itself is quite open, in the sense that any voltage control algorithm can be integrated into it for a particular area. For example, if the state estimator has a partial solution, then the model-based controller could be used with minor modification in the areas with valid state estimation solutions, while the alternate controller could be applied to those areas without valid state estimation solutions. Moreover, for those problematic areas with large amount of generators inside, the hybrid multi-phase automatic voltage controller that will be presented could also be integrated into the scheme easily.

4.1.2 Tests on WECC System

Since the standard IEEE 30 bus system is too small to be divided to several control areas, the tests are performed on the WECC system only. Again, the WECC 2001-2003 Winter (case ID 213SNK) planning case is used and modified for test purpose. Except the candidate control devices available in west Oregon area listed in Table 3.5, additional devices in Seattle/Tacoma area and Spokane area are chosen as candidate control devices and these control devices and their initial settings are listed in Table 4.1 and Table 4.2.

Device Type	Bus / Transformer	Capacity / Range	Setting / Status
Capacitor	ADDY 2 230	49.1	OFF
	BELL MI 230	64.5, 64.5, 64.5	OFF
	BONNERS 115	11.9, 11.9	OFF
	COLV BPA 115	13.5, 13.5, 15.0	OFF
	CUSICK 230	50.9	OFF
	DEER PRK 115	15.0	OFF
	SAND CRK 115	11.9, 11.9	OFF
	TRENTWOD 115	25.4, 25.4	OFF
Generator	BOUNDARY 230	1.009 ~ 1.079	1.039
	LIT GOOS 500	1.040 ~ 1.110	1.080

Table 4.1 Additional control devices available in Spokane area.

Device Type	Bus / Transformer	Capacity / Range	Setting / Status
Capacitor	FAIRMONT 115	10.6, 15.6, 21.0, 22.8	OFF
	KITSAP 115	37.3, 60.7, 60.7	OFF
	OLYMPIA 115	55.6	OFF
	OLYMPIA 230	21.0	OFF
	SHELTON 115	21.0, 21.0	OFF
	TACOMA 230	58.9	OFF
Generator	PAUL 500	1.050 ~ 1.110	1.080

Table 4.2 Additional control devices available in Seattle/Tacoma area.

In the following simulations, the local control areas are constructed such that the buses within 6 tiers of the control bus are included. The step-size for LTC tap changing is set to one tap at a time and the step-size for generator voltage adjusting is set to 0.01 p.u. The rules for calculating the costs of control actions are same as before, i.e. the cost for switching out a capacitor or reactor bank is zero, the cost for switching in a capacitor or reactor bank is 100.0, the cost for LTC tap changing is 200.0, and cost for generator voltage adjusting is set to 300.0. For any type of device, the cost of next action will increase by 10.0, and decrease by 1.0 at each time step. The control objective is to maintain all bus voltages within 2% band around the pre-defined voltage profile, and the maximum allowed voltage deviation is 5% away from the optimal value. The voltage penalty coefficient λ is set to 1.0 and the maximum voltage penalty P_0 is set to 7.5 for test purpose.

The first simulation scenario is that both west Oregon and Seattle areas of the Pacific Northwest system experience line outages and/or load variations, thus voltage problems occurs simultaneously in both areas, and then the lines go back to service with load back to normal. The control results using the multiple problematic area control are shown in Table 4.3.

Tim Step	Area	ΔV_{max} (Before Control)	Control Device (Bus)	Control Action	ΔV_{max} (After Control)
Stage 1: Line Outage: ECHOLAKE 500 – RAVER 500 Line Outage: ALVEY 500 – MARION 500					
1	1	-0.058 BANGOR 115	FAIRMONT 115 22.8 Mvar	ON	-0.054 BANGOR 115
	2	-0.048 TOLEDO 69.0	MARION 500 -248 Mvar	OFF	-0.038 TOLEDO 69.0
2	1	-0.054 BANGOR 115	FAIRMONT 115 21 Mvar	ON	-0.050 BANGOR 115
	2	-0.038 TOLEDO 69.0	MARION 500 -149 Mvar	OFF	-0.034 TOLEDO 69.0
3	1	-0.050 BANGOR 115	KITSAP 115 60.7 Mvar	ON	-0.025 BURNT WD 115
	2	-0.034 TOLEDO 69.0	TOLEDO 230 30 Mvar	ON	-0.021 ELKTON 69.0
4	1	-0.025 BURNT WD 115	ALBANY 115 50 Mvar	ON	-0.024 COYO D1 250
	2	-0.021 ELKTON 69.0	Out of range		
5	1	-0.024 COYO D1 250	JOHN DAY 500	1.050 →1.060	No Violation
Stage 2: Load Increase: MASON 115 → [P_L = 151 MW, Q_L = 50 Mvar] Load Increase: ALVEY 115 → [P_L = 154 MW, Q_L = 51 Mvar] DIXONVLE 115 → [P_L = 259 MW, Q_L = 107 Mvar]					
6	1	-0.049 MASON 115	KITSAP 115 60.7 Mvar	ON	-0.040 MASON 115
	2	-0.033 DIXONVLE 115	DIXONVLE 115 -149 Mvar	OFF	-0.027 DIXONVLE 115
	3	-0.032 MUR COVE 115	Out of range		
7	1	-0.040 MASON 115	OLYMPIA 230 152.4 Mvar	ON	-0.028 DIXONVLE 115
	2	-0.027 DIXONVLE 115	ALVEY 115 19.5 Mvar	ON	-0.027 MASON 115
8	1	-0.028 DIXONVLE 115	LANE 115 30.4 Mvar	ON	-0.027 DIXONVLE 115
	2	-0.027 MASON 115	SHELTON 115 21 Mvar	ON	
9	1	-0.027 DIXONVLE 115	DIXONLE 230 →| DIXONLE 115 (2)	11/17→ 10/17	-0.023 DIXONVLE 115
10	1	-0.023 DIXONVLE 115	DIXONLE 230 →| DIXONLE 115 (1)	11/17→ 10/17	No Violation
Stage 3: Line In-service: ECHOLAKE 500 – RAVER 500 Line In-service: ALVEY 500 – MARION 500 Load Decrease: ALVEY 115 → [P_L = 4.4 MW, Q_L = 1.4 Mvar] DIXONVLE 115 → [PL = 130 MW, QL = 57.7 Mvar]					
11	1	No Violation			

Table 4.3 Multiple area voltage control results [Oregon and Seattle areas].

The second simulation scenario is that both west Oregon and Spokane areas of the Pacific Northwest system experience line outages and/or load variations, thus voltage problems occurs simultaneously in both areas, and then the lines go back to service with load back to normal. Six load buses in Spokane area are chosen for the test: CHENEY 115, CRESTN 115, DEER PRK 115, GREEN BL 115, PRIEST 115, and SPRNGHIL 115. The control results using the multiple problematic area control are shown in Table 4.4.

Tim Step	Area	ΔV_{max} (Before Control)	Control Device (Bus)	Control Action	ΔV_{max} (After Control)
Stage 1: Line Outage: BELL MI 230 – COULEE 230, BELL BPA – 500 TAFT 500 [1] Line Outage: ALVEY 500 – MARION 500					
1	1	-0.052 MT HALL 115	BONNERS 115 11.9 Mvar	ON	-0.034 BONNERS 115
	2	-0.045 TOLEDO 69.0	MARION 500 -248 Mvar	OFF	-0.038 TOLEDO 69.0
	3	-0.032 VALY WAY 115	TRENTWOD 115 5.4 Mvar	ON	-0.022 DEER PRK 115
2	1	-0.038 TOLEDO 69.0	MARION 500 -149 Mvar	OFF	-0.034 TOLEDO 69.0
	2	-0.034 BONNERS 115	BONNERS 115 11.9 Mvar	ON	
	3	-0.022 DEER PRK 115	CUSICK 230 50.9 Mvar	ON	
3	1	-0.034 TOLEDO 69.0	DIXONVLE 115 -149 Mvar	OFF	-0.032 TOLEDO 69.0 -0.026 COYO D1 250
4	1	-0.032 TOLEDO 69.0	TOLEDO 230 30 Mvar	ON	
5	1	-0.026 COYO D1 250	CHEMAWA 230 54 Mvar	ON	-0.026 COYO D1 250
6	1	-0.026 COYO D1 250	JOHN DAY 500	1.050 $\rightarrow$1.060	No Violation
Stage 2: Load Increase: on 6 buses $\rightarrow$ [P_L + 121 MW, Q_L + 47 Mvar] Load Increase: ALVEY 115 $\rightarrow$ [P_L = 154 MW, Q_L = 51 Mvar] DIXONVLE 115 $\rightarrow$ [P_L = 259 MW, Q_L = 107 Mvar]					
7	1	-0.032 DEER PRK 115	DEER PRK 115 15.0 Mvar	ON	-0.029 DIXONVLE 115
	2	-0.027 DIXONVLE 115	ALVEY 115 19.5 Mvar	ON	
	3	-0.024 SAND CRK 115	SAND CRK 115 11.9 Mvar	ON	-0.027 GREEN BL 115
	4	-0.021 CHENEY 115	Out of range		
8	1	-0.029 DIXONVLE 115	LANE 115 30.4 Mvar	ON	-0.028 DIXONVLE 115
	2	-0.027 GREEN BL 115	TRENTWOD 115 25.4 Mvar	ON	-0.027 CRESTN 115

9	1	-0.028 DIXONVLE 115	JOHN DAY 500	1.060 →1.070	-0.028 DIXONVLE 115
	2	-0.027 CRESTN 115	BELL MI 230 64.5 Mvar	ON	
10	1	-0.028 DIXONVLE 115	JOHN DAY 500	1.070 →1.080	-0.028 DIXONVLE 115
11	1	-0.028 DIXONVLE 115	JOHN DAY 500	1.080 →1.090	-0.027 DIXONVLE 115
12	1	-0.027 DIXONVLE 115	JOHN DAY 500	1.090 →1.100	-0.026 DIXONVLE 115
13	1	-0.026 DIXONVLE 115	DIXONLE 230 →| DIXONLE 115 (2)	11/17→ 10/17	-0.021 DIXONVLE 115
14	1	-0.021 DIXONVLE 115	DIXONLE 230 →| DIXONLE 115 (1)	11/17→ 10/17	No Violation
Stage 3: Line In-service: BELL MI 230 – COULEE 230, BELL BPA – 500 TAFT 500 [1] Load Decrease: on 6 buses → [P_L, Q_L back to original normal values] Line In-service: ALVEY 500 – MARION 500 Load Decrease: ALVEY 115 → [P_L = 4.4 MW, Q_L = 1.4 Mvar] DIXONVLE 115 → [PL = 130 MW, QL = 57.7 Mvar]					
15	1	No Violation			

Table 4.4 Multiple area voltage control results [Oregon and Spokane areas].

It can be observed from above tables that at the beginning of each iteration, the controller will group the violation buses into different problematic areas and then tries to find the best control devices available in each control areas, send out parallel switching commands. At some intermediate stages, the voltage violation buses maybe out of control range for some control areas. But as the control devices are switched in the other areas, this center of the voltage violations may moved to a new bus and the problematic areas may be merged to form a new problematic area. This means that there are still some minor interactions between different control areas, which are supposed to be totally separated. This problem could be solved by either enlarging the control area or by forming control area using other methods such as electric distance concept. In fact, this interaction will not affect the selection of the best control devices in each area, so as long as the interaction effects are small, it could be neglected.

The control sequences in above tables clearly show the preference of control devices and their actions. The reactors are normally switched out before capacitors are switched in. The LTC taps are changed and generator-controlled bus voltages are adjusted only if there is no suitable capacitor/reactor bank available. Also it is noted that the generator-controlled bus voltage settings are continuously adjusted in Table 4.4, because the voltage settings are treated as discrete "tap" in this formulation. The multiple adjustments could be removed either by using linear approximation to evaluate the voltage changes for multiple voltage tap adjustment or formulating generator voltage adjusting as a continuous problem as shown in next section.

4.2 Multiple-phase Hybrid Voltage Control

It is indicated in some literatures [1] – [3] that although extensive use of capacitor banks can increase the practical transfer limits of real power, it may results in a brittle, voltage collapse-prone network. Thus it is necessary to consider generators as major voltage control devices for more secure operation, especially for those power systems with large amount of generation resources close to their load centers. This leads to the problem of coordinating generator controls and discrete device controls. Some control schemes in the literatures deal with the problem as a continuous problem under the OPF framework, where discrete devices are first treated as continuous variables and then a closest discrete value is chosen from the OPF solution. Such approaches have the limitations such as poor convergence and hunting. Other schemes deal with the problem as a pure discrete problem, such as the discrete controller presented in the last chapters. The generator voltage settings are basically treated as discrete "tap" with several fixed values. This may lead to the inaccuracy and repeated changes of same generator setting in contiguous steps. In this section, a multi-phase hybrid automatic voltage control scheme is proposed to treat the continuous generator settings and discrete control devices in their true form and in the meantime, take reactive power security into consideration.

4.2.1 Multiple-phase Hybrid Control Scheme

The control scheme has three operation phases: In the first phase and second phase, the controller will try to maintain system voltage profiles and keep adequate generator reactive reserves at the same time. In the third phase, which is meant to be under extreme or emergency operating conditions, the controller will use all of the available reactive reserves to restore system voltages. In Phase I, the controller tries to maintain prescribed voltage profiles by adjusting high side voltages of generators within a certain local problematic area, while keeping the generator VAR outputs within their reserved limits. In this phase, the reserved VAR limits of the generators are set to a certain percentage of the full steady state VAR limits of the generators. In other words, we reserve some of the VAR capacity of the generators for dynamic voltage support and for voltage security. When the controller can no longer maintain voltages by adjusting generator VAR outputs in Phase I, that is, when all of the generators have reached their reserved VAR limits within the local area or the controller could not restore the voltage back to normal even with the reactive outputs reaching reserved VAR limits, the controller will operate in Phase II, where it switches local discrete devices to correct the voltage profile, which may in turn relieve the reactive power demands on generators, thus make the generator VAR outputs reduced and the controller goes back to operate in Phase I again. When the controller can no longer maintain voltages by adjusting generator VAR outputs in Phase I and there is no more discrete devices available for Phase II, the controller will enter Phase III, where the full reactive power capacity of generators will be utilized to restore the voltage as close as possible to the prescribed values.

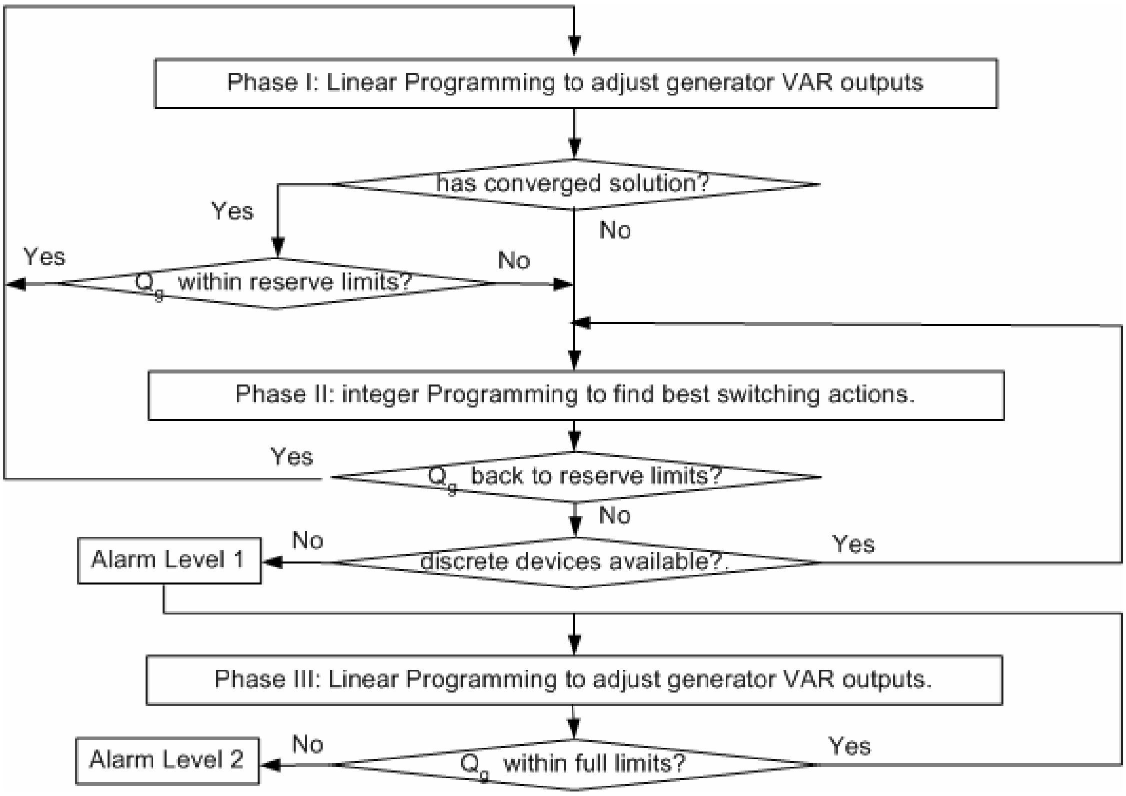

Figure 4.2 Phase transition diagram of the multi-phase hybrid voltage control.

In the first phase and third phase, the controller employs generators as continuous control devices, and the reactive power demand is distributed among generators within respective local areas using linear programming. In the second phase, the controller utilizes discrete devices within local areas, and the previous discrete formulation presented in chapter 3 is used to determine proper switching actions. The controller will send alarms to operators if reactive power reserve or full limits are hit in the third phase. Figure 4.2 illustrates the phase transition diagram of the controller.

The above control scheme is hybrid in the sense that it integrates continuous and discrete formulation into one scheme. The controller is meant to be used in those power systems with large amount of generation resource available and close to load centers. Under normal operating conditions such as morning load pickups, the controller will act in the way similar to that of AGC, trying to adjust generator reactive outputs to maintain the desired voltage profile. The discrete control devices are treated as supplemental reactive power to generator reactive reserves, which need to be kept at certain level such that there could be enough fast reactive power support in case of emergency. The formulation details of the three phases are presented in the following section.

4.2.2 Formulation of the Optimization

With the three phases clearly defined above, now the problem of choosing "best" control actions in each phase can be formulated as linear programming or integer programming optimization problem as follows.

(1). Phase I: Linear programming.

In the first phase, linear programming is employed to distribute reactive power demand among generators that operate in aligned mode. The objective is to maintain all bus voltages within 2% variation range of their desired values with the minimum changes of the generator voltage settings and/or maximum level of generator reactive power reserves. Meanwhile, the total reactive power outputs need to be kept within the generator reactive power reserve limits (for example, 75% of full limits). The linear programming problem is formulated as

$$\min : \alpha\sum_{1}^{N_G}\left|\Delta V_{Gi}\right| + (1-\alpha)\sum_{1}^{N_G}\left|\Delta Q_{Gi}\right|$$
$$s.t.: pQ^{r}_{Gi\min} \le Q_{Gi} \le pQ^{r}_{Gi\max}; i = 1...N_G \qquad (4.1)$$
$$V_{j\min} \le V_j \le V_{j\max}; j = 1...N$$

In above formulation, ΔV_{Gi} and ΔQ_{Gi} are voltage setting and reactive power output change of *ith* generator. $Q_{Gi} = Q^0_{Gi} + \Delta Q_{Gi}$ is the reactive power output of *ith* generator after control action. $Q^r_{Gi\min}$ and $Q^r_{Gi\max}$ are lower and upper reserved limits of the reactive power output. $V_j = V^0_j + \Delta V_j$ denotes the bus voltage after control action. $V_{j\min}$ and $V_{j\max}$ represent lower and upper limits of the bus voltage. p is the percentage of full reactive power limit as reserve limit for phase I. α represents a weighting factor between 0 and 1. N and N_G are the number of buses the number of control generators inside the local area, respectively.

Note that after obtaining ΔQ_G under given $\Delta V^{\exp}_G$ using equation (2.30) of local voltage estimator for generator, the sensitivity of generator reactive power output change to its voltage setting change can be derived as follows

$$\beta_i = \Delta Q_{Gi} \big/ \Delta V^{\exp}_{Gi}; i = 1...N_G \qquad (4.2)$$

Normally, the sensitivity can be assumed to be positive. If under certain conditions, the sensitivity of a generator becomes negative, then this generator will be excluded as a candidate control device.

From equation (2.16) of local voltage estimator for generator, the load bus voltage change can be written as

$$\Delta V_j = \sum_{i=1}^{N_G} s_{j,i}\Delta Q_{Gi}; j = 1...N \qquad (4.3)$$

Using equations (4.2) and (4.3), the above LP problem (4.1) can be reformulated as

$$
\begin{aligned}
&\min : \sum_{1}^{N_G} [\alpha + (1-\alpha)\beta_i] |\Delta V_{Gi}| \\
&s.t.: \Delta Q^r_{Gi\min} \le \beta_i \Delta V_{Gi} \le \Delta Q^r_{Gi\max}; i = 1 \ldots N_G \\
&\quad \Delta V_{j\min} \le \sum_{i=1}^{N_G} s_{j,i} \beta_i \Delta V_{Gi} \le \Delta V_{j\max}; j = 1 \ldots N
\end{aligned}
\tag{4.4}
$$

Here ΔV_{Gi} denotes the generator voltage setting change. $\Delta Q^r_{Gi\min} = pQ^r_{Gi\min} - Q^0_{Gi}$ and $\Delta Q^r_{Gi\min} = pQ^r_{Gi\min} - Q^0_{Gi}$ are lower and upper limits of the generator reactive power change. $\Delta V_{j\min} = V_{j\min} - V^0_j$ and $\Delta V_{j\max} = V_{j\max} - V^0_j$ are lower and upper limits of the bus voltage change.

Note that parameter α could be adjusted to reflect the preference of either minimizing voltage changes or minimizing reactive power output changes. The cost function can be readily modified to incorporate other objectives such as reactive reserve maximization, or reactive loss minimization.

(2). Phase II: Integer programming.

In the second phase, the total reactive power outputs hit the generator reactive power reserve limits within the local area or the linear programming in the first phase could not converge to a solution. Thus the available discrete control devices within the local area will be utilized to maintain the desired voltage profile. The integer programming formulation (3.2) is used here and re-written as follows

$$
\begin{aligned}
&\min : \sum_{i=1}^{N_D} |k_i| \left[C_i(k_i) + \lambda \sum_{j=1}^{N} P_i(\Delta V_{i,j}) \right] \\
&s.t.: \sum_{i=1}^{N_D} |k_i| \le N_{sw}; \quad k_i \in \{-1, 0, 1\}
\end{aligned}
\tag{4.5}
$$

In the formulation, k_i represents the switching type: -1 for switching out capacitor/reactor, one tap decrease of LTC or one step decrease of generator voltage setting, 0 for no control action and +1 for switching in capacitor/reactor, one tap increase of LTC or one step increase of generator voltage setting. $C_i(k_i)$ denotes the cost of the *ith* control device under control action type k_i. $\Delta V_{i,j}$ is the voltage change on j_{th} bus caused control action of *ith* device. $P_i(\Delta V_{i,j})$ denotes the voltage penalty cost of *jth* bus under *ith* control action, as shown in Figure 3.3. λ represents the weighting factor of voltage violation penalty cost. N, N_D and N_{sw} are the number of buses inside the local area, the number of feasible control devices, and the maximum number of control actions, respectively.

Note that after switching of the discrete control devices, the nearby generators will be relieved from the reactive power demand and thus the total reactive power outputs may come back to be within the reactive power reserve limits, and the controller may go back to operate in Phase I again.

(3). Phase III: Linear programming.

When the total reactive power outputs hit the generator reactive power reserve limits and no more discrete control devices are available to provide supplemental reactive support, the controller will operate in Phase III. In this phase, the system is under much stress and the full generator reactive capacity will be utilized in an aligned mode to restore the system voltages or at least mitigate the voltage violations. The linear programming formulation is different from that in Phase I, with the objective of minimizing voltage violations under the constraints of full generator reactive power limits. The formulation is written as

$$
\begin{aligned}
&\min: \sum_{j=1}^{N} \left| V_j - V_j^{\exp} \right| \\
&s.t.: Q_{Gi\min} \le Q_{Gi} \le Q_{Gi\max}; i = 1 \ldots N_G
\end{aligned}
\tag{4.6}
$$

In the formulation, $V_j = V_j^0 + \Delta V_j$ represents the bus voltage after control action. $V_j^{\exp}$ denotes the desired bus voltage. $Q_{Gi} = Q_{Gi}^0 + \Delta Q_{Gi}$ is the reactive power output of generator i after control action. $Q_{Gi\min}$ and $Q_{Gi\max}$ are lower and upper full limits of the generator reactive power output. N and N_G are the number of buses the number of control generators inside the local area, respectively.

Using equations (4.2) and (4.3), the above linear programming problem can be reformulated as

$$
\begin{aligned}
&\min: \sum_{j=1}^{N} \left| V_j^0 - V_j^{\exp} + \sum_{i=1}^{N_G} s_{j,i} \beta_i \Delta V_{Gi} \right| \\
&s.t.: \Delta Q_{Gi\min} \le \beta_i \Delta V_{Gi} \le \Delta Q_{Gi\max}; i = 1 \ldots N_G
\end{aligned}
\tag{4.7}
$$

Here ΔV_{Gi} denotes the voltage setting change of generator *i*. $\Delta Q_{Gi\min} = Q_{Gi\min} - Q_{Gi}^0$ and $\Delta Q_{Gi\min} = Q_{Gi\min} - Q_{Gi}^0$ are lower and upper full limits of the generator reactive power output change.

Now considering the following equivalence of minimization problem

$$
\min: \sum_{j=1}^{N} \left| u_j \right| \Leftrightarrow \begin{cases} \min: \sum_{j=1}^{N} y_j \\ s.t.: -y_j \le u_j \le y_j, y_j \ge 0, j = 1, \ldots, N \end{cases}
\tag{4.8}
$$

The linear programming problem (4.7) can be transformed to

$$
\begin{aligned}
&\min: \sum_{j=1}^{N} y_j \\
&s.t.: -y_j \le V_j^0 - V_j^{\exp} + \sum_{i=1}^{N_G} s_{j,i}\beta_i \Delta V_{Gi} \le y_j ; y_j \ge 0; j = 1...N \\
&\quad \Delta Q_{Gi\min} \le \beta_i \Delta V_{Gi} \le \Delta Q_{Gi\max}; i = 1...N_G
\end{aligned}
\tag{4.9}
$$

To make the controller more practical, several modifications have been made to above Phase I and III linear programming formulation such that the controller could reach feasible solution in most cases. These modifications include (a). To make the generator's voltage adjusted in same direction, set the limits according to the current condition. If the voltage is low, then set the lower limits of the generator's reactive power to zero. If the voltage is high, then set the upper limits to zero. (b). Always check lower limit against corresponding upper limit of each generator reactive output. If a lower limit is larger than corresponding upper limit, then set them equal, which in effect inhibit the generator from any control action. (c). For Phase I controller, since the number of load buses is generally much more than the number of the generators in any control area, the number of constraints is much more than the number of free control variables. This often makes the linear programming problem infeasible. To deal with this problem, some preliminary examination of the constraints is performed by setting control variables to their lower/upper limits. If the constraints are still not satisfied in this extreme case, then the corresponding constraints will be relaxed, which is equivalent to relax the voltage constraints on some load buses.

The computations in the formulation above do not require the state estimator model. All measurements are directly from SCADA, thus it is meant to be fast and aimed at real-time implementation with short iteration time (say 30 seconds). However, if the state estimator model is available and valid, the above formulation could be easily modified to utilize the model data for computation.

4.2.3 Tests on IEEE 30 Bus System

The simulations of hybrid voltage controller and power flow on IEEE 30 bus system are conducted with MATLAB programs. The available control devices in IEEE 30 bus system and their initial settings are listed in Table 3.2. In the following tests, the local control areas are chosen such that the buses within 3 tiers of the control bus are included. The step-sizes for LTC tap changing is set to be 0.01 p.u. The costs of different control device's actions are calculated according the following rules: the cost for switching out a capacitor or reactor bank is set to zero, the cost for switching in a capacitor or reactor bank is set to 10.0, and the cost for LTC tap changing is set to 20.0. Since generators are not used as discrete controls, their step-sizes and costs of switching are not set in the tests. For any type of device, the cost of next action will increase by 5.0, and decrease by 1.0 at each time step. The control objective is to maintain all bus voltages within 2% band around the normal voltage profile, and the maximum allowed voltage deviation is 5% away from the normal value. The voltage penalty coefficient λ is set to 1.0 and the maximum voltage penalty P_0 is set to 1.0 for test purpose. The weighting factor α is set to 0.7 and the percentage p is set to 0.75 in the tests.

Many scenarios with different load levels, load distributions and topology have been tested on the system. Table 4.5 shows the control actions under the scenario that the system experience some line outage and load increases, then the line goes back to service and loads return to normal values.

Tim Step	Phas	ΔV_{max} (Before Control)	Control Device (Bus)	Control Action	ΔV_{max} (After Control)
Stage 1: Line Outage: Line Bus 16 – Bus 17					
1	I	-0.0492 Bus 17	Gen. Bus 2, Bus 8	Infeasible	
	II	-0.0492 Bus 17	Bus 10 19.0 Mvar	ON	-0.0279 Bus 24
2	I	-0.0279 Bus 24	No gen. inside		
	II	-0.0279 Bus 24	Bus 24 4.3 Mvar	ON	-0.0216 Bus 17
3	I	-0.0216 Bus 17	Gen Bus 2		No Violation
			Gen Bus 8	1.0000 →1.0062	
			Gen Bus 11		
Stage 2: Load Increase: Bus 16 → [P_L = 4.375 MW, Q_L = 2.25 Mvar] Bus 17 → [P_L = 11.25 MW, Q_L = 7.25 Mvar]					
4	I	-0.0216 Bus 17	Gen Bus 2, Bus 8, Bus 11	Infeasible	
	II	-0.0216 Bus 17	LTC Bus 6 →|– Bus 9	0.988→ 0.978	-0.0212 Bus 17
5	I	-0.0216 Bus 17	Gen Bus 2		No Violation
			Gen Bus 8	1.0062 →1.0094	
			Gen Bus 11	1.0720 →1.0732	
Stage 3: Load Increase: Bus 16 → [P_L = 5.469 MW, Q_L = 2.813 Mvar] Bus 17 → [P_L = 14.063 MW, Q_L = 9.063 Mvar]					
6	I	-0.0253 Bus 17	Gen Bus 2, Bus 8, Bus 11	Infeasible	
	II	-0.0253 Bus 17	LTC Bus 6 →|– Bus 10	0.979→ 0.969	-0.0231 Bus 17
7	I	-0.0231 Bus 17	Gen Bus 2, Bus 8, Bus 11	Infeasible	
	II	-0.0231 Bus 17	LTC Bus 28 →|– Bus 27	0.978→ 0.968	-0.0223 Bus 17
8	I	-0.0223 Bus 17	Gen Bus 2, Bus 8, Bus 11	Infeasible	
	II	-0.0223 Bus 17	LTC Bus 4 →|– Bus 12	0.942→ 0.932	-0.0218 Bus 17
9	I	-0.0218 Bus 17	Gen Bus 2	1.0330 →1.0332	No Violation
			Gen Bus 8	1.0094 →1.0146	
			Gen Bus 11	1.0732 →1.0744	
Stage 4: Load Increase: Bus 16 → [P_L = 6.836 MW, Q_L = 3.516 Mvar] Bus 17 → [P_L = 17.578 MW, Q_L = 11.328 Mvar]					
10	I	-0.0266 Bus 17	Gen Bus 2, Bus 8, Bus 11	Infeasible	
	II	-0.0266 Bus 17	LTC Bus 6 →|– Bus 9	0.978→ 0.968	-0.0238 Bus 17

11	I	-0.0238 Bus 17	Gen Bus 2, Bus 8, Bus 11	Infeasible	
	II	-0.0238 Bus 17	LTC Bus 6 →|– Bus 10	0.969→ 0.959	-0.0216 Bus 17
12	I	-0.0216 Bus 17	Gen Bus 2		No Violation
			Gen Bus 8		
			Gen Bus 11	1.0744 →1.0794	
Stage 5: Line In-service: Line Bus 16 – Bus 17 Load Decrease: Bus 16 → [P_L = 5.469 MW, Q_L = 2.813 Mvar] Bus 17 → [P_L = 14.063 MW, Q_L = 9.063 Mvar]					
13	–	No Violation			

Table 4.5 Results of multi-phase hybrid voltage control (IEEE 30 – A).

Now if we further limit the number of taps that LTC transformers can change, as shown in Table 4.6, then at stage 4 the controller will operate in Phase III and the results are listed in Table 4.7.

Device Type	Transformer	Range	Setting
LTC Transformer	Bus 6 →|– Bus 9	0.9780 ~ 1.0180	0.988
	Bus 6 →|– Bus 10	0.9690 ~ 1.0090	0.979
	Bus4 →|– Bus 12	0.8420 ~ 0.9720	0.942
	Bus 28 →|– Bus 27	0.9680 ~ 1.0080	0.978

Table 4.6 Modified LTC tap range on IEEE 30 bus system.

Tim Step	Phas	ΔV_{max} (Before Control)	Control Device (Bus)	Control Action	ΔV_{max} (After Control)
Stage 1 to Stage 3: Same as in Table 4.5.					
1	I	-0.0492 Bus 17	Gen. Bus 2, Bus 8	Infeasible	
	II	-0.0492 Bus 17	Bus 10 19.0 Mvar	ON	-0.0279 Bus 24
…	…	……	……	…	……
9	I	-0.0218 Bus 17	Gen Bus 2	1.0330 →1.0332	No Violation
			Gen Bus 8	1.0094 →1.0146	

			Gen Bus 11	1.0732 →1.0744	
Stage 4: Load Increase: Bus 16 → [P_L = 6.836 MW, Q_L = 3.516 Mvar] Bus 17 → [P_L = 17.578 MW, Q_L = 11.328 Mvar]					
10	I	-0.0266 Bus 17	Gen Bus 2, Bus 8, Bus 11	Infeasible	
	II	-0.0266 Bus 17	No discrete control		
	III	-0.0266 Bus 17	Gen Bus 2	1.0332 →1.0377	No Violation
			Gen Bus 8	1.0146 →1.0208	
			Gen Bus 11	1.0744 →1.0923	
Stage 5: Line In-service: Line Bus 16 – Bus 17 Load Decrease: Bus 16 → [P_L = 5.469 MW, Q_L = 2.813 Mvar] Bus 17 → [P_L = 14.063 MW, Q_L = 9.063 Mvar]					
13	–	No Violation			

Table 4.7 Results of multi-phase hybrid voltage control (IEEE 30 – B).

From above tables, it can be seen that at each stage, the hybrid voltage controller first operates in Phase I, trying to find all of the available control generators inside a local area, and using linear programming algorithm to obtain best voltage settings to maintain desired load bus voltage profile. If the linear programming algorithm successfully finds solution, then voltage setpoint adjusting commands are sent, and the load bus voltages are restored. If there is no generator available or the generator's reactive power is not enough to recover the load bus voltages (i.e. the linear programming algorithm could not reach a solution), then the controller will operate in Phase II. In this phase, the controller will act as a discrete controller presented in chapter 3 without generator controls, locating the worst violation bus first, then trying to identify the most effective discrete control devices depending on their relative priority and switching costs. After the switching, if either the problematic center bus changes or the generator reactive power outputs are relieved and back to their limits, the controller may go back to operate in Phase I again. If under some conditions such as stage 4 in Table 4.7, the controller could not find appropriate discrete control devices to alleviate the voltage problem, the controller will operate in Phase III. In this phase, the generator's full reactive power capacity will be used to minimize the differences between bus voltages and the desired voltage profile. It is also noted from the above table that even some generators are inside the local area, they are not necessarily change their settings, either because they are far away from problematic center or because their sensitivities are too small to be effective in alleviating the voltage problem.

4.2.4 Tests on WECC System

In this section, feasibility tests of the hybrid voltage controller formulated in section 4.2 will be performed on an actual WECC 2001-2003 Winter planning case (case ID 213SNK) with more than 6000 buses. The hybrid controller is simulated with C/C++ program, while the WECC system is simulated with BPA Power Flow package [39]. For test purpose, the selected candidate devices as listed in Table 3.5 are adjusted to reduce the number of capacitors and increase the number of generators. Table 4.8 lists the control devices and their initial settings. Note that the bus names listed as generator type controls are actually generator-controlled high-side voltage buses. The corresponding control generators are not listed here, but can be easily identified in the WECC case file. The KEELER-SVC bus is originally a "BQ' type of bus, but is modified to be treated as generator-controlled "BC' type of bus.

Device Type	Bus / Transformer	Capacity / Range	Setting / Status
Capacitor	ALBANY 115	50.0	OFF
	ALVEY 115	19.5, 19.5, 25.6	OFF

	ALVEY 230	58.9, 58.9, 58.9, 117.8	OFF
	CHEMAWA 115	23.7	OFF
	CHEMAWA 230	54.0	OFF
	LANE 115	30.4	OFF
	LANE 230	108.2	OFF
	TILLAMOK 115	30.4, 22.8	OFF
	TOLEDO 69.0	27.1, 15.4, 15.4	OFF
	TOLEDO 230	30.0	OFF
Reactor	DIXONVLE 500	-149.0	ON
	MARION 500	-248.0, -149.0	ON
LTC Transformer	ALVEY 230 →|– ALVEY 115 3	1/9 ~ 9/9	4/9
	ALVEY 230 →|– ALVEY 115 4	1/9 ~ 9/9	4/9
	ALVEY 500 →|– ALVEY 230 5	1/9 ~ 9/9	9/9
	DIXONVLE 230 →|– DIXONVLE 115 1	1/17 ~ 17/17	11/17
	DIXONVLE 230 →|– DIXONVLE 115 2	1/17 ~ 17/17	11/17
Generator	JOHN DAY 500	-1096.0 ~ 796.0	1.05
	BIG EDDY 230	-569.0 ~ 407.0	1.05
	BONNVILE 230	-200.0 ~ 312.0	1.039
	MCNARY 230	-430.0 ~ 262.0	1.050
	SWIFT 230	-153.0 ~ 153.0	1.050
	KEEL-SVC 230	-450.0 ~ 800.0	1.043

Table 4.8 Control devices available in west Oregon area.

In the following simulations, the local control areas are constructed such that the buses within 6 tiers of the control bus are included. The step-size for LTC tap changing is set to one tap at a time and the following rules are applied to calculate the costs of different control actions: the cost for switching out a capacitor or reactor bank is zero, the cost for switching in a capacitor or reactor bank is 100.0, and the cost for LTC tap changing is 200.0. Since generators are not used as discrete controls, their step-sizes and costs of switching are not set in the tests. For any type of device, the cost of next action will increase by 10.0, and decrease by 1.0 at each time step. The control objective is to maintain all bus voltages within 2% band around the pre-defined voltage profile, and the maximum allowed voltage deviation is 5% away from the optimal value. The voltage penalty coefficient λ is set to 1.0 and the maximum voltage penalty P_0 is set to 7.5 for test purpose. The weighting factor α is set to 0.5 and the percentage p is set to 0.75 in the simulations.

Numerous tests have been conducted on the WECC planning cases under different topology and loading conditions, only parts of the results are shown here. The first simulation scenario shows how the multi-phase hybrid controller responds to load increases in west Oregon area. Eight load buses in western Oregon area are chosen for the tests: ROSS 230, ALCOA 230, RIVRGATE 230, ROSS 115, SIFT TP1 230, SIFT TP2 230, ST JOHNS 230, and WOODLAND 230. The second scenario assume the power system has some further changes in topology and loads before the controller restoring voltages in the first stage, the controller will operate in different phase and make different control decisions. The control results are presented in Table 4.9 and table 4.10.

<table>
<tr><th>Tm Stp</th><th>Area</th><th>Phas</th><th>ΔV_{max} (Before Control)</th><th>Control Device (Bus)</th><th>Control Action</th><th>ΔV_{max} (After Control)</th></tr>
<tr><td colspan="7">Stage 1: Load increase: ROSS 230 → [P_L = 450.0 MW, Q_L = 142.0 Mvar]
ALCOA 230 → [P_L = 45.0 MW, Q_L = 14.2 Mvar]
RIVRGATE 230 → [P_L = 45.0 MW, Q_L = 14.2 Mvar]
ROSS 115 → [P_L = 45.0 MW, Q_L = 14.2 Mvar]
SIFT TP1 230 → [P_L = 45.0 MW, Q_L = 14.2 Mvar]
SIFT TP2 230 → [P_L = 45.0 MW, Q_L = 14.2 Mvar]
ST JOHNS 230 → [P_L = 45.0 MW, Q_L = 14.2 Mvar]
WOODLAND 230 → [P_L = 45.0 MW, Q_L = 14.2 Mvar]</td></tr>
<tr><td rowspan="3">1</td><td rowspan="2">1</td><td>I</td><td>-0.041 TOLEDO 69.0</td><td>No feasible gen.</td><td></td><td></td></tr>
<tr><td>II</td><td>-0.041 TOLEDO 69.0</td><td>MARION 500 -248 Mvar</td><td>OFF</td><td>-0.034 TOLEDO 69.0</td></tr>
<tr><td>2</td><td>I</td><td>-0.025 BRBTN SW 115</td><td>No feasible gen.</td><td></td><td></td></tr>
</table>

		II	-0.025 BRBTN SW 115	No discrete control		
	3	I	-0.022 BALD MT 69.0	No feasible gen.		
		II	-0.022 BALD MT 69.0	No discrete control		
2	1	I	-0.034 TOLEDO 69.0	No feasible gen.		
		II	-0.034 TOLEDO 69.0	MARION 500 -149Mvar	OFF	-0.030 TOLEDO 69.0
	2	I	-0.025 BRBTN SW 115	No feasible gen.		
		II	-0.025 BRBTN SW 115	No discrete control		
	3	I	-0.021 BALD MT 69.0	No feasible gen.		
		II	-0.021 BALD MT 69.0	No discrete control		
3	1	I	-0.030 TOLEDO 69.0	No feasible gen.		
		II	-0.030 TOLEDO 69.0	DIXONVLE 500 -149 Mvar	OFF	-0.027 TOLEDO 69.0
	2	I	-0.025 BRBTN SW 115	No feasible gen.		
		II	-0.025 BRBTN SW 115	No discrete control		
	3	I	-0.021 BALD MT 69.0	No feasible gen.		
		II	-0.021 BALD MT 69.0	No discrete control		
4	1	I	-0.027 TOLEDO 69.0	No feasible gen.		
		II	-0.027 TOLEDO 69.0	LANE 230 108 Mvar	ON	-0.026 ROSS 345
	2	I	-0.025 WALNUT 115	No feasible gen.		
		II	-0.025 WALNUT 115	No discrete control		
	3	I	-0.021 BALD MT 69.0	No feasible gen.		
		II	-0.021 BALD MT 69.0	No discrete control		
5	1	I	-0.026 ROSS 345	4 gen. inside	Infeasible	
		II	-0.026 ROSS 345	CHEMAWA 230 54 Mvar	ON	-0.026 ROSS 345
6	1	I	-0.026 ROSS 345	4 gen. inside	Infeasible	
		II	-0.026 ROSS 345	No discrete control		
		III	-0.026 ROSS 345	BONNVILE 230	1.039 →1.053	No Violation
				MCNARY 230		
				SWIFT 230	1.050 →1.081	
				KEEL-SVC 230	1.043 →1.055	

Table 4.9 Results of multi-phase hybrid voltage control (WECC - A).

Tm Stp	Area	Phas	ΔV_{max} (Before Control)	Control Device (Bus)	Control Action	ΔV_{max} (After Control)
Stage 1: same as in Table 4.9						
1	1	I	-0.041 TOLEDO 69.0	No feasible gen.		
		II	-0.041 TOLEDO 69.0	MARION 500 -248 Mvar	OFF	-0.034 TOLEDO 69.0
	2	I	-0.025 BRBTN SW 115	No feasible gen.		
		II	-0.025 BRBTN SW 115	No discrete control		
	3	I	-0.022 BALD MT 69.0	No feasible gen.		
		II	-0.022 BALD MT 69.0	No discrete control		
…	…	…	……	……	…	……
5	1	I	-0.026 ROSS 345	4 gen. inside	Infeasible	
		II	-0.026 ROSS 345	CHEMAWA 230 54 Mvar	ON	-0.026 ROSS 345
Stage 2: Line Outage: ALVEY 500 – MARION 500 Load Increase: ALVEY 115 → [P_L = 300 MW, Q_L = 100 Mvar] DIXONVLE 115 → [PL = 140 MW, QL = 53 Mvar]						
6	1	I	-0.032 VILLAGEG 115	No feasible gen.		
		II	-0.032 VILLAGEG 115	ALVEY 230 117.8 Mvar	ON	-0.028 TOLEDO 69.0
	2	I	0.022 GAR1EAST 500	No feasible gen.		
		II	0.022 GAR1EAST 500	No discrete control		
7	1	I	-0.028 TOLEDO 69.0	No feasible gen.		
		II	-0.028 TOLEDO 69.0	ALVEY 230 58.9 Mvar	ON	-0.026 ROSS 345
	2	I	-0.025 WALNUT 115	No feasible gen.		
		II	-0.025 WALNUT 115	No discrete control		
	3	I	-0.021 BALD MT 69.0	No feasible gen.		
		II	-0.021 BALD MT 69.0	No discrete control		
8	1	I	-0.026 ROSS 345	BONNVILE 230	1.039 →1.044	-0.025 TOLEDO 69.0
				MCNARY 230		
				SWIFT 230	1.050 →1.078	
				KEEL-SVC 230	1.043 →1.059	
9	1	I	-0.025 TOLEDO 69.0	No feasible gen.		
		II	-0.025 TOLEDO 69.0	ALVEY 230 58.9 Mvar	ON	-0.023 TOLEDO 69.0
10	1	I	-0.023 TOLEDO 69.0	No feasible gen.		
		II	-0.023 TOLEDO 69.0	ALVEY 115 25.6 Mvar	ON	-0.022 TOLEDO 69.0
11	1	I	-0.022 TOLEDO 69.0	No feasible gen.		

		II	-0.022 TOLEDO 69.0	ALBANY 115 50.0 Mvar	ON	-0.021 TOLEDO 69.0
12	1	I	-0.021 TOLEDO 69.0	No feasible gen.		
		II	-0.021 TOLEDO 69.0	ALVEY 115 25.6 Mvar	ON	No Violation

Table 4.10 Results of multi-phase hybrid voltage control (WECC - B).

It can be observed from above tables that at each stage, the controller first groups the violation buses into different problematic areas and operates in Phase I. It tries to find the available control generators in each local area, using linear programming algorithm to calculate optimal generator voltage adjustments such that load bus voltage profiles are maintained as desired. If the linear programming algorithm successfully finds solutions for one or more control areas, then parallel switching commands are sent, and the load bus voltages may be restored for those areas, or the problem center may change and problematic areas may merge into new areas. If there is no generator available or the generator's reactive power is not enough to recover the load bus voltages (i.e. the linear programming algorithm could not reach a solution), then the controller will operate in Phase II, trying to find the best (highest priority and lowest cost) discrete control devices available for switching. If such control devices exists, then after switching either the problematic center bus changes or the generator reactive outputs are back to their limits, the controller may go back to operate in Phase I again. If under certain condition, the controller could not find appropriate discrete control devices to switch, then the controller will operate in phase III, and the generator's full reactive power capacity will be utilized to restore the voltage or at least alleviate the voltage problem.

It is worth mentioning that although some generators are inside a local area, they are not necessarily change their settings, such as MCNARY 230 in step 6 of Table 4.9 and step 8 in Table 4.10, because either they are far away from problematic center or their sensitivities are too small or their reactive power outputs reach their limits. It is also noted that although the control solutions in Phase I are supposed to bring bus voltages back to normal range, this is not always the case, especially with the constraint relaxing technique. For example, in step 8 of Table 4.10 the controller successfully reach a solution in Phase I, but the voltage on TOLEDO 69.0 remains outside the normal range after control actions, since the voltage constraint on TOLEDO 69.0 is relaxed in the linear programming formulation. In effect, the voltages on most buses are still brought back to normal range, and the voltage on TOLEDO 69.0 can be restored later by switching discrete devices. Finally it is noted that in above tables, the reactors are switched out before the capacitors are switched in, which shows that the preferences of the operators are properly implemented into the algorithm.

4.3 Summary

To deal with voltage problems happened simultaneously in several places in large power systems, the on-line slow voltage control scheme in last chapter is extended to divides the network into separate control areas dynamically according to current system conditions and make control decisions for each area respectively. The scheme itself is open, in the sense that any voltage control algorithm can be integrated into it, including the model-based algorithm and the alternate control algorithm. The simulation results on the actual WECC planning case show that the controller is effective in alleviate multiple voltage problems simultaneously.

For power systems with a large amount of generation resources, a multi-phase hybrid voltage control scheme is proposed to coordinate continuous generation controls and discrete controls while taking reactive power security into consideration. The controller is meant to act in the way similar to that of AGC under normal operating conditions such as morning load pickups, adjusting generator reactive outputs to maintain the desired voltage profile with the discrete devices as supplemental reactive power resource. The controller operated in three phases and use linear programming / integer programming to search for the best control actions in each phase. The test results on the standard IEEE 30-bus system and the actual WECC planning case clearly show that the hybrid scheme is feasible, scalable to large-scale power system and suitable for on-line implementation.

Chapter 5

Conclusions and Future Works

This chapter summarizes the main results of the research by providing general conclusions and discussions on the key contributions, which is followed by suggestions for possible extensions of the work reported in this dissertation.

5.1 Conclusions

In view of a state estimator model maybe unavailable or unreliable, this dissertation proposes an alternate heuristic slow voltage controller that can be easily integrated with the model-based controller and motivated towards implementation under a common framework in the western Oregon area of Pacific Northwest. An integer-programming formulation is presented with preferences of control actions built into the switching cost function, and the objective is to keep the voltages within certain range around optimal profile with minimum switching cost. The alternate controller operates independent of the state estimator model and can be used as back-up controller, or used to reinforce the decisions made by the model-based controller.

A local voltage estimator is formulated based on linearized reactive power flow model to approximate switching effects by utilizing only the local SCADA measurements around the control devices. The control effects of capacitor/reactor switching, LTC tap changing, and generator voltage adjusting are quickly assessed in a unified way by treating them as some reactive power injection changes.

Parallel control of multiple problematic areas of a large power system is also addressed. The system is dynamically divided into separated control areas around several problem center buses and simultaneous corrective control actions are made such that voltage problems occurred in different areas are quickly alleviated.

To coordinate continuous generator controls and discrete device controls for large power systems with lots of generators as main voltage controls, a hybrid multi-phase automatic voltage control scheme is proposed to maintain system voltage profile while taking reactive power security into consideration. The controller operates in three phases with the optimization problems in each phase formulated as continuous or discrete problems and solved using linear programming or integer programming respectively.

Simulation results on the IEEE 30 bus test system and an actual WECC planning case show that the above schemes are effective in handling the voltage problem, scalable to large-scale power system and suitable for on-line implementation.

5.2 Future Works

As with any work of research, there is always more that can be done. Aside from further testing of the algorithms with more cases and on other power systems, there are several extensions and modifications which could be explored.

In the local voltage estimator, it is assumed that the SCADA measurements are available and valid inside the small local area, but this is not always the case. Although the unavailable data could be replaced with the last good measurements or last good state estimator results if there is no significant change in network topology and loading conditions within certain time period, it is necessary to find a simple way to detect the bad measurements or at least report the obvious erroneous measurements.

Apart from the using local voltage estimator to approximate the effects of control actions, pattern recognition approach with the help of engineering experience might be also worth doing. This approach actually involves defining the typical cases offline by pattern classification or clustering algorithm and then identifying a typical case that is closest to current operating conditions by pattern recognition.

It is also possible to consider other objective functions such as loss minimization, reactive margin maximization and operating cost minimization under the possible reactive power market environment.

Bibliography

[1] C. W. Taylor, *Power System Voltage Stability*, McGraw-Hill Inc., 1994.

[2] P. Kundur, *Power System Stability and Control*, McGraw-Hill Inc., 1994.

[3] T. V. Cutsem, "Voltage Instability: Phenomena, Countermeasures, and Analysis Methods", *Proceedings of the IEEE*, Vol. 88, No. 2, pp. 208-227, February 2000.

[4] B. Kirby and E. Hirst, "Ancillary Service Details: Voltage Control", *Report ORNL/CON-453*, Oak Ridge National Laboratory, Oak Ridge, TN, December 1997.

[5] C. W. Taylor, V. Venkatasubramanian, and Y. Chen, "Wide-Area Stability and Voltage Control," *Proceedings of VII Symposium of Specialist in Electric Operational and Expansion Planning (VII SEPOPE)*, Brazil, May 2000.

[6] C. W. Taylor, "Response-Based, Feedforward Wide-Area Control", *Position Paper for NSF/DOE/EPRI Sponsored Workshop on Future Research Directions for Complex Interactive Electric Networks*, Washington D.C., November 2000.

[7] K. T. Vu, C. Liu, C. W. Taylor, and K. M. Jimma, "Voltage Instability: Mechanisms and Control Strategies", *Proceedings of the IEEE*, Vol. 83, No. 11, pp. 1442-1455, November 1995.

[8] B. Stott and E. Hobson, "Power System Security Control Calculation Using Linear Programming, Part 1 and 2", *IEEE Transactions on Power Apparatus and Systems*, Vol. PAS-97, No. 5, pp. 1713-1731, October 1978.

[9] D. I. Sun, B. Ashley, B. Brewer, A. Hughes, and W. F. Tinney, “Optimal Power Flow by Newton Approach”, *IEEE Transactions on Power Apparatus and Systems*, Vol. PAS-103, No. 2, pp. 2864-2880, October 1984.

[10] O. Alsac, J. Bright, M. Prais, and B. Stott, “Further Developments in LP-Based Optimal Power Flow”, *IEEE Transactions on Power Systems*, Vol. 5, No. 3, pp. 697-711, August 1990.

[11] W. F. Tinney, J. M. Bright, K. D. Demaree, and B. A. Hughes, “Some Deficiencies in Optimal Power Flow”, *IEEE Transactions on Power Systems*, Vol. 3, No. 2, pp. 676-683, May 1988.

[12] C. Liu and K. Tomsovic, “An Expert System Assisting Decision-Making of Reactive Power/Voltage Control”, *IEEE Transactions on Power Systems*, Vol. PWRS-1, No. 3, pp. 195-201, August 1986.

[13] S. J. Cheng, O. P. Malik, and G. S. Hope, “An Expert System for Voltage and Reactive Power Control of a Power System”, *IEEE Transactions on Power Systems*, Vol. 3, No. 4, pp. 1449-1455, November 1988.

[14] W. R. Wagner, A. Keyhani, S. Hao, and T. C. Wong, “A Rule-Based Approach to Decentralized Voltage Control”, *IEEE Transactions on Power Systems*, Vol. 5, No. 2, pp. 643-651, May 1990.

[15] T. F. Godart and H. B. Puttgen, “A Reactive Path Concept Applied within a Voltage Control Expert System”, *IEEE Transactions on Power Systems*, Vol. 6, No. 2, pp. 787-793, May 1991.

[16] K. Tomsovic, “A Fuzzy Linear Programming Approach to the Reactive Power/Voltage Control Problem”, *IEEE Transactions on Power Systems*, Vol. 7, No. 1, pp. 287-293, February 1992.

[17] R. Yohoyama, T. Niimura, and Y. Nakanishi, “A Coordinated Control of Voltage and Reactive Power by Heuristic Modeling and Approximate Reasoning”, *IEEE Transactions on Power Systems*, Vol. 8, No. 2, pp. 636-645, May 1993.

[18] C-T. Su and C-T. Lin, “Application of a Neural Network and Heuristic Model for Voltage-Reactive Power Control”, *Electric Power Systems Research*, Vol. 34, No. 3, pp. 143-148, May 1995.

[19] J.P. Paul, J.T. Leost, and J.M. Tesseron, “Survey of the Secondary Voltage Control in France: Present Realization and Investigations,” *IEEE Transactions on Power Systems*, Vol. PWRS-2, No.2, pp. 505-511, 1987.

[20] M. Ilic, J. Christensen, and K.L. Eichorn, “Secondary Voltage Control Using Pilot Point Information”, *IEEE Transactions on Power Systems*, Vol. 3, No. 2, May 1988.

[21] P. Lagonotte, J.C. Sabonnadiere, J.Y. Leost, and J.P. Paul, “Structural Analysis of the Electrical System: Application to the Secondary Voltage Control in France”, *IEEE Transactions on Power Systems*, Vol. 4, No. 2, pp. 479-484, May 1989.

[22] S. Corsi, P. Marannino, N. Losignore, G Moreschini, and G. Piccini, “Coordination Between the Reactive Power Scheduling Function and the Hierarchical Voltage Control of the EHV ENEL System”, *IEEE Transactions on Power Systems*, Vol. 10, No. 2, pp. 686-694, May 1995.

[23] M. Ilic, X. Liu, G. L.eung, M. Athans, C. Vialas, and P. Pruvot, “Improved Secondary and New Tertiary Voltage Control,” *IEEE Transactions on Power Systems*, Vol. 10, No. 4, Nov. 1995.

[24] J. L. Sancha, J. L. Fernandez, A. Cortes, and J. T. Abarca, “Secondary Voltage Control: Analysis, Solutions and Simulation Results for Spanish Transmission System”, *IEEE Transactions on Power Systems*, Vol. 11, No. 2, pp. 630-638, May 1996.

[25] H. Vu, P. Pruvot, C. Launay, and Y. Harmand, “An Improved Voltage Control on Large Scale Power System”, *IEEE Transactions on Power Systems,* Vol. 11, No. 3, pp. 1295-1303, August 1996.

[26] A. Conjo and M. J. Aguilar, “Secondary Voltage Control: Nonlinear Selection of Pilot uses, Design of an Optimal Control Law, and Simulation Results”, *IEE Proceedings of Generation, Transmission, and Distribution*, Vol. 145, No. 1, January 1998.

[27] J. Van Hecke, N. Janssens, J. Deuse, and F. Promel, “Coordinated Voltage Control Experience in Belgium”, *CIGRE Session Report 38-111*, Paris, September 2000.

[28] M. Ilic and W. Stobart, “Development of A Smart Algorithm for Voltage Monitoring and Control”, *IEEE Transactions on Power Systems*, Vol. 5, No. 4, November 1990.

[29] A. Zobian and M. Ilic, “A Steady State Voltage Monitoring and Control Algorithm Using Localized Least Square Minimization of Load Voltage Deviations”, *IEEE Transactions on Power Systems*, Vol. 11, No. 2, pp. 929-938, May 1996.

[30] C. Yu, Y.T. Yoon, M. Ilic, and A. Catelli, "On-line Voltage Regulation: The Case of New England", *IEEE Transactions on Power Systems*, Vol. 14, pp. 1477-1483, November 1999.

[31] Y. Chen, *Development of Automatic Slow Voltage Control for Large Power Systems*, Ph.D. dissertation, School of Electrical Engineering And Computer Science, Washington State University, Pullman, WA, August 2001.

[32] J. J. Grainger and W. D. Stevenson, Jr., *Power System Analysis*, McGraw-Hill Inc., 1994.

[33] A. J. Wood and B. F. Wollenberg, *Power Generation, Operation and Control,* John Wiley & Sons, 1996.

[34] http://www.ee.washington.edu/research/pstca/

[35] N. Christofides, A. Mingozzi, P. Toth, and C. Sandi, *Combinatorial Optimization*, John Wiley & Sons, 1979.

[36] G. L. Nemhauser and L. A. Wolsey, *Integer and Combinatorial Optimization,* John Wiley & Sons, 1988.

[37] M. S. Bazaraa and J. J. Jarvis, *Linear Programming and Network Flows*, John Wiley & Sons, 1977.

[38] J. P. Ignizio and T. M. Cavalier, *Linear Programming*, Prentice-Hall Inc., 1994.

[39] Bonneville Power Administration, *IPF Batch PowerFlow (BPF) User's Guide*, Portland, OR, 1998.

[40] T. S. Corman, C. E. Leiserson, R. L. Rivest, and C. Stein, *Introduction to Algorithms*, Second Edition, The MIT Press, 2001.

[41] http://www.gnu.org/software/glpk

APPENDIX A

IEEE 30 Bus Test System

The system data and one-line diagram of IEEE 30 bus standard test system is available on at the website of power research group of University of Washington [34].

A.1 One-line Diagram of IEEE 30 Bus Test System [34]

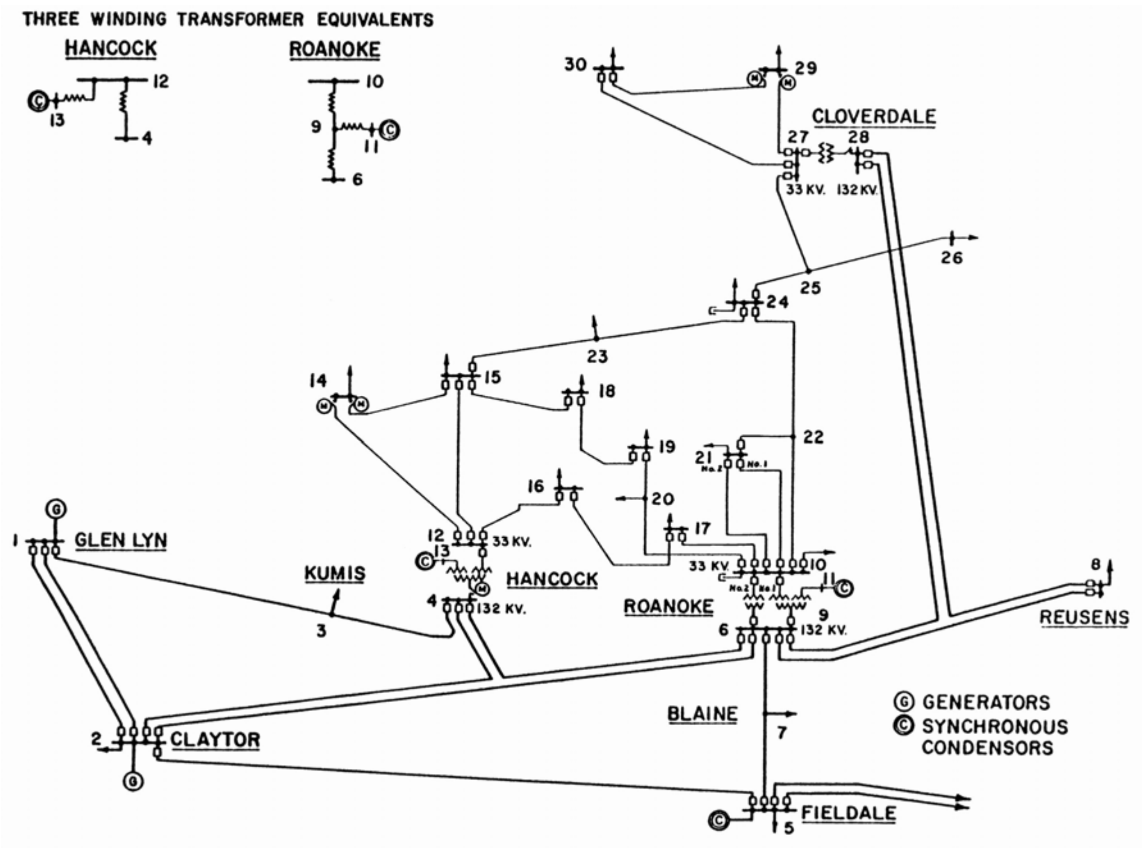

Figure A.1 One-line Diagram of IEEE 30 Bus Test System [34].

A.2 System Data of IEEE 30 Bus Test System [34]

```
08/20/93 UW ARCHIVE                    100.0  1961 W IEEE 30 Bus Test Case
BUS DATA FOLLOWS                       30 ITEMS
  1 Glen Lyn  132  1  1  3  1.060     0.0    0.0    0.0  260.2   -16.1  132.0  1.060   0.0   0.0   0.0   0.0     0
  2 Claytor   132  1  1  2  1.043   -5.48   21.7   12.7   40.0    50.0  132.0  1.045  50.0 -40.0   0.0   0.0     0
  3 Kumis     132  1  1  0  1.021   -7.96    2.4    1.2    0.0     0.0  132.0  0.0     0.0   0.0   0.0   0.0     0
  4 Hancock   132  1  1  0  1.012   -9.62    7.6    1.6    0.0     0.0  132.0  0.0     0.0   0.0   0.0   0.0     0
  5 Fieldale  132  1  1  2  1.010  -14.37   94.2   19.0    0.0    37.0  132.0  1.010  40.0 -40.0   0.0   0.0     0
  6 Roanoke   132  1  1  0  1.010  -11.34    0.0    0.0    0.0     0.0  132.0  0.0     0.0   0.0   0.0   0.0     0
  7 Blaine    132  1  1  0  1.002  -13.12   22.8   10.9    0.0     0.0  132.0  0.0     0.0   0.0   0.0   0.0     0
  8 Reusens   132  1  1  2  1.010  -12.10   30.0   30.0    0.0    37.3  132.0  1.010  40.0 -10.0   0.0   0.0     0
  9 Roanoke   1.0  1  1  0  1.051  -14.38    0.0    0.0    0.0     0.0    1.0  0.0     0.0   0.0   0.0   0.0     0
 10 Roanoke    33  1  1  0  1.045  -15.97    5.8    2.0    0.0     0.0   33.0  0.0     0.0   0.0   0.0   0.19    0
 11 Roanoke    11  1  1  2  1.082  -14.39    0.0    0.0    0.0    16.2   11.0  1.082  24.0  -6.0   0.0   0.0     0
 12 Hancock    33  1  1  0  1.057  -15.24   11.2    7.5    0.0     0.0   33.0  0.0     0.0   0.0   0.0   0.0     0
 13 Hancock    11  1  1  2  1.071  -15.24    0.0    0.0    0.0    10.6   11.0  1.071  24.0  -6.0   0.0   0.0     0
 14 Bus 14     33  1  1  0  1.042  -16.13    6.2    1.6    0.0     0.0   33.0  0.0     0.0   0.0   0.0   0.0     0
 15 Bus 15     33  1  1  0  1.038  -16.22    8.2    2.5    0.0     0.0   33.0  0.0     0.0   0.0   0.0   0.0     0
 16 Bus 16     33  1  1  0  1.045  -15.83    3.5    1.8    0.0     0.0   33.0  0.0     0.0   0.0   0.0   0.0     0
 17 Bus 17     33  1  1  0  1.040  -16.14    9.0    5.8    0.0     0.0   33.0  0.0     0.0   0.0   0.0   0.0     0
 18 Bus 18     33  1  1  0  1.028  -16.82    3.2    0.9    0.0     0.0   33.0  0.0     0.0   0.0   0.0   0.0     0
 19 Bus 19     33  1  1  0  1.026  -17.00    9.5    3.4    0.0     0.0   33.0  0.0     0.0   0.0   0.0   0.0     0
 20 Bus 20     33  1  1  0  1.030  -16.80    2.2    0.7    0.0     0.0   33.0  0.0     0.0   0.0   0.0   0.0     0
 21 Bus 21     33  1  1  0  1.033  -16.42   17.5   11.2    0.0     0.0   33.0  0.0     0.0   0.0   0.0   0.0     0
 22 Bus 22     33  1  1  0  1.033  -16.41    0.0    0.0    0.0     0.0   33.0  0.0     0.0   0.0   0.0   0.0     0
 23 Bus 23     33  1  1  0  1.027  -16.61    3.2    1.6    0.0     0.0   33.0  0.0     0.0   0.0   0.0   0.0     0
 24 Bus 24     33  1  1  0  1.021  -16.78    8.7    6.7    0.0     0.0   33.0  0.0     0.0   0.0   0.0   0.043   0
 25 Bus 25     33  1  1  0  1.017  -16.35    0.0    0.0    0.0     0.0   33.0  0.0     0.0   0.0   0.0   0.0     0
 26 Bus 26     33  1  1  0  1.000  -16.77    3.5    2.3    0.0     0.0   33.0  0.0     0.0   0.0   0.0   0.0     0
 27 Cloverdle  33  1  1  0  1.023  -15.82    0.0    0.0    0.0     0.0   33.0  0.0     0.0   0.0   0.0   0.0     0
 28 Cloverdle132   1  1  0  1.007  -11.97    0.0    0.0    0.0     0.0  132.0  0.0     0.0   0.0   0.0   0.0     0
 29 Bus 29     33  1  1  0  1.003  -17.06    2.4    0.9    0.0     0.0   33.0  0.0     0.0   0.0   0.0   0.0     0
 30 Bus 30     33  1  1  0  0.992  -17.94   10.6    1.9    0.0     0.0   33.0  0.0     0.0   0.0   0.0   0.0     0
-999
BRANCH DATA FOLLOWS                41 ITEMS
  1   2   1  1 1 0  0.0192   0.0575   0.0528   0   0   0   0 0  0.0     0.0 0.0   0.0   0.0   0.0   0.0
  1   3   1  1 1 0  0.0452   0.1652   0.0408   0   0   0   0 0  0.0     0.0 0.0   0.0   0.0   0.0   0.0
  2   4   1  1 1 0  0.0570   0.1737   0.0368   0   0   0   0 0  0.0     0.0 0.0   0.0   0.0   0.0   0.0
  3   4   1  1 1 0  0.0132   0.0379   0.0084   0   0   0   0 0  0.0     0.0 0.0   0.0   0.0   0.0   0.0
  2   5   1  1 1 0  0.0472   0.1983   0.0418   0   0   0   0 0  0.0     0.0 0.0   0.0   0.0   0.0   0.0
  2   6   1  1 1 0  0.0581   0.1763   0.0374   0   0   0   0 0  0.0     0.0 0.0   0.0   0.0   0.0   0.0
  4   6   1  1 1 0  0.0119   0.0414   0.0090   0   0   0   0 0  0.0     0.0 0.0   0.0   0.0   0.0   0.0
  5   7   1  1 1 0  0.0460   0.1160   0.0204   0   0   0   0 0  0.0     0.0 0.0   0.0   0.0   0.0   0.0
  6   7   1  1 1 0  0.0267   0.0820   0.0170   0   0   0   0 0  0.0     0.0 0.0   0.0   0.0   0.0   0.0
  6   8   1  1 1 0  0.0120   0.0420   0.0090   0   0   0   0 0  0.0     0.0 0.0   0.0   0.0   0.0   0.0
  6   9   1  1 1 0  0.0      0.2080   0.0      0   0   0   0 0  0.978   0.0 0.0   0.0   0.0   0.0   0.0
  6  10   1  1 1 0  0.0      0.5560   0.0      0   0   0   0 0  0.969   0.0 0.0   0.0   0.0   0.0   0.0
  9  11   1  1 1 0  0.0      0.2080   0.0      0   0   0   0 0  0.0     0.0 0.0   0.0   0.0   0.0   0.0
  9  10   1  1 1 0  0.0      0.1100   0.0      0   0   0   0 0  0.0     0.0 0.0   0.0   0.0   0.0   0.0
  4  12   1  1 1 0  0.0      0.2560   0.0      0   0   0   0 0  0.932   0.0 0.0   0.0   0.0   0.0   0.0
 12  13   1  1 1 0  0.0      0.1400   0.0      0   0   0   0 0  0.0     0.0 0.0   0.0   0.0   0.0   0.0
 12  14   1  1 1 0  0.1231   0.2559   0.0      0   0   0   0 0  0.0     0.0 0.0   0.0   0.0   0.0   0.0
 12  15   1  1 1 0  0.0662   0.1304   0.0      0   0   0   0 0  0.0     0.0 0.0   0.0   0.0   0.0   0.0
 12  16   1  1 1 0  0.0945   0.1987   0.0      0   0   0   0 0  0.0     0.0 0.0   0.0   0.0   0.0   0.0
 14  15   1  1 1 0  0.2210   0.1997   0.0      0   0   0   0 0  0.0     0.0 0.0   0.0   0.0   0.0   0.0
```

16	17	1	1	1	0	0.0524	0.1923	0.0	0	0	0	0	0	0.0	0.0	0.0	0.0	0.0	0.0	0.0
15	18	1	1	1	0	0.1073	0.2185	0.0	0	0	0	0	0	0.0	0.0	0.0	0.0	0.0	0.0	0.0
18	19	1	1	1	0	0.0639	0.1292	0.0	0	0	0	0	0	0.0	0.0	0.0	0.0	0.0	0.0	0.0
19	20	1	1	1	0	0.0340	0.0680	0.0	0	0	0	0	0	0.0	0.0	0.0	0.0	0.0	0.0	0.0
10	20	1	1	1	0	0.0936	0.2090	0.0	0	0	0	0	0	0.0	0.0	0.0	0.0	0.0	0.0	0.0
10	17	1	1	1	0	0.0324	0.0845	0.0	0	0	0	0	0	0.0	0.0	0.0	0.0	0.0	0.0	0.0
10	21	1	1	1	0	0.0348	0.0749	0.0	0	0	0	0	0	0.0	0.0	0.0	0.0	0.0	0.0	0.0
10	22	1	1	1	0	0.0727	0.1499	0.0	0	0	0	0	0	0.0	0.0	0.0	0.0	0.0	0.0	0.0
21	22	1	1	1	0	0.0116	0.0236	0.0	0	0	0	0	0	0.0	0.0	0.0	0.0	0.0	0.0	0.0
15	23	1	1	1	0	0.1000	0.2020	0.0	0	0	0	0	0	0.0	0.0	0.0	0.0	0.0	0.0	0.0
22	24	1	1	1	0	0.1150	0.1790	0.0	0	0	0	0	0	0.0	0.0	0.0	0.0	0.0	0.0	0.0
23	24	1	1	1	0	0.1320	0.2700	0.0	0	0	0	0	0	0.0	0.0	0.0	0.0	0.0	0.0	0.0
24	25	1	1	1	0	0.1885	0.3292	0.0	0	0	0	0	0	0.0	0.0	0.0	0.0	0.0	0.0	0.0
25	26	1	1	1	0	0.2544	0.3800	0.0	0	0	0	0	0	0.0	0.0	0.0	0.0	0.0	0.0	0.0
25	27	1	1	1	0	0.1093	0.2087	0.0	0	0	0	0	0	0.0	0.0	0.0	0.0	0.0	0.0	0.0
28	27	1	1	1	0	0.0	0.3960	0.0	0	0	0	0	0	0.968	0.0	0.0	0.0	0.0	0.0	0.0
27	29	1	1	1	0	0.2198	0.4153	0.0	0	0	0	0	0	0.0	0.0	0.0	0.0	0.0	0.0	0.0
27	30	1	1	1	0	0.3202	0.6027	0.0	0	0	0	0	0	0.0	0.0	0.0	0.0	0.0	0.0	0.0
29	30	1	1	1	0	0.2399	0.4533	0.0	0	0	0	0	0	0.0	0.0	0.0	0.0	0.0	0.0	0.0
8	28	1	1	1	0	0.0636	0.2000	0.0428	0	0	0	0	0	0.0	0.0	0.0	0.0	0.0	0.0	0.0
6	28	1	1	1	0	0.0169	0.0599	0.0130	0	0	0	0	0	0.0	0.0	0.0	0.0	0.0	0.0	0.0

-999
LOSS ZONES FOLLOWS 1 ITEMS
1 IEEE 30 BUS
-99
INTERCHANGE DATA FOLLOWS 1 ITEMS
-9
1 2 Claytor 132 0.0 999.99 IEEE30 IEEE 30 Bus Test Case
TIE LINES FOLLOWS 0 ITEMS
-999
END OF DATA

APPENDIX B

README of the Programs

B.1 Standard programs used and case studied

In the simulations of WECC system, BPA standard power flow program (Cygwin version) [39] is used to approximate the system's response to any control action. Before the simulations, the power flow for the original case is calculated by BPA power flow program and the resulting voltage profile is treated as the desired voltage profile. At the beginning of each time step of the simulations, the BPA power flow program is called to calculate the actual power flow on the large system. The resulting "*.PFO" file is read and treated as the SCADA measurements, and based on these "measurements" the control decision is made.

To solve the large-scale linear programming problems in Chapter 4, the GLPK (GNU Linear Programming Kit) package [41] is used. This package includes a set of routines written in ANSI C and organized in the form of a callable library, which is intended for solving large-scale linear programming (LP), mixed integer programming (MIP), and other related problems.

The BPA planning case studied is 2001 to 2003 winter planning case with case ID: 213SNK. The total number of buses of the case is 6815 and the total number of lines is

9245. For test purpose, about 20 to 30 discrete devices in the western Oregon area are considered as candidate controls.

To simulate the response of IEEE 30 bus system, a simple power flow program is implemented with MATLAB language that takes advantage of the built-in matrix manipulation and sparse matrix storage. Solving a set of linear equations is a built-in function and therefore made it an attractive choice for quick implementation and testing of ideas.

The IEEE 30 bus system is a standard test system, the system data and one-line diagram of IEEE 30 bus is available on at the website of power research group of University of Washington [34] and listed in Appendix A.

B.2 MATLAB files

1) **bpa_ctrl.m:** main program

   The main program read in the standard case file, and calls the power flow program to obtain the desired voltage profile first. Then for each time step, the power flow is calculated and the result is saved as the control results from SCADA. It also controls the loop of the stages, and calls different controller subroutines to determine the best control actions.

2) **devIPctrl.m:** discrete controller (integer programming) subroutine

   The subroutine uses integer programming to search for the discrete control devices with lowest total switching cost and highest priority.

3) **estimate.m:** voltage estimator subroutine

The subroutine calculates the estimated local bus voltages after control actions, which will be used to calculated the voltage penalty costs later.

4) **fd_pf.m / nr_pf.m:** Fast-Decoupled / Newton-Raphson power flow subroutine

These subroutines calculate the power flow with fast-decoupled or Newton-Raphson algorithms.

5) **findctrlact.m:** control action finding subroutine

The subroutine finds appropriate control actions for all control devices under current network topology and loads conditions.

6) **findonelocal.m:** local control are formation subroutine

The subroutine formulates appropriate local area around a specific bus using breadth-first search algorithm.

7) **genLPctrlOne.m:** Phase I hybrid controller subroutine

The subroutine solves linear programming to obtain the best generator voltage setpoints to restore the bus voltages

8) **genLPctrlThree.m:** Phase III hybrid controller subroutine

The subroutine solves linear programming to minimize the difference between local bus voltages and the desired voltage profile.

9) **ieee30chg.m / ieee30state.m:** IEEE 30 bus base case / stage definition subroutine

These subroutines modify the original IEEE 30 bus system data to form base case and the changes at each stage.

10) **lfdfPQ.m:** IEEE 30 bus base case / stage definition subroutine

The subroutine calculates the sensitivities of the bus voltages to any control actions

11) **readcdf.m:** IEEE Common Data Format file reading subroutine

The subroutine read in the Common Data Format file to proper data structures.

12) **savecontrol.m:** control result saving subroutine

The subroutine save the control results into a text file for further investigation.

B.3 C/C++ files

1) **voltctrl_estim.c:** main program

The main program read in the WECC *.NET case file, and calls the BPA power flow program to obtain the desired voltage profile first. Then for each time step, the BPA power flow is called and the result in *.PFO file is saved as the control results from SCADA. It also controls the loop of the stages and control steps, and calls the controller subroutine to determine the best control actions.

2) **voltctrl_estim.h:** header file for the program

The header file includes definitions of constants, data structures and function prototype declarations.

3) **control.c:** includes subroutines implementing the voltage controllers

getAllCtrl_Act(): Obtains appropriate control action for each device.

tryLPCtrl_I(): Phase I hybrid voltage controller subroutine.

tryLPCtrl_III(): Phase III hybrid voltage controller subroutine.

findAllCtrl_Gen(): Locates all control generators for each control area.

formLPprog_I(): Formulate linear programming problem for Phase I controller.

formLPprog_III(): Formulate linear programming problem for Phase III controller.

tryIPCtrl_II(): Discrete controller (integer programming) subroutine.

findOneCtrl_Dev(): Find the best control device inside a control area.

calcSwitch_Cost(): Calculate the switching cost for certain control action.

updatAllDev_Rec(): Update the control device status after control actions.

4) **estimate.c:** includes subroutines implementing the voltage estimator

calcLine_Flow(): Calculate line P/Q flows from bus voltages and angles .

calcLine_LFDF(): Calculate line flow (P/Q) sensitivities to voltages.

calcLTC_LFDF(): Calculate line flow (P/Q) sensitivities to LTC taps.

formB_Matrix(): Formulate B matrix from measurements.

estimBus_Volt(): Estimate bus voltages after control actions.

5) **miscs.c:** includes miscellaneous subroutines supporting the program

runBpa_Pf(): Call BPA power flow to run a specified case.

findSel_LocalBus(): Locates all selected local load buses.

findMax_Diff(): Local the worst violation bus inside each area.

findCtrl_Reg(): Formulate separated problematic areas.

findAll_Loc():Find local buses and local lines of all the control buses.

6) **read.c:** includes subroutines to read case/result/control files

readAll_CASE(): Read in case definition file.

readAllBus_NET(): Read in bus data *.NET file to proper data structures.

readAllBus_PFO(): Read in bus voltage from BPA power flow result *.PFO file.

readAllDev_CTRL1(): Read in control device status file.

readAllLine_NET(): Read in line data *.NET file to proper data structures.

readAllCtrl_PARA(): Read in controller parameters file.

readAllLine_CHG(): Read in line outage data for each case.

readAllBus_CHG(): Read in bus load change data for each case.

readLP_SOL(): Read in GLPK solution file for linear programming problems.

7) **write.c:** includes subroutines to write case/result/control files

writeNew_PFC(): Write a *.PFC BPA power flow control file for a case.

writeCase_CHG1():Write case change to a *.CHG BPA power flow change file.

writeCtrl_CHG():Write control change to a *.CHG BPA power flow change file.

writeCtrl_RES(): Save the control results to a text file.

writeCtrl_COST(): Save the costs of control actions for comparing purpose.

writeNext_CTRL(): Save the control device status to file.

writeLP_LPT_I(): Write the formulated Phase I LP problems to a *.LPT file.

writeLP_LPT_III(): Write the formulated Phase III LP problems to a *.LPT file.